Development of Novel Semisolids for the Treatment of Chronic Skin Diseases

Dissertation

der Mathematisch-Naturwissenschaftlichen Fakultät

der Eberhard Karls Universität Tübingen

zur Erlangung des Grades eines

Doktors der Naturwissenschaften

(Dr. rer. nat.)

vorgelegt von

Ziwei Zhang

aus Heilongjiang

China

Tübingen

2018

Gedruckt mit Genehmigung der Mathematisch-Naturwissenschaftlichen Fakultät der Eberhard Karls Universität Tübingen.

Tag der mündlichen Qualifikation:	14.12.2018
Dekan:	Prof. Dr. Wolfgang Rosenstiel
1. Berichterstatter:	Dr. Dominique J. Lunter
2. Berichterstatter:	Prof. Dr. Rolf Daniels

Acknowledgement

In May of 2015, I decided to pursue a PhD degree in Tübingen, a small picturesque and tranquil town far away from the hustle and bustle. As the Chinese proverb says, "Time flies like an arrow, days and months as a weaver's shuttle." Now at the epilogue of my PhD, I feel extremely grateful for the wonderful people I have met here.

Foremost, I express my sincere appreciation to Prof. Dr. Rolf Daniels for giving me the opportunity to be part of his research group, for his enthusiasm, kind guidance and insightful suggestions throughout my PhD.

I express my deepest gratitude to my supervisor Dr. Dominique J. Lunter for introducing me to this wonderful world of Raman microspectroscopy, for her excellent guidance and invaluable encouragement, and for her unreserved help and support throughout my work. Even today, after almost four years, I still remember our first meeting and I distinctly remember thinking to myself after the meeting how nice it would be to work with her. I feel incredibly fortunate to meet such a nice and supportive advisor.

I thank Prof. Dr. Martin A. Wahl for giving constructive criticisms, suggestions and comments in the PhD seminars.

I am very thankful to Milica Lukić and Ivana Pantelić in the University of Belgrade for their generous help with *in vivo* studies.

I thank my lab mates and colleagues in Pharmaceutical Technology for all their help. Especially, I would like to thank Markus Schmidberger for the German translation of the summary section in the thesis. Thanks to Klaus Weyhing for his kind introduction and reparation of lab instruments as well as teaching me "Schwäbisch". I would like to thank my Erasmus master student, Luis Quintairos, for his work in fluorescent staining.

I would also like to thank my thesis committee for their time and patience.

Finally, I owe inexpressible gratitude to my parents and my brother for all the love and support. Special thanks to my boyfriend Zhihua Huang for always being there with me in all ups and downs.

I would like to dedicate this dissertation to my parents,

Da Zhang and Yuanping Wang

谨以此论文，献给我的父母

张达 王元萍

Table of contents

Abbreviations

%	Percent
°C	Celsius Degree
µm	Micrometre
ANOVA	Analysis of variance
BC	Basic cream
CA-SCS	Cetearyl alcohol (and) sodium cetearyl sulfate
C-C	Carbon-carbon bond
CCD	Charge Coupled Device
CER	Ceramide
CHOL	Cholesterol
cm	Centimetre
CRM	Confocal Raman microspectroscopy
CSA	Cetylstearyl alcohol
CV	Coefficient of variation
DSC	Differential scanning calorimetry
EI	Erythema index
FFA	Free fatty acids
FTIR	Fourier-transform infrared
g	Gram
g/ml	Gram per milliliter
GC	Gas chromatography
GM	Geometric mean
GMS	Glycerol monostearate
h	Hour
HLB	Hydrophile-lipophile balance
HPMC	Hydroxypropyl methyl cellulose
HPTLC	High performance thin layer chromatography
L-BC	Physiological lipids incorporated in basic cream
LC	Liquid chromatography
L-NiC	Physiological lipids incorporated in non-ionic cream
LPP	Long periodicity phase
MCT	Medium-chain triglyceride

mg	Miligram
min	Minute
ml	Milliliter
MS	Mass spectrometry
n.s.	No significance
NiC	Non-ionic cream
NMR	Nuclear magnetic resonance
PEG-20-GMS	PEG-20-glycerol monostearate
pH	Negative log of activity of hydrogen ions
PS 60	Polysorbate 60
SC	Stratum corneum
SCM	Stratum corneum moisturization
SLS	Sodium lauryl sulfate
SNK	Student-Newman-Keuls test
SPP	Short periodicity phase
TEWL	Transepidermal water loss
v/v	Volume percent

Summary

Most chronic skin diseases are accompanied by a deficient skin barrier function and basic therapeutics are used to treat this. Formulations which are used for the maintenance therapy may contain emulsifiers and they are suspected to withdraw lipids from skin. This would worsen the conditions of diseased skin. Therefore, the aims of this PhD thesis are: (1) to analyze the capability of emulsifiers and formulations (that contain these emulsifiers) to extract lipids from the skin, (2) to investigate the lipid conformational changes after the treatment of emulsifiers and formulations and (3) to develop new formulations which do not withdraw lipids from the skin but rather to deliver them into it. This would substantially improve the skin conditions and the patients' well-being.

The present PhD thesis is generally divided into three parts: in the first and second parts, non-destructive and non-invasive confocal Raman microspectroscopy (CRM) was firstly employed to characterize lipid componential and conformational changes after emulsifiers and formulations treatment. Various emulsifiers showed distinct potencies to extract lipids and cause disordered lipid ordering, whereas investigated formulations did not lead to lipid reduction, but rather altered lipid conformation at different extent. Correlation between conventional methods and CRM was discussed. Based on the results in this study, CRM has the potential to be a standardized analytical method for skin lipids characterization with easy sample preparation and immediate analytical readout.

In the third section, skin repair formulations, which aim at delivering physiological lipids into the skin to repair defective barrier function, were developed. Application of the creams led to substantially increased lipid levels in the lipid-deficient skin in *ex vivo* study. Twice-a-day application of skin repair creams provided a reinforcement of the skin barrier as transepidermal water loss (TEWL) was significantly decreased. As they are based upon monographed creams, they can be prepared in pharmacies and have a potential to be used as cream bases for individualised pharmacotherapy. This would be of interest to develop formulations for patients suffering from chronic skin problems, especially those that are characterized by impaired barrier function.

Zusammenfassung

Die meisten chronischen Hauterkrankungen werden von einer mangelhaften Hautbarrierefunktion begleitet und werden oft mit Basistherapeutika behandelt. Formulierungen, die in der Basistherapie eingesetzt werden, können Emulgatoren enthalten und stehen im Verdacht, Lipide aus der Haut zu extrahieren. Dies würde den Zustand erkrankter Haut verschlechtern. Das Ziel dieser Arbeit ist, (1) die Fähigkeit von Emulgatoren (und Formulierungen, die diese Emulgatoren enthalten), Lipide aus der Haut zu extrahieren, (2) die Lipid-Konformationsänderungen nach der Behandlung mit Emulgatoren und Formulierungen zu untersuchen und (3) neue Formulierungen zu entwickeln, die Lipide nicht aus der Haut herauslösen, sondern sie vielmehr in diese abgeben. Dies würde den Hautzustand und somit das Wohlbefinden der Patienten wesentlich verbessern.

Im ersten und zweiten Teil dieses Projekts wurde zunächst die zerstörungsfreie und nicht-invasive konfokale Raman-Mikrospektroskopie (CRM) zur Charakterisierung von Lipidkompositions- und Konformationsänderungen nach der Emulgator- und Formulierungsbehandlung untersucht. Die eingesetzten Emulgatoren unterscheiden sich im Extraktionsvermögen und ihrem Einfluss auf die Lipidordnung. Wohingegen die getesteten Formulierungen nicht zu einer Lipidreduktion führen, sondern zu einer veränderten Lipidkonformation. Im Vergleich zu etablierten Methoden hat sich die CRM als eine zuverlässige und effektive Alternative zur Quantifizierung von Hautlipiden und zur Beschreibung von Strukturveränderungen der Lipide bewährt. Durch einfache Probenvorbereitung und schnelle Dateninterpretation ist die CRM als standardisierte analytische Methode zur Charakterisierung der Hautlipide geeignet.

Im dritten Abschnitt wurden Formulierungen entwickelt, die darauf abzielen, physiologische Lipide in die Haut zu bringen, um die defekte Barrierefunktion zu reparieren. Die hergestellten Formulierungen zeigen eine homogene Textur. Die Anwendung der Cremes führt in der Lipid-defizienten Haut im Vergleich zur Kontrolle in ex-vivo-Studien zu wesentlich erhöhten Lipidkonzentrationen. Die zweimal tägliche Applikation der entwickelten Cremes sorgt für eine Stärkung der Hautbarriere, wodurch der transepidermale Wasserverlust (TEWL) signifikant verringert wird. Da sie auf monographierten Grundlagen basieren, können sie in Apotheken hergestellt werden. Zusätzlich haben sie auch das Potenzial, als Basis für eine individualisierte

Pharmakotherapie eingesetzt zu werden. Dies ist von Interesse, um Formulierungen für Patienten zu entwickeln, die an chronischen Hautproblemen leiden; insbesondere solche, die durch eine beeinträchtigte Barrierefunktion gekennzeichnet sind.

List of publications

The work presented in the thesis has been published in international peer-reviewed journals. Three research papers were published in fulfilment of the requirement of this cumulative thesis.

Accepted papers

Publication 1

Ziwei Zhang and Dominique Lunter, Confocal Raman microspectroscopy as an alternative method to investigate the extraction of lipids from stratum corneum by emulsifiers and formulations. European Journal of Pharmaceutics and Biopharmaceutics. 127:61-71 (2018). doi: 10.1016/j.ejpb.2018.02.006

Publication 2

Ziwei Zhang and Dominique Lunter, Confocal Raman microspectroscopy as an alternative to differential scanning calorimetry to detect the impact of emulsifiers and formulations on stratum corneum lipid conformation. European Journal of Pharmaceutical Sciences. 121:1-8 (2018). doi: 10.1016/j.ejps.2018.05.013

Publication 3

Ziwei Zhang, Milica Lukic, Snezana Savic and Dominique Lunter, Reinforcement of barrier function – skin repair formulations to deliver physiological lipids into skin. International Journal of Cosmetic Science. 40:494-501 (2018). doi: 10.1111/ics.12491

Personal contribution

Publication 1

Confocal Raman microspectroscopy as an alternative method to investigate the extraction of lipids from stratum corneum by emulsifiers and formulations.
Ziwei Zhang and Dominique Lunter *
European Journal of Pharmaceutics and Biopharmaceutics.
Volume 127, 8 February 2018, Pages 61-71.
DOI: 10.1016/j.ejpb.2018.02.006

Idea: Dominique Lunter and Ziwei Zhang
Study design: Ziwei Zhang and Dominique Lunter
Experiment: Ziwei Zhang
Evaluation: Ziwei Zhang and Dominique Lunter
Manuscript: Ziwei Zhang and Dominique Lunter

Publication 2

Confocal Raman microspectroscopy as an alternative to differential scanning calorimetry to detect the impact of emulsifiers and formulations on stratum corneum lipid conformation.
Ziwei Zhang and Dominique Lunter *
European Journal of Pharmaceutical Sciences.
Volume 121, 30 August 2018, Pages 1-8.
DOI: 10.1016/j.ejps.2018.05.013

Idea: Dominique Lunter and Ziwei Zhang
Study design: Ziwei Zhang and Dominique Lunter
Experiment: Ziwei Zhang
Evaluation: Ziwei Zhang and Dominique Lunter
Manuscript: Ziwei Zhang and Dominique Lunter

Publication 3

Reinforcement of barrier function – skin repair formulations to deliver physiological lipids into skin.

Ziwei Zhang, Milica Lukic, Snezana Savic and Dominique Lunter *

International Journal of Cosmetic Science.
Volume 40, 1 September 2018, Pages 494-501.
DOI: 10.1111/ics.12491

Idea: Dominique Lunter and Ziwei Zhang
Study design: Ziwei Zhang, Milica Lukic, Snezana Savic and Dominique Lunter
Experiment: Ziwei Zhang and Milica Lukic
Evaluation: Ziwei Zhang, Milica Lukic and Dominique Lunter
Manuscript: Ziwei Zhang, Dominique Lunter and Milica Lukic

EBERHARD KARLS
UNIVERSITÄT
TÜBINGEN

Mathematisch-Naturwissenschaftliche Fakultät

Erklärung nach § 5 Abs. 2 Nr. 8 der Promotionsordnung der Math.-Nat. Fakultät
-Anteil an gemeinschaftlichen Veröffentlichungen-
Nur bei kumulativer Dissertation erforderlich!

Declaration according to § 5 Abs. 2 No. 8 of the PhD regulations of the Faculty of Science
-Collaborative Publications-
For Cumulative Theses Only!

Last Name, First Name: Zhang, Ziwei

List of Publications

1. Zhang, Z. and Lunter, D.J. Confocal Raman microspectroscopy as an alternative method to investigate the extraction of lipids from stratum corneum by emulsifiers and formulations. Eur J Pharm Biopharm. 127:61-71 (2018).
2. Zhang, Z. and Lunter, D.J. Confocal Raman microspectroscopy as an alternative to differential scanning calorimetry to detect the impact of emulsifiers and formulations on stratum corneum lipid conformation. Eur J Pharm Sci. 121:1-8 (2018).
3. Zhang, Z., Lukic, M., Savic, S. and Lunter, D. Reinforcement of barrier function – skin repair formulations to deliver physiological lipids into skin. Int J Cosmet Sci. 40: 494-501 (2018).

Nr.	**Accepted publication yes/no**	**List of authors**	Position of candidate in list of authors	Scientific ideas by the candidate (%)	Data generation by the candidate (%)	Analysis and Interpretation by the candidate (%)	Paper writing done by the candidate (%)
			Optionally, you can also declare the above-stated categories in a written statement on a separate sheet of paper.				
1	Yes	2	1	50%	100%	75%	75%
2	Yes	2	1	50%	100%	75%	75%
3	Yes	4	1	50%	90%	70%	70%

I confirm that the above-stated is correct.

_____

Date, Signature of the candidate

I/We certify that the above-stated is correct.

_____

Date, Signature of the doctoral committee or at least of one of the supervisors

List of oral and poster presentations

Oral and poster presentations in academic conferences during the period of this thesis are separately listed.

Oral presentation 1

Ziwei Zhang and Dominique Lunter, Confocal Raman microspectroscopy as an alternative to differential scanning calorimetry to detect the impact of emulsifiers and formulations on stratum corneum lipid conformation. Skin forum, Jun. 20-21, 2018, Tallinn. *The best oral presentation prize.*

Oral presentation 2

Ziwei Zhang and Dominique Lunter, Confocal Raman microspectroscopy as an alternative to differential scanning calorimetry to detect the impact of emulsifiers and formulations on stratum corneum lipid conformation. 30th International Federation of Societies of Cosmetic Chemists (IFSCC) Congress, Oct. 18-22, 2018, Munich.

Poster presentation 1

Ziwei Zhang and Dominique Lunter, Confocal Raman microspectroscopy as an alternative to differential scanning calorimetry to detect the impact of emulsifiers and formulations on stratum corneum lipid conformation. Skin forum, Jun. 20-21, 2018, Tallinn.

Poster presentation 2

Ziwei Zhang and Dominique Lunter, Influence of surfactants and formulations on stratum corneum lipids. Deutsche Pharmazeutische Gesellschaft (DPhG) Annual Meeting, Oct. 4-7, 2016, Munich.

1. Introduction

1.1 Background

As the major interface between internal tissues and the external environment, skin plays an important role in protecting the human body. The main barrier function of the skin is located in stratum corneum (SC), which is the outermost layer of the skin. Two essential functions of the SC are to prevent excessive water loss from human body and to serve as the first line against exterior influences (e.g. chemical, physical and microbiological invasion). As the only continuous domain in SC, intercellular lipids are of great importance for a competent cutaneous barrier function. However, the depletion or disturbance of the major lipids in SC (which can be caused by chemicals such as emulsifiers) is thought to be one of the etiological factors to produce dryness and barrier disruption in skin conditions [1-3]. Over the last three decades, a number of findings have proved that many skin diseases such as atopic dermatitis, psoriasis and lamellar ichthyosis are associated with impaired barrier function, which are mainly caused by abnormalities in epidermal lipids in patients, especially a marked depletion of SC lipids. A brief summary of common skin diseases with associated alteration in the SC lipids as well as the pathogenetic changes are shown in Table 1. Basic therapy is normally used to treat these skin diseases in clinical practise. However, many formulations used in basic therapy contain emulsifiers, which are suspected to extract endogenous lipids from skin. This would further aggravate the compromised skin conditions. A loss of lipid content contributes to deficient lipid integrity between corneocytes, leading to an impaired skin barrier. As a result, this may allow the entrance of potentially harmful substances, chemicals and microbes, which can inflame and irritate the skin. In return, this inflammation may further worsen the skin barrier function, closing the vicious circle [4].

Based on the abovementioned facts, we can see that, on one hand, examination of skin lipid properties is of great importance in the diagnosis of skin diseases as well as in heathy skin screening. Such lipid characterisation should include two aspects: lipid composition and conformation. On the other hand, it is essentially vital to develop novel formulations which do not withdraw lipids but rather to replenish the lipid amount in SC, aiming at recovering the skin barrier function along with the treatment of dermatologic diseases.

Table 1 *Overview of common skin diseases and alterations in lipid properties.*

No.	Skin diseases	Changes in lipid composition	Changes in lipid conformation	Effects on the skin barrier function	Pathogenesis	References
1	Atopic dermatitis	Decreased levels of total CER [NP], CER [EOS], bound ω-hydroxyceramides and long-chain FFAs (C20-26) including cis-6-hexadecenoic acid, increased levels of CER [AS], bound FFA and CHOL	Altered LPP, short SPP and reduced orthorhombicity	Significant increase in TEWL, higher permeability, reduction in skin hydration (dry skin)	Upregulation of sphingomyelin deacylase and glucosylceramide deacylase, impaired conversion of linoleic acid to γ-linoleic acid, increased level of ceramidase, decreased level of prosaposin	[5-17]
2	Psoriasis	Decreased level of total CER, especially with a phytosphingosine base, concurrent increases in CER with a sphingosine base, no change in FFA level	Altered LPP and short SPP	Progressive increase in TEWL	Decreased expression of serine palmitoyltransferase and prosaposin	[5, 6, 18, 19]
3	Lamellar ichthyosis	Decreased levels of acyl CER (especially CER [EOS]) and FFA	Altered LPP, short SPP and reduced orthorhombicity	Disruption of skin barrier function	A congenital recessive skin disorder caused by mutation of ‘transglutaminase’ gene 1	[20-22]
4	Netherton syndrome	Decreased CER [EOS], [EOP], [EOH], [EOdS] and [NP]	Altered LPP, short SPP and reduced orthorhombicity	Severe skin barrier defects	Autosomal recessive disorder due to mutations of both copies of the SPINK5 gene (localized to band 5q31-32)	[23]

No.	Skin diseases	Changes in lipid composition	Changes in lipid conformation	Effects on the skin barrier function	Pathogenesis	References
5	Type 2 Gaucher disease	Increased level of glucosylceramide to CER ratio	Altered lipid organization	Ichthyosiform skin	The level of glucocerebrosidase is significantly reduced, and thus the conversion of glucosylceramides to corresponding CERs decreased	[24-26]
6	Sjögren-Larsson syndrome	Decreased levels of CER [EOS], CER [NP] and CER [AP], increased levels of FFA and membrane-bound CERs	Altered lipid organization	TEWL not affected; hyperkeratosis may compensate the barrier dysfunction	An inborn error of lipid metabolism caused by deficient activity of fatty alcohol - NAD oxidoreductase	[27-29]
7	Essential FFA deficiency	Reduced ratio of CER [EOS] linoleate to CER [EOS] oleate	Altered lipid structure	Epidermal hyperproliferation	Replacement of linoleic acid with oleic acid	[1, 16]
8	X-linked ichthyosis	Decreased levels of total neutral lipids and free sterols; no change in sterol esters or total sterols	Altered lipid organization	Disruption of normal skin barrier function	Deficiency in steroid sulfatase	[30]
9	Bullous ichthyosiform erythroderma	Decreased level of total CER	Altered lipid organization	Disruption of normal skin barrier function	Abnormality of keratins 1 and 10	[28, 31]
10	Aged dry skin	Decreased lipid levels	Disturbance of SC lamellar structure	Compromised skin barrier	Elevated ceramidase activity	[32]

In order to characterize the changes in skin lipid composition and conformation, reliable and efficient analytical methods are well in need. Traditional lipid quantification methods include gas chromatography (GC), liquid chromatography (LC), mass spectrometry (MS), high-performance thin-layer chromatography (HPTLC) and most commonly a combination of at least two of them. However, by means of all these conventional methods, samples undergo different levels of preliminary treatment before the actual analysis. This might lead to the risks of loss, contamination or even chemical alteration of analytes. Besides, the whole analytical process, sample preparation in particular, is time-consuming. On the other hand, to explore the lipid arrangement in SC, a number of studies have been carried out by means of various methods, including but not limited to electron microscopy [33], small angle and wide angle X-ray scattering [34, 35], NMR spectroscopy [36], Fourier transform infrared (FTIR) spectroscopy [37] as well as differential scanning calorimetry (DSC) [38]. Thanks to these technologies, more comprehensive knowledge on the sophisticated lipid structure is obtained. Nevertheless, these methods can only provide information on intercellular lipid organization, but are not capable of analysing lipid content. Moreover, for example, in DSC study, samples are normally destroyed after the measurement and cannot be analysed by other instruments. All of the facts mentioned above encourage to look for a new way to investigate the lipid composition and to describe the lipid structural arrangement between corneocytes. Therefore, a reliable, non-destructive and time-efficient method, which can provide information on both lipid composition and conformation, is of exceptional interest. The solution that is proposed in this PhD thesis is confocal Raman microspectroscopy.

As shown in Table 1, a decreased level of SC lipids is shown in many skin diseases which are accompanied with impaired barrier function. Therefore, therapeutic strategies should be employed to repair the barrier function along the treatment of skin diseases, even if barrier impairment is not causative for them. Topical preparations are generally recommended as a key and basic step in treating chronic skin diseases [39, 40]. The traditional approach is the “outside-in” approach [41], in which non-physiological lipids of high concentrations are primarily applied onto the skin in order to enhance barrier function, such as petrolatum [42, 43]. These products normally show a lower compliance among patients, since they are not easy to spread and leave an oily feeling on skin. Furthermore, even though they effectively reduce water loss in

a short time, they are not essentially able to repair the lipid deficiency [44]. Hence, another therapeutic concept has gained great popularity - to restore the lipid content in SC. In this PhD thesis, a skin repair formulation is developed, aiming at direct replenishment of the missing lipids and thus to improve the skin barrier.

To conclude, the task of the current PhD project is therefore to probe the skin lipid properties in terms of concentration and conformation by means of confocal Raman microspectroscopy. This is done in order to evaluate CRM as a reliable technique for SC lipid analysis, as well as to understand the correlations between lipid composition, lipid organization and skin barrier function. Another task is to develop new formulations to reinstate the homeostasis of skin lipids in order to bring back the normal skin conditions.

1.2 General basics

1.2.1 Current knowledge on stratum corneum lipids

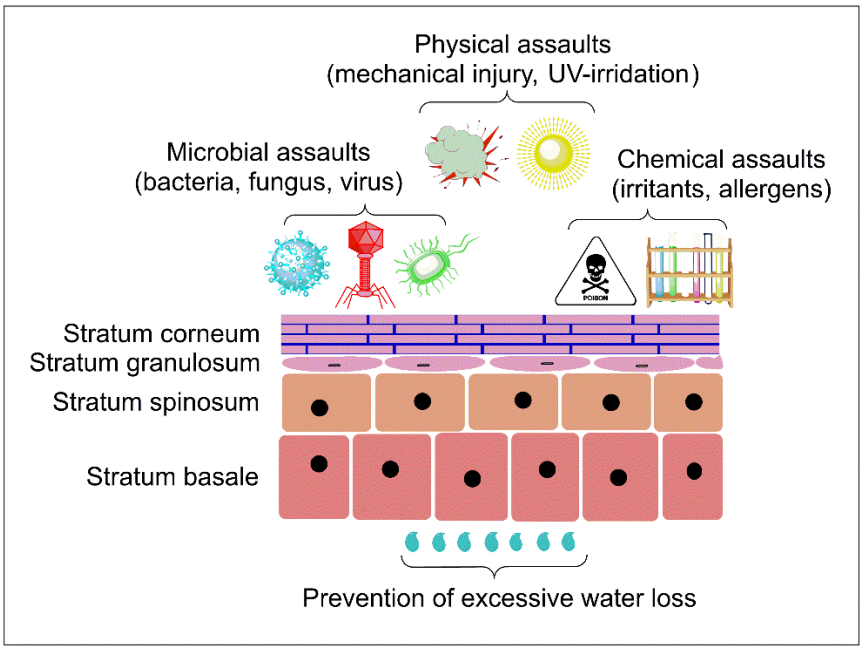

Figure 1 *Schematic drawing of skin structure and skin barrier function*

Epidermis is the outmost layer in skin and comprises four different layers. These layers include superficial stratum corneum (SC), stratum granulosum (SG), stratum spinosum (SS) as well as the innermost stratum basale (SB) layer (Figure 1). Firstly

in the 1940s, it was postulated that the superficial layer of SC, is responsible for the skin barrier function [45]. Typically, SC is 10-20 µm thick. However, its thickness can vary greatly depending on the body site, age, gender and race. SC consists of 10-15 layers of keratin-enriched corneocytes and intercellular lipids. The flattened corneocytes are oriented approximately parallel to the skin surface, surrounded by crystalline intercellular lipid domains. SC structure typically is described as the biphasic “mortar and bricks” model, in which mortar is a mixture of lipids and glues corneocytes together [46].

The lipid matrix consists of a heterogeneous mixture of cholesterol, long-chain ceramides and free fatty acids in a molar ratio of approximately 1:1:1 [47]. Experiments have demonstrated the intercellular lipids are highly arranged in lamellar phases oriented approximately parallel to the surface of corneocytes. Such complex composition and peculiar organization constitute the molecular structure of lipid domains and provides remarkable physical protection properties. However, undesired factors, such as emulsifiers-induced lipid extraction or conformational changes, may lead to an impaired skin barrier function, which can cause further skin problems. In our previous research, it was found that various emulsifiers extracted intercellular lipids from SC at different extent and thus led to disruptive skin integrity [48]. Hence, skin lipid analysis is of paramount importance in dermatological diagnosis and disease treatment.

On the other hand, the barrier function of the SC is also directly related to the conformational order of lipids in this layer [49]. The structure of the SC lipids resembles a multiple lamellar structure. At physiological temperature, the lipid matrix is shown in a typical all-*trans* conformational packing, where lipids are highly organized in ordered orthorhombic state [50, 51]. However, lipid structural changes can take place upon certain stimulations, which could dramatically influence the condition of the skin. Once the intercellular lipids change to more *gauche*-conformation (more disordered state), a compromised skin barrier is presented. Many skin diseases, e.g. lamellar ichthyosis, psoriasis and atopic dermatitis are associated with structural changes in the lipid matrix (Table 1). Therefore, analyses of the structural state of the cutaneous lipids are of great importance.

1.2.2 Confocal Raman microspectroscopy

When a beam of light is incident on a sample, most of the light is scattered by the sample in a way that the scattered light has the same wavelength as the incident light, this phenomenon is called Rayleigh scattering or elastic scattering. However, there is a small fraction of photons, which interacts with the molecules of the sample. As a result, the back scattered light has a different energy compared to the incident photons. This phenomenon is known as Raman scattering or inelastic scattering, which was first observed by C.V. Raman in 1928 [52]. These effects are explained schematically in Figure 2. The shift in energy gives information about the vibrational modes in the system. Based on this, confocal Raman microscope was invented.

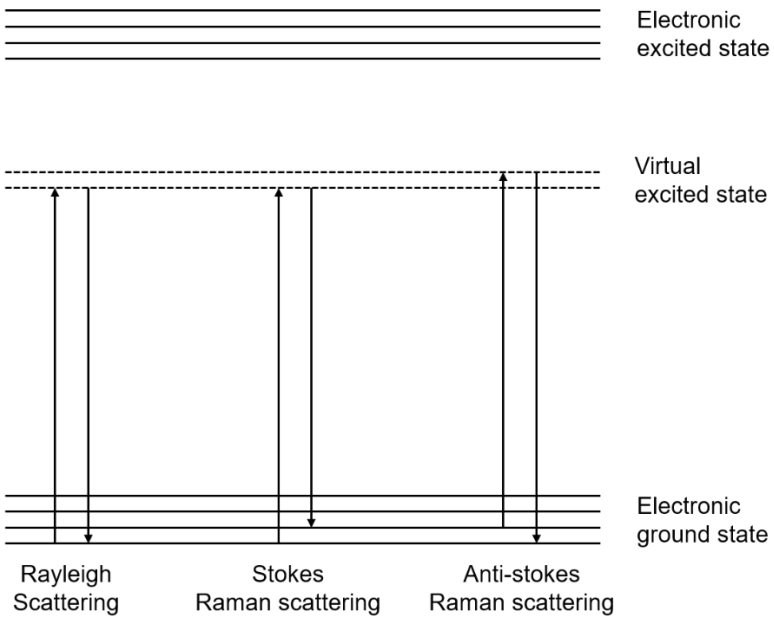

Figure 2 *Jablonski diagram representation of Rayleigh and Raman scattering*

Confocal Raman microspectroscopy (CRM), as a label-free, non-invasive and non-destructive analytical technique, is increasingly used in pharmaceutical field, especially in skin research to provide a structural fingerprint by which molecules can be identified. CRM instrument couples a Raman spectrometer to a standard optical microscope (see Figure 3). The principle of CRM is as follows: a laser beam is focused on the sample through a microscope objective. Backscattered light of the sample is then collected and collimated by the same objective and guided through a tiny pinhole. Thereafter, the scattered light is dispersed by the Raman spectrometer and finally

projected on a Charge Coupled Device (CCD) detector. This is essentially a large array of detectors that enables simultaneous recording of a complete Raman spectrum in a single exposure, since spontaneous Raman scattering is typically very weak.

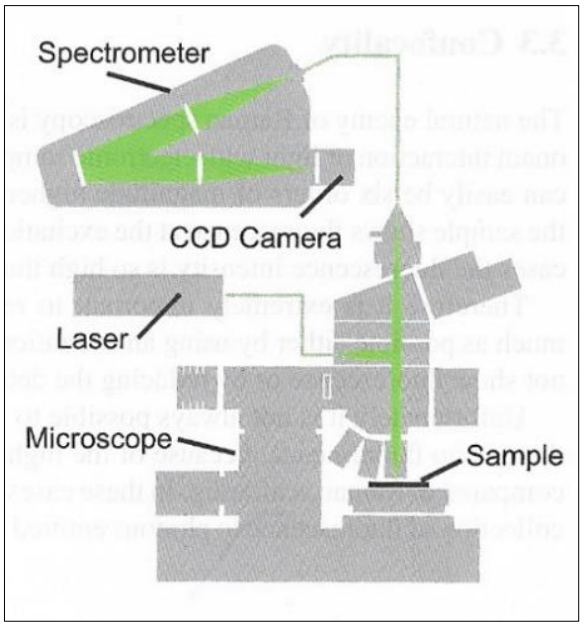

Figure 3 *Confocal Raman microspectroscopy setup used in this study [53]*

CRM can provide chemical information by peaks/bands at specific wavenumbers in the recorded Raman spectrum, without requiring dyes, stains, radioactive labels etc. Due to the linear dependency of Raman scattering on molecule amount, relative concentration of certain substances (such as SC lipids) can be determined by their contribution to the Raman bands. Thus, relative lipid concentration in SC can be measured. Furthermore, CRM is very sensitive to scattering by non-polar groups (e.g. C-C) [49]. It has a high potential for studying conformational changes in hydrocarbon backbones and is thereby applicable to the study of lipid conformational transitions. In addition, skin samples can be measured directly in 3 dimensions without complex pre-treatment. CRM measurement takes relatively short time (several seconds to minutes). Based on these advantages, CRM was firstly employed in this thesis to measure the skin lipid content as well as lipid structural arrangement at molecular level. Hence, changes in skin lipids can be comprehensively investigated in both aspects of composition and conformation by CRM.

1.2.3 Lipids replenishment therapy

When normal lipid bilayers are disturbed due to various external and internal factors, skin barrier is at a certain extent destroyed (Figure 4A), leading to skin dryness, pruritus, infection or inflammation. In some circumstances, if the barrier function of the skin is mildly compromised, a repair sequence is rapidly initiated with an increased synthesis of all the SC lipids to reinstate homeostasis [54-56]. However, in most diseased conditions, the rate of lipid synthesis is disrupted and rapid replenishment of the depleted SC lipids might not be possible. Therefore, through intervening the lipid synthesis procedure, lipid content between corneocytes is recovered. This can be achieved by incorporating physiological lipids in therapeutic formulations and transporting them into skin, which triggers the intrinsic pathways in the epidermis to promote the production of intercellular lipids in SC (Figure 4B). As this approach essentially addresses the issue of lipid deficiency, it is thus termed as “inside-out” method. Compared with traditional methods, which occlude the skin surface to reduce TEWL, this skin repair formulation leads to an increase in the total lipid amount for a longer period and thereby is considered more effective in restoring impaired skin barrier function.

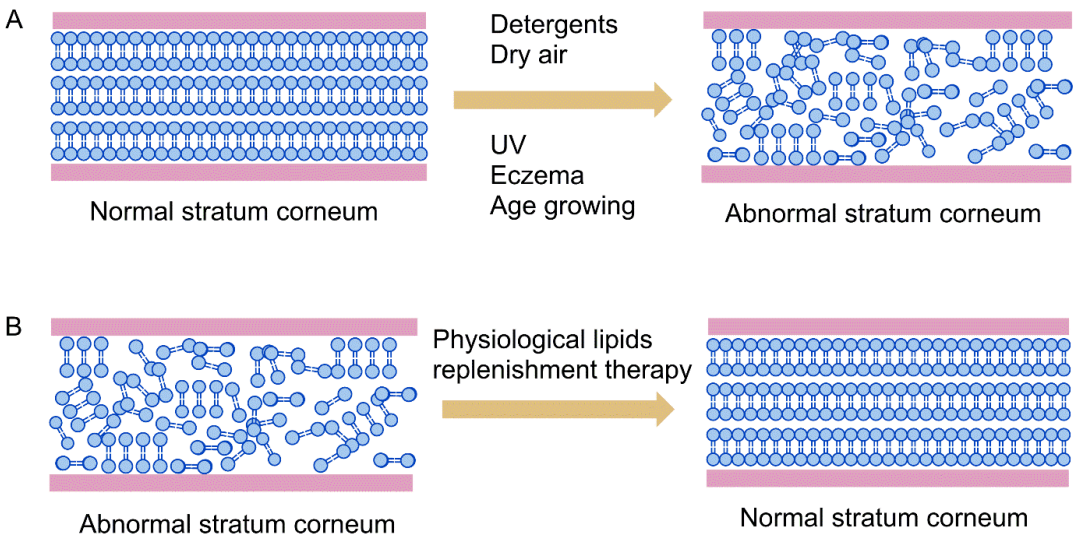

Figure 4 *Schematic of disordered stratum corneum lipids and the lipids replenishment therapy:* ▪ *corneocytes layers and* ■ *lipid region.*

2. Objectives

The objective of the PhD thesis is, first of all, to characterize the SC lipid changes after the treatment with different emulsifiers and formulations. To this end, SC lipid composition and SC thickness were analysed by CRM and traditional methods, including high-performance thin-layer chromatography (HPTLC), fluorescent staining as well as histology study. Correlation between these methods was established to evaluate CRM as a reliable alternative to conventional methods in the measurement of lipid content and SC thickness. Secondly, the influence of emulsifiers and formulations on the lipid conformation was investigated by CRM. Results of CRM were correlated to those of a classical method of differential scanning calorimetry (DSC), assessing CRM as an effective technique to describe the intercellular lipid arrangement. Last but not least, since many chronic skin diseases are associated with reduced lipid content in SC, formulations which can deliver physiological lipids into skin and improve the impaired barrier function were developed, characterized and evaluated.

Following objectives should be elaborated in the framework of this thesis:

- Establishment of CRM methods to detect skin lipid content, conformation and SC thickness.
- Quantification of SC lipid extracts by means of HPTLC.
- Investigation of SC thermal behaviour by means of DSC.
- Histological study of skin after emulsifiers and formulations treatment.
- Correlation establishment between CRM and traditional lipid analytical methods.
- Formulation development, characterization (polarized light microscopy and rheology) and evaluation (stability, ex vivo and in vivo efficacy) of skin repair creams.

3. Results and discussion

3.1 Confocal Raman microspectroscopy as an alternative method to investigate lipid extraction from stratum corneum

The purpose of this study was to understand the effects of emulsifiers and formulations treatment on SC lipids. To this end, common methods, such as HPTLC and fluorescent staining techniques, were performed to evaluate the lipid componential changes. As an alternative, non-destructive CRM was firstly employed in the present study to assess such effects with easy sample preparation and immediate analytical readout in contrast to the aforementioned conventional methods.

3.1.1 Raman spectral variability and peak normalization

Skin constituents can be assessed by CRM. To counteract interindividual variability spectra need to be normalized to an internal standard. This is often done using the so-called “keratin peak” in the high wavenumber region (Figure 5). In this section, we evaluated several skin peaks in the fingerprint region for their suitability as the internal standard in order to omit spectra acquisition in the high wavenumber region. This would decrease the spectra acquisition time and would thus be advantageous to speed up the analysis.

The peaks of interest are: v (C-C)-mode at 1002-1014 cm^{-1}, the δ (CH_2, CH)-mode at 1294-1334 cm^{-1}, the δ (CH_2, CH_3)-mode at 1425-1495 cm^{-1} and the v (C=O) mode at 1630-1714 cm^{-1} (Figure 5). Spectra from three skin donors were used to assess the variability of the spectra of isolated SC. The peak areas under the curve are given in Table 2. Generally, the variability between different donors is higher than the variability within one donor. The peak areas were found not to differ significantly between samples from one donor but do differ significantly between samples from different donors (Kruskal-Wallis-test; $p<0.05$). Evaluating the standard deviation of the peaks, it becomes clear that the δ (CH_2, CH_3)-mode as well as the v (C=O)-mode give the lowest variability within samples from one donor as well as between samples from different donors. However, the δ (CH_2, CH_3)-mode at 1425-1495 cm^{-1} mainly arises from lipids and is often referred to as the lipid peak. Investigation on SC lipid content in this study is thus based on this peak. Therefore, v (C=O)-mode at 1630-1714 cm^{-1}, showing the least variation, is chosen as the normalization standard. Lipid peaks need

to be normalized to this peak prior to further comparison to counteract inter- and intra-individual variability.

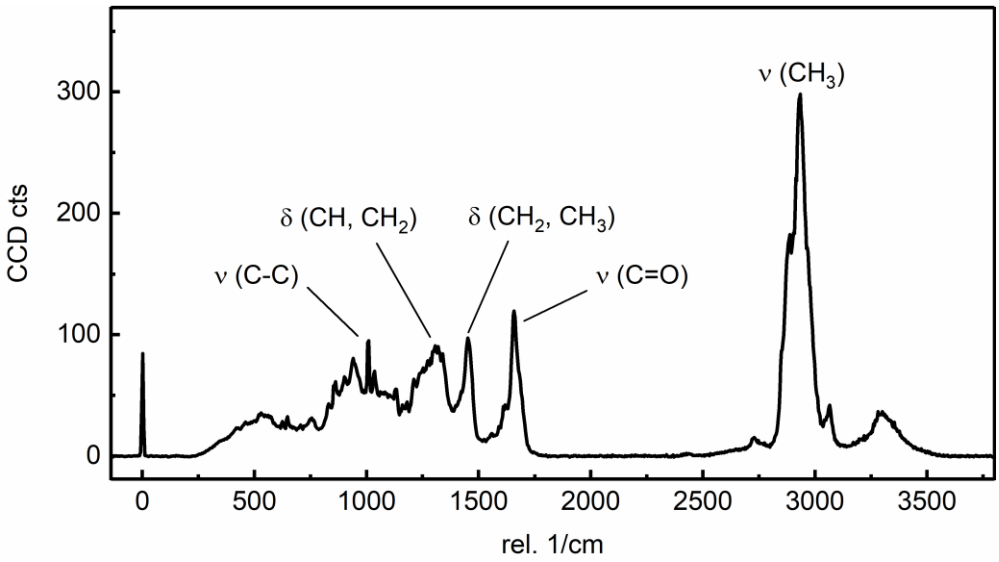

Figure 5 *A typical Raman spectrum of the porcine stratum corneum in the full region*

Table 2 *Peak areas of selected skin peaks [arbitrary units], nine measurements per donor, three donors.*

Peak vibration	Integrated wavenumber range (cm^{-1})	Intra-individual		Inter-individual	
		GM	CV [%]	GM	CV [%]
ν (C-C)	1002 - 1014	705.1	21.7	914.5	32.1
δ (CH, CH_2)	1294 - 1334	2585.0	19.4	3451.6	33.0
δ (CH_2, CH_3)	1425 - 1495	3918.5	16.3	5087.1	29.6
ν (C=O)	1630 - 1714	6118.2	18.5	7974.2	30.3

3.1.2 Lipid analysis by CRM

To investigate the impact of emulsifiers and formulations on SC lipids, four different formulations, including monographed basic cream [57], hydrophilic cream [58], non-ionic cream [58] and an HPMC stabilized emulsion including medium-chain triglyceride (MCT) [59] were used. Additionally, all emulsifiers which were incorporated in those formulations were tested in aqueous solution/dispersion in the respective

concentrations as present in the formulations. CRM and HPTLC were employed to analyse the changes in SC lipid concentration after treatment. Furthermore, lipid extraction was visualized by fluorescence staining and SC thickness was measured by histology and CRM. Correlation between CRM and HPTLC results was conducted. This was done to assess if CRM can be used as a reliable and beneficial method in the application of skin lipid analysis.

From CRM spectra of isolated SC sheets, normalized lipid signals were calculated by the following equation:

$$Normalized\ \delta(CH_2, CH_3) = \frac{AUC\ \delta(CH_2,CH_3)}{AUC\ \nu(C=O)} \qquad (1)$$

where AUC is the integrated area under specified peak in a single CRM spectrum.

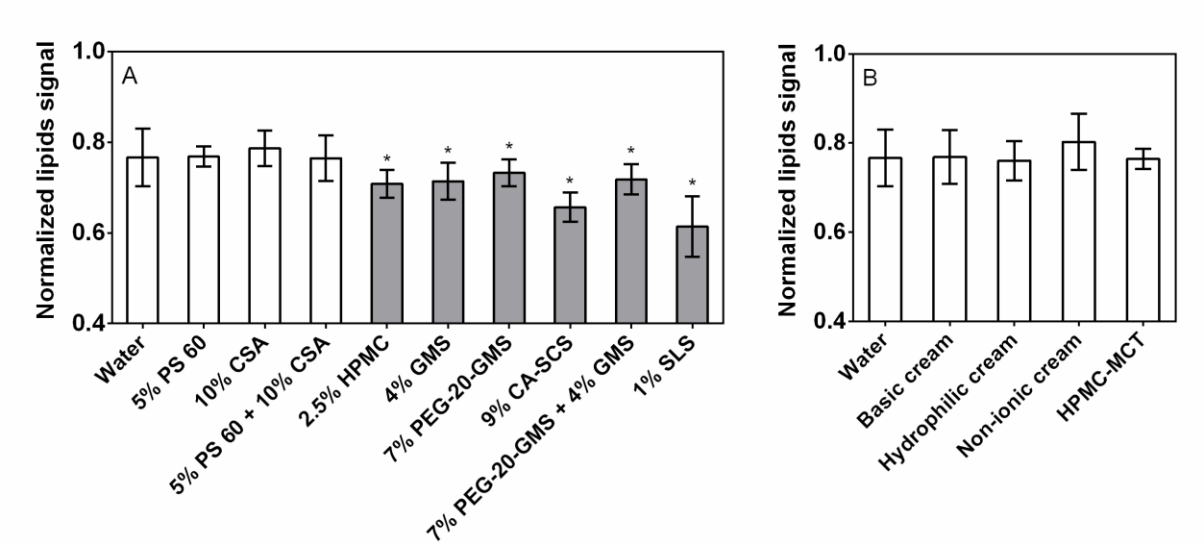

Figure 6 *Normalized stratum corneum lipid-signal at 1425 - 1495 cm^{-1} after treatment, A: emulsifiers treatment, B: formulations treatment, mean ± SD, n = 9, * significant difference (ANOVA, SNK; p < 0.05).*

As shown in Figure 6A, water treated SC presented a normalized lipid signal of 0.76. Compared to the water treated reference, PS 60, CSA and their mixture treated SC showed no significant changes, indicating they had no obvious effect on the intercellular lipid domains in SC. Whereas in other emulsifiers treated SC samples, significant decreases in lipid peaks could be seen. The lipid signal was reduced by GMS, PEG-20-GMS and their mixture as well as HPMC to a similar extent, from 5 to

8%. For ionic CA-SLS, a more pronounced reduction of 11% was found. SLS, as the positive control, led to the most substantial reduction by 25%. These results indicate a decrease of lipid content in the intercellular region of SC after treatment with various emulsifiers. According to Söderlind's group, lipid extraction from SC can be explained by the inherent solubility-enhancement of emulsifiers [60]. During the incubation period in Franz diffusion cells, surface-active emulsifiers, serving as solubilizer, improve the solubility of lipids in the donor compartment. In other words, they facilitate lipid extraction from SC. Therefore, it can be concluded that, various kinds of emulsifiers have different capabilities to extract lipids from the stratum corneum.

However, in contrast to the single emulsifiers, none of the tested formulations had any effect on lipid content of the SC although formulations contained emulsifiers in the same concentration as the emulsifier solutions (Figure 6B). This indicates that the emulsifiers are bound to the interfacial layers in the creams or emulsions. Interactions with the oil phase of the formulations are strong enough to saturate all binding sites and therefore emulsifiers cannot engage in the interactions with the SC lipids.

3.1.3 Lipid analysis by HPTLC

As a conventional skin lipids analytical method, HPTLC was implemented to verify the results of CRM. HPTLC results are given in Figure 7. Compared with the reference (water treated), all studied formulations, PS 60, CSA, as well as their mixture showed no obvious distinction in any extract levels, indicating no lipid extraction by any treatment. However, HPMC, GMS, PEG-20-GMS and their mixture presented differently decreased levels of lipids, values ranging from 5 % to 10 %. This trend is more obvious in CA-SLS treated SC. Besides, as a positive control, SLS treated SC exhibited the most substantial reduction of lipid extracts by 27%. These results demonstrated decreases in the remaining lipid content post incubation with various emulsifiers, implying lipid withdrawal during emulsifiers treatment in Franz cells. This conclusion is consistent with those of CRM analysis. Thus, from this point of view, CRM can be proven as a potential reliable and effective assessing method for lipid analysis in dermatology field.

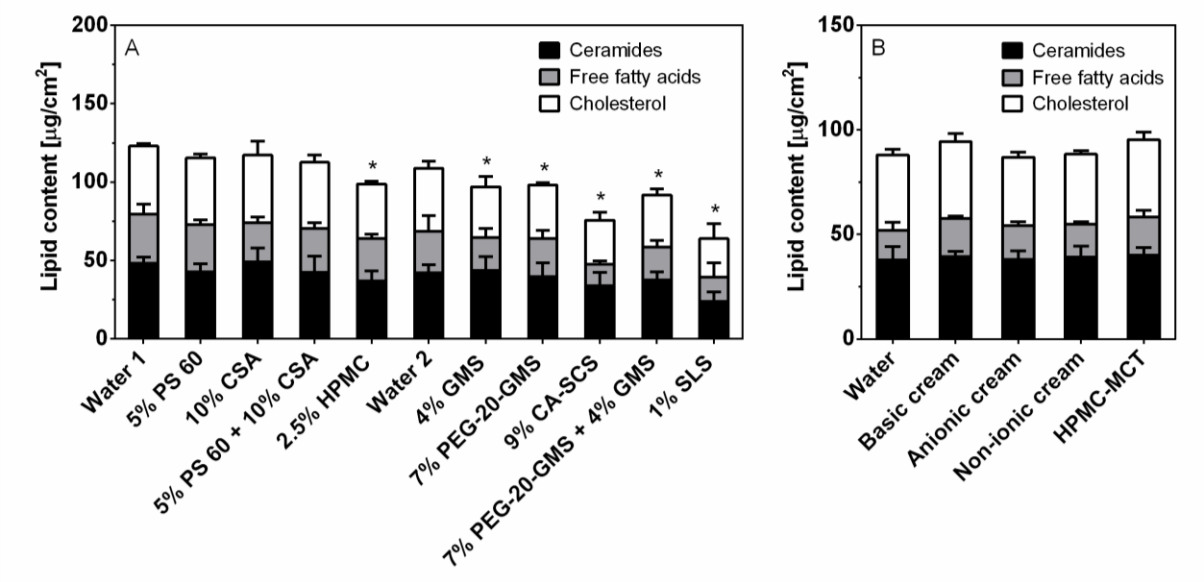

Figure 7 *Levels of major stratum corneum lipids, ceramides, free fatty acids and cholesterol following lipid extraction and high-performance thin-layer chromatography separation. A: emulsifiers treatment study, water 1 to HPMC are samples from one donor and water 2 to SLS are from another donor; B: formulations treatment, mean ± SD, n = 3, * significant difference (ANOVA, SNK; p < 0.05) [48].*

3.1.4 SC barrier disruption study

In order to additionally evaluate the barrier disruption of SC by emulsifiers and formulations treatment, a tissue staining technique with pyranine was conducted. This method was previously used to estimate in vivo subclinical injury caused by SLS [61]. SC with less barrier integrity is stained more intensely compared to normal SC, which is nowadays believed as pyranine binds to keratin filaments that are exposed to the dye since intercellular lipids are extracted [61]. In our study, SLS treated SC showed a markedly increased intensity in contrast to the reference, which complies with the reported literature [61]. Other investigated emulsifiers and formulations exhibited different extent of increased fluorescent intensity, indicating different abilities of lipid extraction and barrier impairment. Specifically, CA-SLS caused the most intense fluorescence, followed by GMS, PEG-20-GMS and their mixture as well as HPMC in a similar level. PS 60, CSA, their mixture as well as formulations showed no increases. These results are in accordance with those of HPTLC and CRM results and give

further proof of the assumption that CA-SLS, GMS, PEG-20-GMS and their mixture withdraw lipids from SC while other emulsifiers and formulations do not.

3.1.5 SC thickness measurement by CRM

Visual inspection of SC sheets after the treatment with different emulsifiers gave clear hints that some sheets were thinner compared to the reference. It thus appeared reasonable to raise the question whether the emulsifiers-induced lipid extraction also affected SC thickness. This hypothesis was assessed by CRM and histology study.

Figure 8 presents SC thickness after the treatment with water, emulsifiers and formulations. Water treated SC exhibited an average thickness of 6.5 ± 1.29 µm. The measured thickness here corresponds to dried SC thickness and is smaller compared to that of native SC [62]. This is due to that native SC contains a certain amount of water, and corneocytes are swollen and larger in volume. All formulations, PS 60, CSA and their mixture treated SC samples showed no obvious difference in contrast with the reference. Whereas, all the rest of the investigated emulsifiers showed significantly reduced thickness of SC: GMS, PEG-20-GMS and their mixture, as well as HPMC exhibited an average thickness of approximately 4 µm, respectively; SLS showed the trend to an even more pronounced reduction of SC thickness of 2.6 µm. It can therefore be said that SC barrier was evidently disrupted by various emulsifiers but not by formulations treatment.

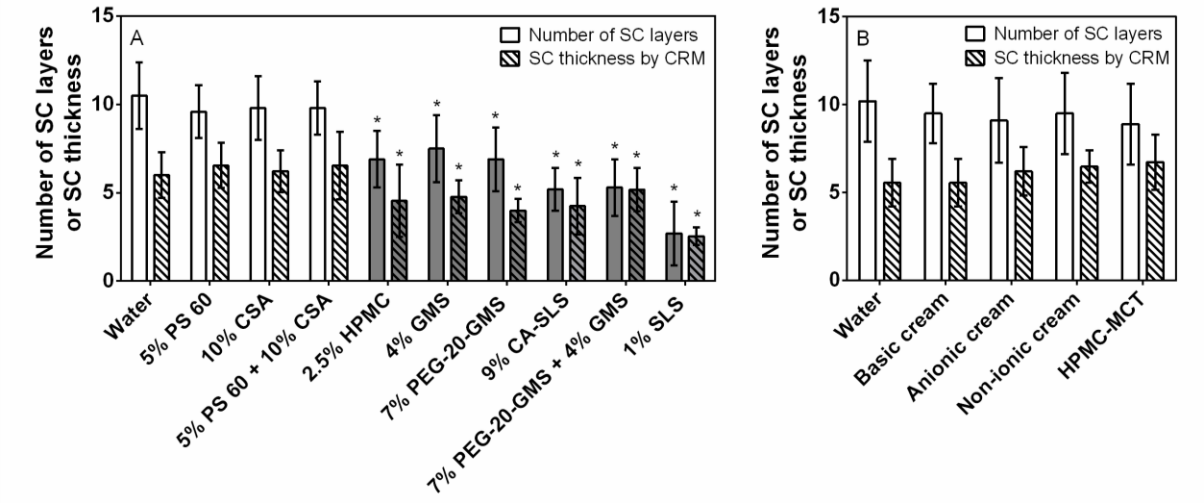

Figure 8 *Comparison of SC thickness and number of corneocytes layers after A: emulsifiers treatment and B: formulations treatment, mean ± SD, n = 3 or 9, * significant difference (ANOVA, SNK; p < 0.05).*

3.1.6 SC thickness estimation by histology

In order to visualize the physical state of SC layers after treatment, a histology study was performed. The histological features of safranin stained cross-sections of porcine skin after emulsifiers treatment were compared. As a reference control, tape-stripping exhibited a pronounced reduction of SC layers. Interestingly, a lower number of corneocytes layers were also observed after treatment with different emulsifiers. The comparison of the number of corneocytes layers after emulsifiers treatment is shown in Figure 8A. It can be seen that there were approximately 10 corneocytes layers in water treated skin, whereas after incubation with various emulsifiers, significant amount of corneocytes layers were removed. The results are thus in line with the findings of SC thickness measurement by CRM.

However, after formulations treatment, corneocytes layers are well maintained. Meanwhile, no significant reduction of lipid-signal after formulations treatment was found in CRM measurement. These results indicate that all investigated formulations do not have an influence on lipid and corneocytes amount.

3.1.7 Correlation between CRM and conventional methods

As the major aim of this study was to investigate the capability of CRM to evaluate the impact of emulsifiers and formulations treatment on SC lipids, SC lipid content and thickness were measured by CRM as well as HPTLC and histology study, respectively. To explore a correlation, the results from CRM were plotted against those from conventional methods (Figure 9 and 10).

CRM led to similar results as the conventional methods. From the correlation plots, it can clearly be seen that there is a strong positive correlation between CRM and conventional methods both for lipids content and SC thickness measurements. This further proves the excellent correlation and shows that CRM can be used as an alternative technique to measure lipid content and SC thickness. Its ease of handling with no sample preparation, extraction or staining needed and short measurement time make it a versatile tool for SC investigation. Nevertheless, if a more detailed analysis of SC lipids (e. g. separate analysis of ceramides, cholesterol or free fatty acids) is aimed for, HPTLC remains the preferable method. For more detailed analyses still more sophisticated methods are required.

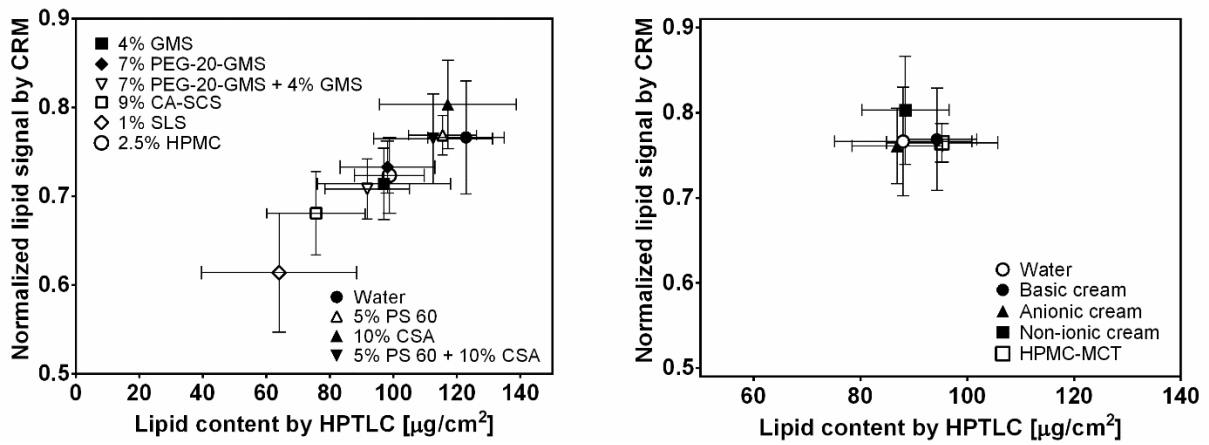

Figure 9 *Correlation plot of SC lipids content measured by CRM (y-axis) and HPTLC (pooled ceramides, cholesterol and free fatty acids content; x-axis); left: after emulsifiers treatment, right: after formulations treatment [48].*

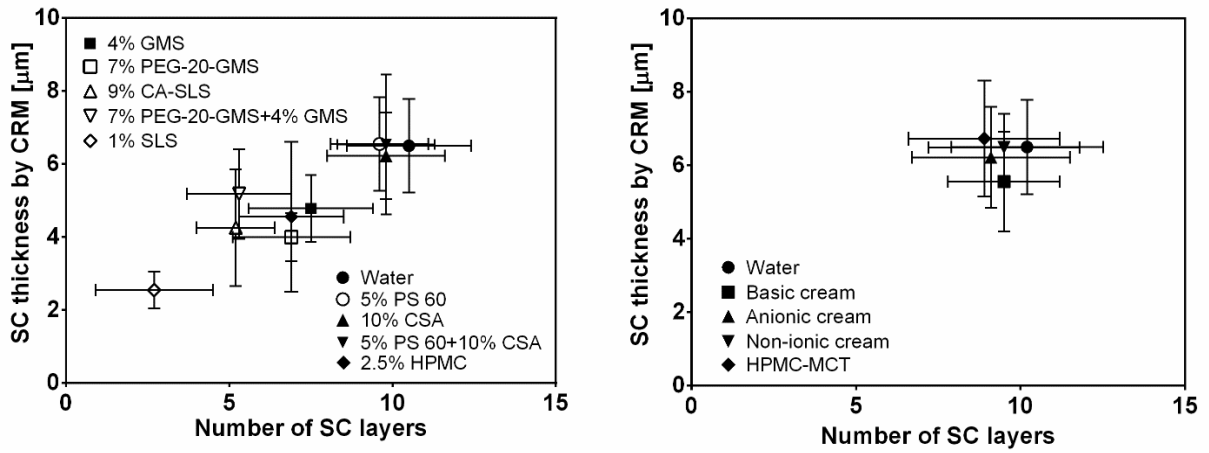

Figure 10 *Correlation plot of SC thickness measured by CRM (y-axis) and histology study with safranin staining; left: after emulsifiers treatment, right: after formulations treatment [48].*

3.1.8 Summary

The first section of the PhD thesis describes CRM as an alternative method to investigate the impact of emulsifiers and formulations on intercellular lipids of SC. CRM and HPTLC were used to analyse the changes in SC lipid content after treatment. Furthermore, lipid extraction was visualized by fluorescence staining and SC thickness was measured by CRM and histology. Various emulsifiers and emulsifier mixtures

showed different impact on SC lipid content and SC thickness. Among all studied emulsifiers CA-SLS showed the strongest lipids extraction ability, followed by GMS and PEG-20-GMS as well as their mixture. Unexpectedly, PS 60 dispersion did not extract SC lipids whereas polymeric HPMC significantly did. Emulsifiers that reduced the lipids content also reduced SC thickness, indicating lipid extraction is the reason for SC thinning. In comparison, none of the tested formulations had any effect on SC lipids. Results from CRM and conventional methods showed a strong positive correlation for both lipid content and SC thickness determination. It can therefore be deduced that with easy sample preparation and fast analytical readout, CRM has the potential to be a standardized analytical method for skin lipids investigation. It can drastically reduce analysation time and give more precise results as the risk of introducing bias is minimized due to the minimal sample pre-processing.

3.2 Confocal Raman microspectroscopy as an alternative to differential scanning calorimetry to detect stratum corneum lipid conformation

In order to further study the influence of emulsifiers and formulations on SC lipid domains, the research focus switches onto the evaluation of lipid organization changes. CRM results were proven in the previous set of experiments to be consistent with those of HPTLC and histological study with better reproducibility and lower data variability [48]. Therefore, in the second section of this PhD thesis, CRM was firstly employed to investigate the lipid conformational changes in contrast to conventional methods (DSC). Correlation between CRM and DSC was explored to evaluate the reliability and efficiency of CRM. To probe the impact of emulsifiers and formulations treatment on SC lipid packing, in the first step, we studied the influence of each single emulsifier and emulsifier mixtures in the same concentrations as used in formulations, and in the second step evaluated the effects of formulations themselves.

3.2.1 Lipid conformation measurement by CRM

Figure 11 highlights three peaks relevant to C-C skeleton stretching in the fingerprint region. The peaks at 1070 cm^{-1} and 1130 cm^{-1} are highly linked to the *all-trans* conformation in lipids, while the peak at 1080 cm^{-1} corresponds to the *gauche* conformation only. According to previous findings, during the lipid transformation from order to disorder, the peak at 1070 cm^{-1} becomes lower and sharper, whereas the peak at 1080 cm^{-1} gets broader and shifts towards the lower wavenumbers [63]. In order to calculate the *trans-gauche* conformation of intercellular lipids in the fingerprint region from the viewpoint of the C-C skeleton vibration, the conformational value was introduced as follows:

$$\text{Comformational value} = \frac{AUC_{\,1080}}{AUC_{\,1130} + AUC_{\,1070}} \qquad (1)$$

where AUC is the integrated area under the specified peak.

This ratio indicates the *gauche* conformation order of the lipids, i.e., a high value represents a tendency towards *gauche* conformation order (less-ordered lateral packing state of lipids), and low value means a prevalence of *trans* conformation order (higher-ordered lateral packing state of lipids) from the viewpoint of C-C skeleton vibration. A detailed description of this procedure has been published [64].

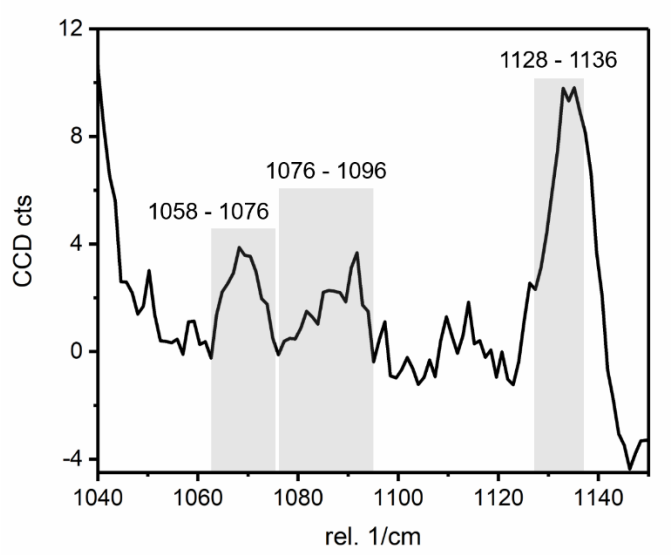

Figure 11 *Lipid-related Raman spectrum of porcine stratum corneum in the region of 1040-1150 cm^{-1} post PCA-based noise reduction procedure with appropriated integration ranges.*

The conformational values of intercellular lipids after treatment with various kinds of emulsifiers are shown in Figure 12A. We can clearly see that the values of HPMC, CA-SLS, GMS, PEG-20-GMS and their mixture treated samples were significantly higher than the reference (water treated samples), indicating that the total intercellular lipids conformation changed to more *gauche* (disordered) states. Furthermore, this result is most obvious for the positive control, SLS treatment, as the ratio increased twice higher than the reference. Whereas for PS 60, CSA as well as their mixture, the calculated conformational values were statistically insignificant compared to the water treated samples, which means the lipid structural arrangement remained to be ordered. Figure 12B shows the conformational values of skin lipids after treatment with different formulations. Among all investigated formulations, basic cream, anionic cream and HPMC-MCT emulsion showed significantly elevated ratios than the reference, indicating the intercellular lipids have more *gauche*-conformation (more disordered state) and a lower ratio of the orthorhombic/hexagonal structures [65]. Whereas for non-ionic cream, the calculated conformational value showed no significant difference in contrast with the reference, implying no obvious influence on the lateral lipids ordering. Therefore, comparison between the formulations suggested that HPMC-MCT emulsion has the most apparent effect, while non-ionic cream has the lowest

impact on the lipid conformational order of the SC. This could be attributed to MCT in the emulsion, as it can dramatically influence intercellular lipid structure in skin [38].

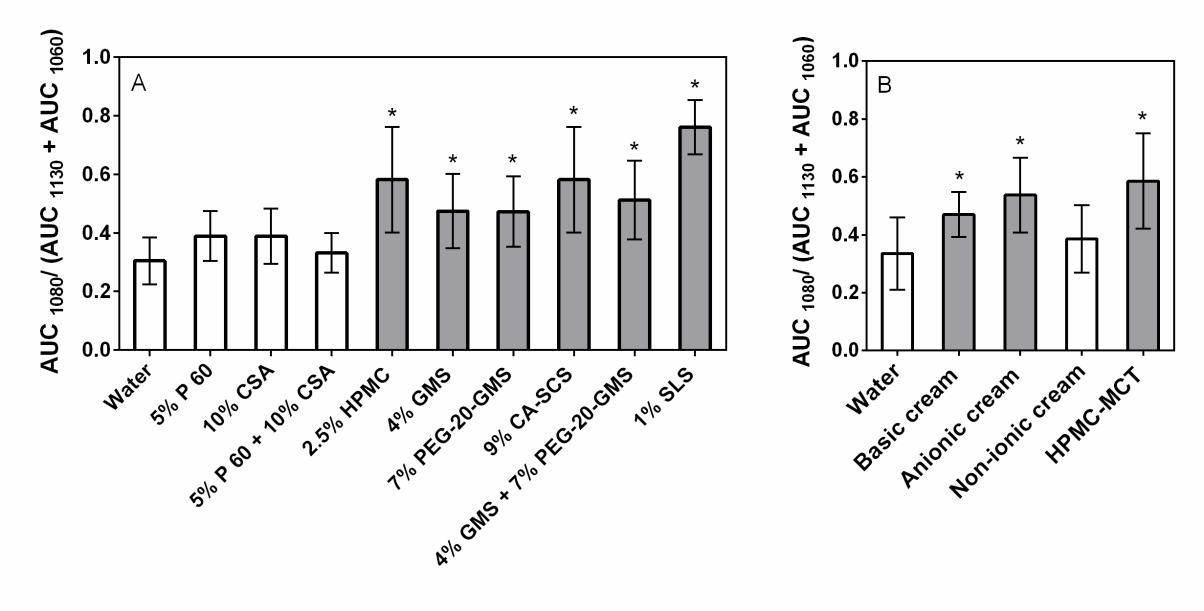

Figure 12 *Comparison of lipid conformational values of porcine skin after treated with emulsifiers (A) and formulations (B), mean ± SD, n = 9, * significant difference (ANOVA, SNK; p < 0.05).*

3.2.2 Lipid ordering study by DSC

DSC is conventionally used to analyse the lipid ordering in the SC. Typically, DSC thermograms of excised porcine SC show two main characteristic endothermic transitions between 0 and 100 °C. The first transition (T1) appears near 60 °C and the second (T2) near 80 °C, both are considered by several investigators to represent a phase transition related to lipids [66]. Since the determination of onset temperature was difficult in this case, the peak minima of profiles were chosen instead [67, 68].

Table 3 lists the T1 and T2 phase transitions of SC after treatment with water and emulsifiers. Compared with water treated SC (reference), various kinds of emulsifiers showed distinct abilities of shifting phase transition temperature. As a positive control, SLS treatment shifted peak temperature the most, indicating the least intercellular lipid order in SC. Among all the studied emulsifiers, anionic CA-SLS treated SC showed the most significant shifts in T1 and T2, yet both were not as obvious as SLS alone. This is due to the fact that, CA-SLS just contains min. 7% sodium SLS and min. 80%

CA (according to European Pharmacopoeia). Interestingly, SC treated with PEG-20-GMS and GMS mixture showed even bigger shift to lower temperature compared to each alone. Presumably, there is a molecular cooperative interaction between these two emulsifiers and thereby leads to a more disordered lipid conformation. PS 60, CSA and their mixture did not shift phase transition significantly in contrast to the reference. These results suggest that they do not affect SC structure. Thus, except for PS 60, CSA and their mixture, other investigated emulsifiers perturb lipid lamellae packing at different extent, resulting in the impaired SC integrity.

Table 3 *Peak minimum temperature of the first (T1) and second (T2) phase transitions of stratum corneum after treatment with emulsifiers, mean ± SD, n = 3, * significant difference (ANOVA, SNK; p < 0.05) [69].*

SC treated with	T1 [°C]	T2 [°C]
Water	63.0 ± 2.6	81.0 ± 2.4
5% PS 60	63.7 ± 2.5	81.5 ± 1.5
10% CSA	61.5 ± 1.9	79.4 ± 1.7
5% PS 60 + 10% CSA	62.8 ± 1.2	81.2 ± 2.6
2.5% HPMC	53.7 ± 1.3 *	73.8 ± 2.5 *
4% GMS	54.6 ± 2.5 *	76.8 ± 2.3 *
7% PEG-20-GMS	53.8 ± 3.1 *	72.1 ± 1.5 *
9% CA-SLS	52.3 ± 2.4 *	66.8 ± 1.9 *
7% PEG-20-GMS + 4% GMS	55.7 ± 2.3 *	70.0 ± 2.8 *
1% SLS	50.4 ± 1.7 *	62.5 ± 1.2 *

Table 4 shows peak minima temperature changes after formulations treatment. For non-ionic cream, such a small shift is considered to be insignificant compared with water treated reference ($p > 0.05$) [70]. Thus, it yields no significant structural alteration in SC. However, for other investigated formulations, they produced obvious changes of lipid structure in SC. Therefore, barrier properties of SC, which relate to certain composition, complex structural arrangement of lipids, are declined after treatment with basic cream, anionic cream and HPMC-MCT emulsion. A comparison among all the formulations suggests HPMC-MCT emulsion is the most effective in terms of

increasing the fluidity of SC. This may be due to MCT, as Müller-Goymann's group also found that MCT incorporated in formulations led to an increased lipid mobility and a less compact microstructure by showing decreased T1 and T2 in DSC thermograms [38]. Interestingly, for both emulsifiers and formulations treatment the conclusions are fully consistent with the results of the CRM measurements.

Table 4 *Peak minimum temperature of the first (T1) and second (T2) phase transitions of stratum corneum after treatment with formulations, mean ± SD, n = 3, * significant difference (ANOVA, SNK; p < 0.05) [69].*

SC treated with	T1 [°C]	T2 [°C]
Water	59.8 ± 1.6	77.4 ± 2.5
Non-ionic cream	58.5 ± 2.4	76.3 ± 1.9
Anionic cream	52.6 ± 3.1 *	75.2 ± 1.2 *
Basic cream	51.8 ± 2.7 *	72.6 ± 2.1 *
HPMC-MCT emulsion	52.3 ± 2.2 *	67.5 ± 2.6 *

3.2.3 Correlation between CRM and DSC

Results from CRM lipid conformation analysis and DSC lipid ordering study were correlated in Figure 13. As can be seen from Figure 13 there is a strong negative correlation between the results of CRM and those of DSC. This shows that the higher conformational values of the lipids (tendency towards *gauche* conformation) correlate very well with lowered phase transition temperature for both emulsifiers and formulations treated SC. This could be explained as follows: after emulsifiers treatment, SC intercellular lipids conformation changed to more *gauche* state, leading to a less ordered structural arrangement. Such increased lipid mobility and less compact microstructure were detected by DSC by showing decreased phase transition temperature in the thermograms. Higher mobility leads to less ordered packing and as a result to increased values in conformational order as detected by CRM. Conformational values calculated from CRM spectra represent lipid conformation from the viewpoint of the C-C skeleton vibration. Meanwhile, in DSC thermal profiles, phase transition temperature shifts indicate changes in the intercellular lipid ordering based on thermodynamic theory. In other words, they can both reflect the structural

arrangement of intercellular lipids and profile the changes of lipid ordering state. CRM has the potential to be used as an alternative to DSC to obtain information on SC lipids conformation.

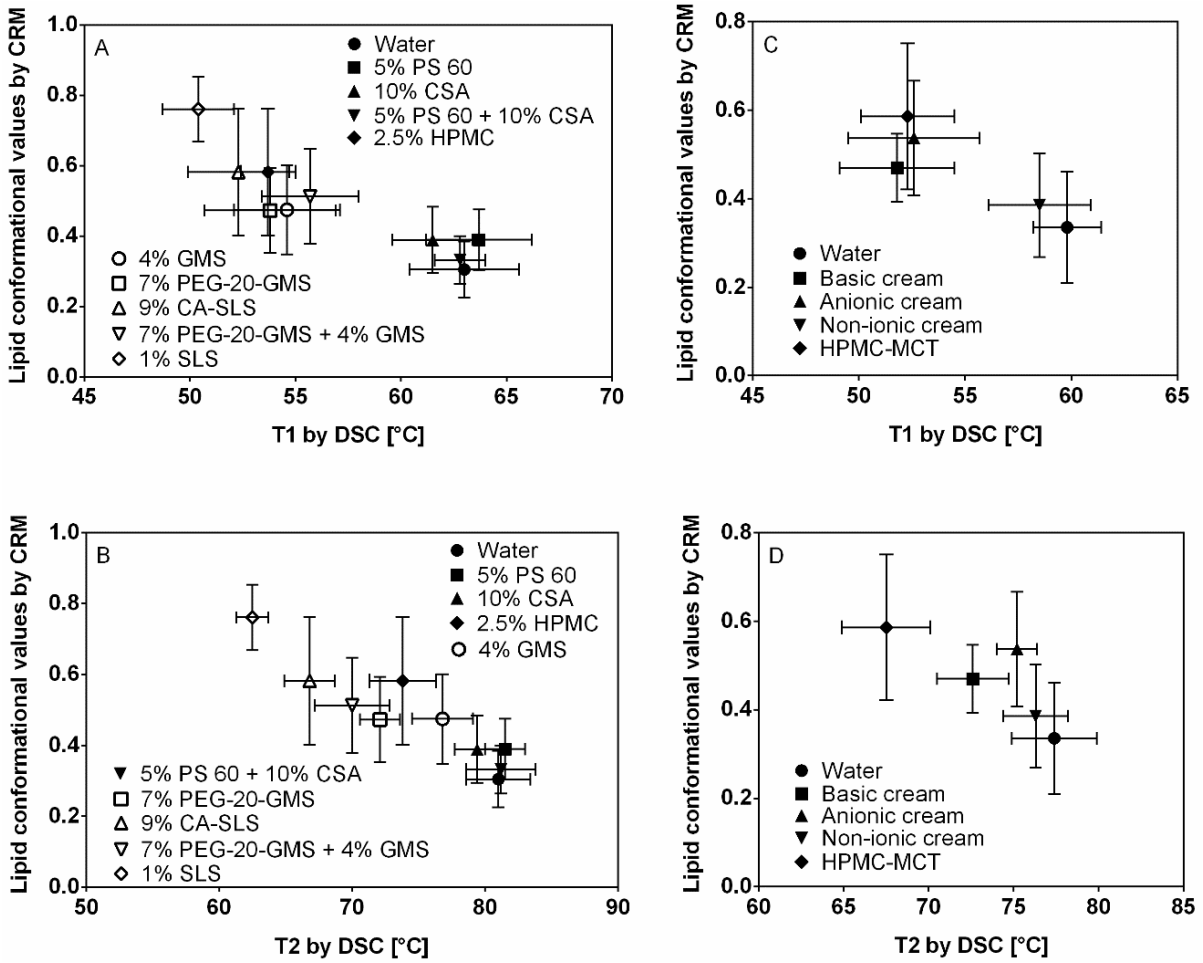

Figure 13 *Correlation between lipid conformational values (by CRM) and lipid phase transition temperature (T1 and T2 in DSC), A and C: emulsifiers treated SC, B and D: formulations treated SC, mean ± SD, n = 3 or 9 [69].*

3.2.4 Summary

DSC is an approved method to characterize the intercellular lipids of SC in detail [71]. Nevertheless, it is relatively time-consuming (depending on the heating rate). In addition, samples are normally destroyed during the measuring process and thus not possible to be further analysed by other techniques. In contrast, CRM can counter all the aforementioned drawbacks. CRM measurement takes relatively shorter time (several seconds to minutes) and it is non-destructive to samples. As already shown

in a previous publication, CRM spectra also provide information regarding the lipid content of SC [48]. To be more precise, CA-SLS, GMS, PEG-20-GMS and their mixture showed potent abilities to extract lipids from SC, while other investigated emulsifiers did not. The present study shows that the same emulsifiers also have significant impact on SC lipids conformation. In combination, we can conclude that emulsifiers that extract lipids also show a tendency to cause lipid conformational changes. Impact of emulsifiers on lipid conformational order and lipid extraction from the SC are highly likely to be two sides of the same story. Their extraction by emulsifiers from SC might facilitate the shift towards less ordered state of SC lipids. On the other hand, less ordered structure may likewise facilitate lipid extraction from the SC. In conjunction with the previous findings, it means lipid content and conformational information could be obtained simultaneously in a single CRM measurement. CRM has the great potential to be an alternative to DSC to detect the impact of emulsifiers and formulations on SC lipid conformation. This work may also serve as a foundation for clinical applications such as healthy skin screening and therapy control, as changes in lipid conformation are important features in many chronic skin diseases.

3.3 Skin repair formulations to deliver physiological lipids into skin

The third section of the current PhD thesis elaborates on a skin repair formulation which aims at recovering the impaired barrier function in many chronic skin diseases. Skin repair creams were prepared using a lab mixer and examined by homogeneity and storage stability. Ex vivo evaluation was performed to compare lipid changes by means of CRM, which was demonstrated to be a reliable and efficient method to quantify global lipids in SC [48]. In addition, in vivo study was conducted to investigate skin recovery potential of cream samples in the living conditions.

3.3.1 Formulations composition and preparation

Basic cream (BC) and non-ionic cream (NiC) showed the least impairment of SC in terms of lipid extraction and conformational alteration in our earlier research [48, 69]. Thus, in this study they both were chosen as base creams to prepare skin repair formulations to replenish lipids in SC. Physiological cholesterol and linoleic acid (molar ratio of 1: 1) were chosen as model lipids and incorporated into BC and NiC. Composition of the investigated formulations are provided in Table 5.

Table 5 *Composition of investigated formulations and evaluation methods*

Lipids incorporated [%]	Base creams	Abbreviations	Evaluation methods		
			Stability study	Ex-vivo study	In-vivo study
0	Basic cream	BC	+	+	-
0	Non-ionic cream	NiC	+	+	-
5.0	Basic cream	L-BC	+	+	+
5.0	Non-ionic cream	L-NiC	+	+	+

Creams were prepared with a lab mixer (Unguator®, Gako International GmbH, Scheßlitz, Germany). Depending on the setting parameters, the components are exposed to different physical forces that may influence the homogeneity of the formulations. Hence, after screening the mixing speed, time and temperature, an optimal method for preparing creams was developed. It includes two steps – a high-speed mixing step for homogenization and a low-speed mixing step for cooling. Specific parameters are shown in Table 6.

Table 6 *An optimal method for preparing cream formulations*

	Speed of the mixing motor [rpm]	Speed of the lifting motor [rpm]	Time [min]
Step 1	2000	1500	9
Step 2	250	800	30

3.3.2 Stability studies of the skin repair creams

Following the above protocol, L-BC and L-NiC were prepared. To characterize the changes in structure and the distribution of creams during storage, stability study was carried out. The samples were stored at 25 °C and characterized by rheology and polarized light microscopy after storage for 1, 2 and 6 months. Figure 14 shows the polarized light microscopic images of the skin repair formulations in the stability test. As seen in Figure 14A, well distributed character was seen for L-BC. Homogeneous cream texture was maintained even after 6 months, indicating the high stability of L-BC (Figure 14B). Therefore, the developed L-BC was proved to be highly structurally stable. Figure 14C to 14E reveal structural changes of L-NiC in the stability study. After 1 month, no clear changes were found in the cream texture (Figure 14D) compared to the initial image (Figure 14C). However, after 2 months square crystals appeared and distributed randomly in the formulation, indicating the instability of L-NiC at room temperature after 2 months (Figure 14E).

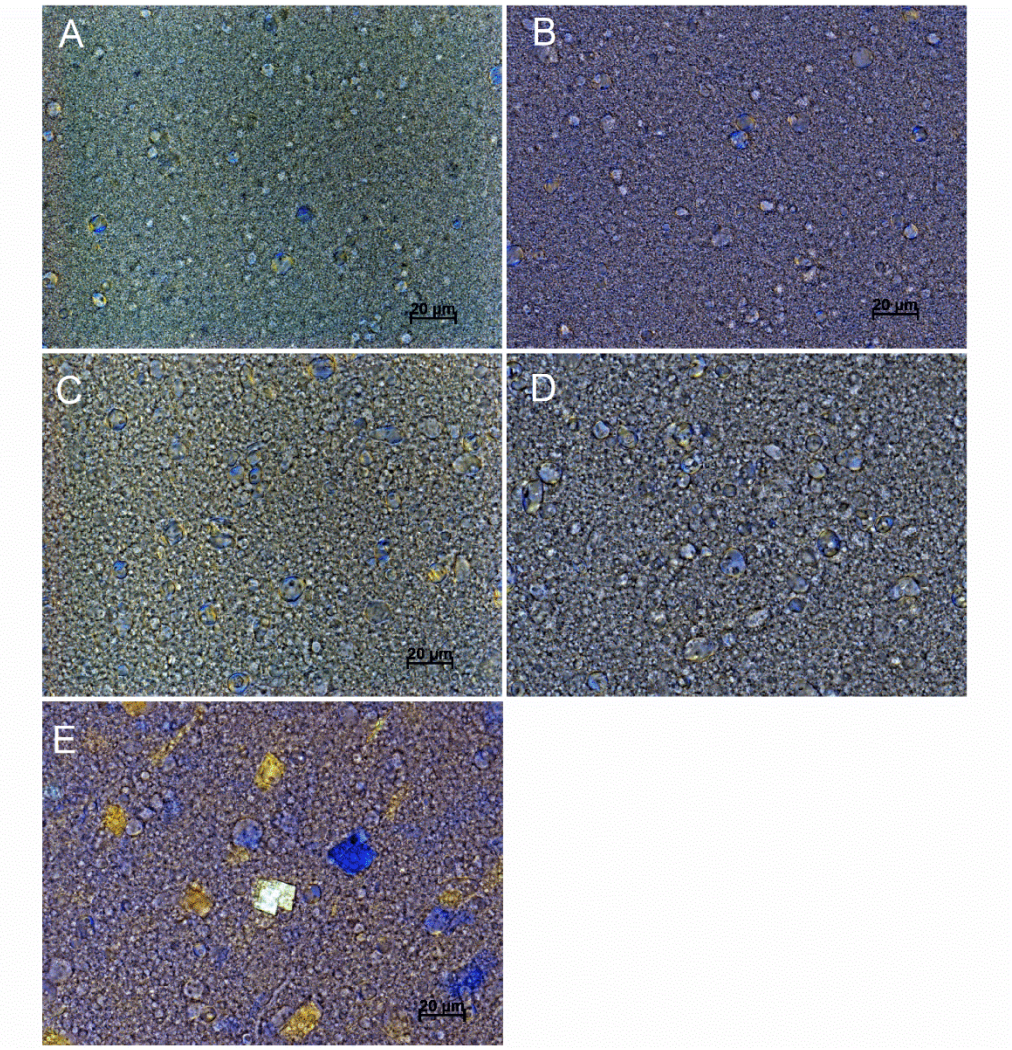

Figure 14 *Polarized light micrographs of developed creams in stability study, A: initial image of L-BC (after 24 h of the preparation), B: L-BC after 6-month storage, C: initial image of L-NiC (after 24 h of the preparation), D: L-NiC after 1-month storage and E: L-NiC after 2-month storage [72].*

The rheological behaviour of skin repair creams in the stability study is shown in Figure 15. It can be seen that, after 6 months, L-BC showed no obvious changes in amplitude sweep compared with the initial values (Figure 15A). In viscosity curves (Figure 15B), there was also no significant variation after storage for 6 months, indicating stable rheological behaviour of L-BC. However, L-NiC showed time-dependent instability. After 2 months, both storage and loss modulus increased dramatically compared to the initial results (Figure 15C). The increase in both moduli could be explained by the coalescent oil droplets and inhomogeneous texture of the formulation. In addition, the

viscosity of L-NiC showed a trend towards higher values (Figure 15D). In combination with microscopic results, these rheological changes could result from the crystals which appeared in the formulations after being stored for 2 months. To address the question what the crystals are, further investigation in the composition of L-NiC was performed using CRM.

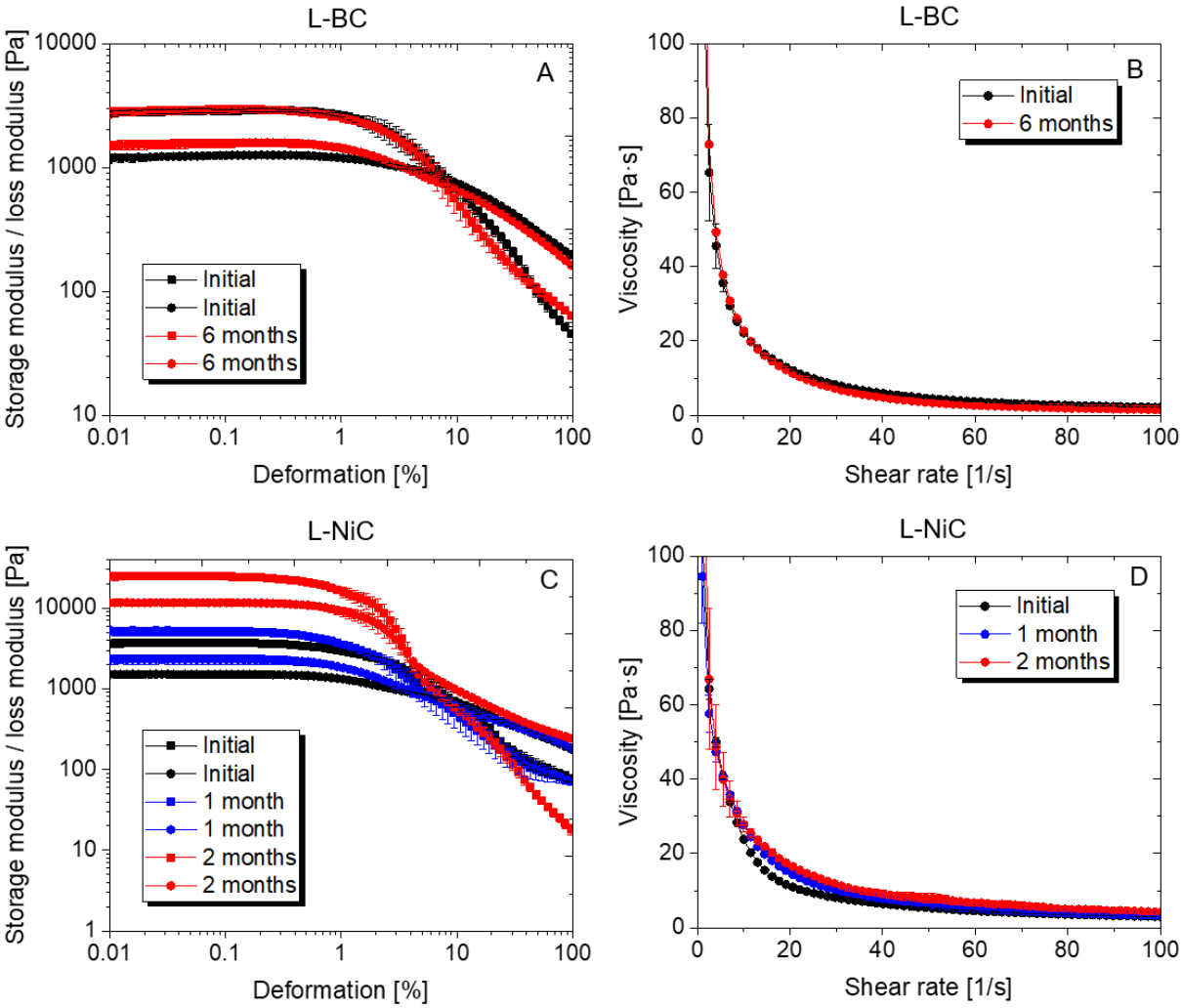

Figure 15 *Rheological behaviour of L-NiC and L-BC in the stability study. A and C results are from oscillatory test; B and D are calculated viscosity results from flow curves, mean ± SD, n = 3.*

Raman colour-coded image of L-NiC was generated to investigate what the crystals are. As shown in Figure 16, highly regular square crystals were found to be pure cholesterol, which crystalized during long-term storage. Such crystallization process is due to a limited solubility of cholesterol in the formulation, leading to a

supersaturated state for cholesterol. This supersaturated state could be attributed to high concentration of cholesterol, low concentration of emulsifiers or weak solubility-enhancing ability of emulsifiers, irrespective which can be a crucial driving force for the formation of crystal lattice. Therefore, in combination with the results of PLM and rheology, it was manifested that L-NiC was not stable after 2-month storage at room temperature, as the added cholesterol crystalized under such conditions.

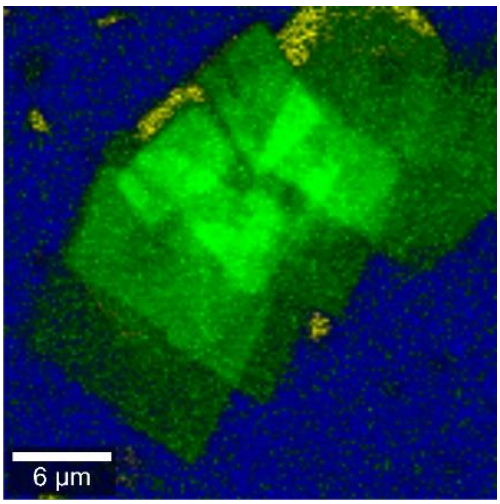

Figure 16 *Raman microscopic colour-coded images of water diluted L-NiC (after 2-month storage at room temperature), blue: water, yellow: white soft paraffin and green: cholesterol.*

3.3.3 Ex vivo evaluation by CRM

Ex vivo experiment was carried out to assess whether the skin repair creams can deliver lipids into SC. For comparison, water treated skin was used as the reference to simulate non-impaired skin. For the rest of the skin samples, SLS treatment was firstly conducted to induce lipid deficiency in SC and thus lead to SC impairment. After SLS treatment, L-BC, L-NiC as well as control formulations of BC and NiC (without lipids) were applied onto the skin, respectively. Additionally, SLS treated skin samples served as a positive control for lipid extraction from SC. From Figure 17A, it can be seen that after SLS treatment, the lipid content significantly reduced compared to the reference (water treated SC). Application of L-BC to SLS impaired skin led to an increase in the lipid amount in SC, indicating L-BC delivered physiological lipids into the lipid-lacking SC. In contrast, BC treated SC did not show any influence on lipid content compared with SLS treatment, as the global amount was still significantly

lower than water treated samples. Therefore, L-BC was proved to be able to deliver lipids into SLS impaired SC, whereas BC did not.

Figure 17B shows the ex vivo evaluation results of L-NiC and NiC. Compared to water treated samples, the lipid content declined significantly after SLS treatment. However, application of L-NiC increased the lipid content in impaired SC prominently. In comparison, NiC treatment did not lead to any change in the lipid amount. This means that L-NiC is capable of transporting lipids into lipid-lacking SC whereas NiC (control formulation) is not. Thus, the developed L-NiC and L-BC were demonstrated to have a promising ability to restore intercellular lipid composition.

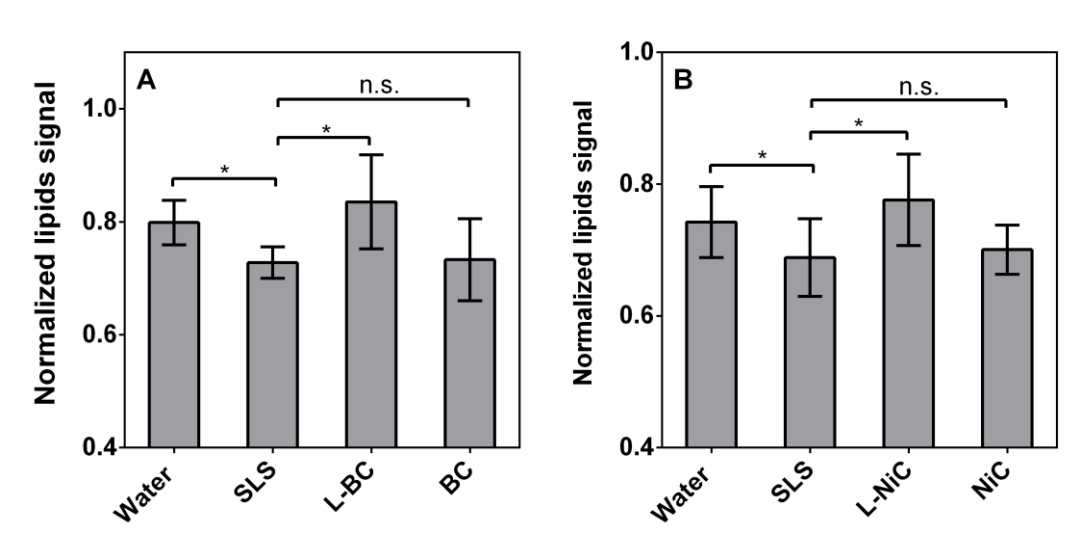

Figure 17 *Comparison of lipid content in porcine stratum corneum after treated with A: BC and L-BC, B: NiC and L-NiC, mean ± SD, n = 9, * significant difference (ANOVA, SNK; $p < 0.05$) [72].*

3.3.4 In vivo skin efficacy study

Previous ex vivo results confirmed the lipids delivery ability of L-BC and L-NiC. Thus, to investigate skin recovery potential of cream samples in the actual living conditions, in vivo study on human volunteers was performed by non-invasive techniques. Biophysical parameters of transepidermal water loss (TEWL) and stratum corneum moisturization (SCM) were measured as indicators to evaluate the efficacy of the investigated creams. To induce barrier impairment, designated skin sites were tape stripped. Thereafter, the sites were either not treated (tape stripped control) or treated

with skin repair creams. One site that was not stripped and not treated was used as untreated control. In Figure 18, the influence of 7-day application of the developed creams on skin barrier function (TEWL) and hydration (SCH) levels is presented.

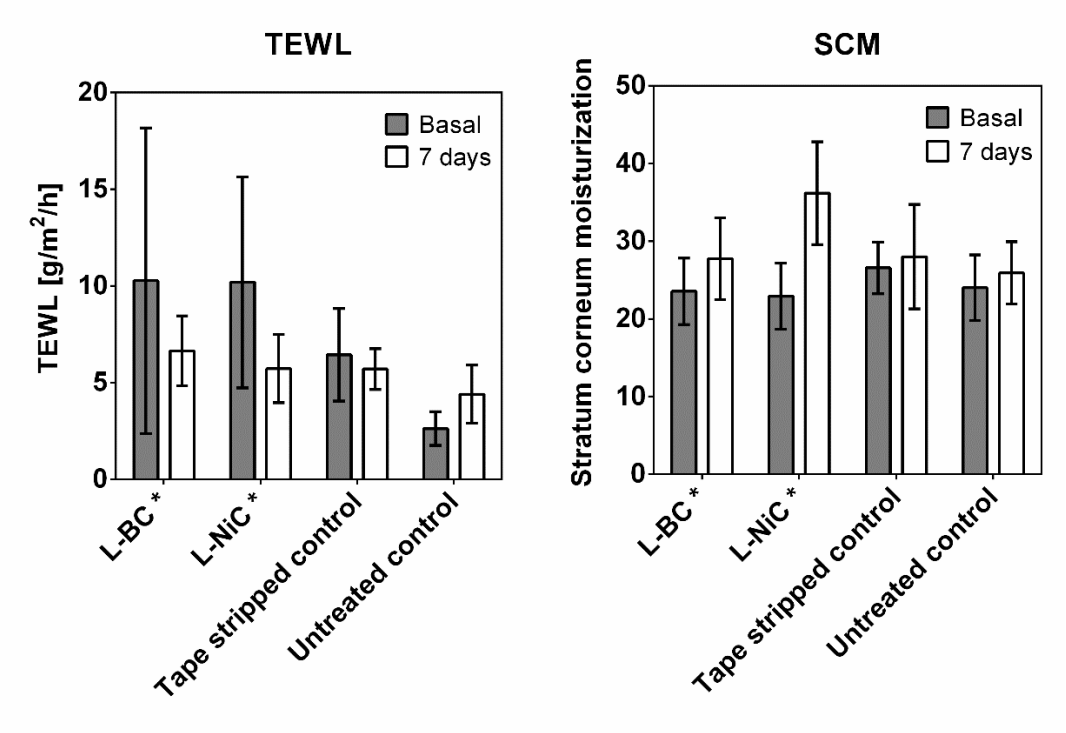

Figure 18 *Results of skin efficacy study for investigated creams, left: transepidermal water loss (TEWL) and right: stratum corneum moisturization (SCM). SCM is in arbitrary units, n=11, mean ± SD [72].*

As shown in Figure 18, for initial/basal values (grey bars), TEWL was statistically increased after tape stripping at all sites, indicating skin barrier disruption after tape stripping procedures. However, after 7-day application of L-BC and L-NiC, significant decrease in TEWL was found for both new creams, suggesting skin barrier function was restored. In contrast, decreases in TEWL were not found in tape stripped control and untreated control. Hence, L-BC and L-NiC were demonstrated to dramatically improve the barrier function of impaired skin by transporting physiological lipids into depleted SC.

There was no statistical difference among initial SC moisturization levels for all sites (grey bars). After 7 days SCM was significantly increased after application of L-NiC and L-BC compared to initial values. However, this was not seen in tape stripped

control and untreated control. Glycerol in L-NiC and propylene glycol in L-BC are well-known moisturizers. Their humectant properties help to retain water in SC and thus lead to high SCM values in the experiment. However, literature reports that SC lipids are also necessary for water retention within skin and for the integrity of the barrier [73], suggesting the delivered lipids played a role in keeping skin moisturized.

Therefore, these improvements in the biophysical parameters proved that L-BC and L-NiC facilitated the skin barrier recovery in the volunteers. Such process can be described as follows: physiological lipids in preparations traverse the SC interstices between corneocytes. When reaching the nucleated cell layers, physiological lipids are taken up by keratinocytes and incorporated into nascent lamellar bodies and eventually secreted into SC intercellular lipid regions [44, 74]. Through this process, L-BC and L-NiC replenished lipids in the depleted skin barrier. Thus, both L-BC and L-NiC showed excellent efficacy in the skin protection and impaired skin recovery.

3.3.5 Summary

Many skin diseases are featured with a reduction in skin lipids and the therapeutic concept in this PhD thesis is to deliver lipids into the skin. Two new formulations, L-BC and L-NiC, containing physiological lipids of cholesterol and linoleic acid were developed. In the ex vivo evaluation experiment, both L-BC and L-NiC showed prominent lipids delivery into SC. Further in vivo study demonstrated that L-BC and L-NiC can facilitate the recovery of impaired skin barrier by showing significantly reduced TEWL values after application. Therefore, the new developed L-BC and L-NiC are able to deliver lipids into skin effectively. L-BC was found to be more stable than L-NiC. Due to the higher stability, L-BC has great potential in clinical use for treating impaired skin barrier associated with depletion of SC lipids. Moreover, it could be an excellent candidate as a base cream to incorporate pharmaceutical actives into the course of an individualized treatment.

4. Conclusion

The lipid matrix is considered to play a crucial role in the skin barrier function. However, undesired factors may lead to lipid alterations in the skin. Emulsifiers, which are widely used in pharmaceutical and cosmetic preparations, are one of those factors. Thus, in the first and second parts of the present PhD thesis, the influence of different emulsifiers and formulations on SC lipid properties was elucidated using CRM and traditional techniques, in both aspects of lipid composition and lipid conformation. Various emulsifiers showed distinct potencies to extract lipids and caused disordered lipid ordering, whereas the investigated formulations did not lead to lipid reduction, but rather altered lipid conformation at different extent. Furthermore, strong correlation between results from CRM and conventional methods was found. CRM possesses a great potential to be a standardized analytical technique in skin lipid quantification and conformational identification.

SC lipid reduction can cause impaired skin barrier function, which is associated with many chronic skin diseases. Therefore, in the third section of the thesis, skin repair formulations, aiming at physiological lipids delivery so as to reinforce barrier function, were developed, characterized and evaluated. Homogeneous cream texture was found in the formulation and remained stable in the long-term stability test. In ex vivo study, application of the creams led to substantially increased lipid levels compared to the reference in the lipid-deficient skin. Moreover, in the in vivo skin efficacy study, application of skin repair creams provided a reinforcement of the skin barrier as transepidermal water loss (TEWL) was significantly decreased. Therefore, they showed excellent effects on replenishing lipid content in SC and recovering impaired barrier function. The prepared skin repair formulations improve skin conditions effectively and thus could be excellent candidates in clinical use as part of maintenance therapy.

5. References

1. Bouwstra, J.A. and M. Ponec, *The skin barrier in healthy and diseased state.* Biochimica et Biophysica Acta (BBA)-Biomembranes, 2006. **1758**(12): p. 2080-2095.
2. Lew, B.-L., et al., *Ceramides and cell signaling molecules in psoriatic epidermis: reduced levels of ceramides, PKC-α, and JNK.* Journal of Korean medical science, 2006. **21**(1): p. 95-99.
3. Jacobs, R., *Depleted skin barrier replenishing skin creams composition and method of application*. 2004, Google Patents.
4. Vávrová, K., et al., *Ceramide analogue 14S24 ((S)-2-tetracosanoylamino-3-hydroxypropionic acid tetradecyl ester) is effective in skin barrier repair in vitro.* European journal of pharmaceutical sciences, 2004. **21**(5): p. 581-587.
5. Berdyshev, E., et al., *Lipid Abnormalities Associated with Skin Lesions in Atopic Dermatitis.* Journal of Allergy and Clinical Immunology, 2017. **139**(2): p. AB87.
6. Farwanah, H., et al., *Ceramide profiles of the uninvolved skin in atopic dermatitis and psoriasis are comparable to those of healthy skin.* Archives of dermatological research, 2005. **296**(11): p. 514-521.
7. Williams, H. and C. Flohr, *How epidemiology has challenged 3 prevailing concepts about atopic dermatitis.* Journal of allergy and clinical immunology, 2006. **118**(1): p. 209-213.
8. Di Nardo, A., et al., *Ceramide and cholesterol composition of the skin of patients with atopic dermatitis.* ACTA DERMATOVENEREOLOGICA-STOCKHOLM-, 1998. **78**: p. 27-30.
9. Imokawa, G., et al., *Decreased level of ceramides in stratum corneum of atopic dermatitis: an etiologic factor in atopic dry skin?* Journal of Investigative Dermatology, 1991. **96**(4): p. 523-526.
10. Janssens, M., et al., *Increase in short-chain ceramides correlates with an altered lipid organization and decreased barrier function in atopic eczema patients.* Journal of lipid research, 2012. **53**(12): p. 2755-2766.
11. Mojumdar, E.H., et al., *Monounsaturated fatty acids reduce the barrier of stratum corneum lipid membranes by enhancing the formation of a hexagonal lateral packing.* Langmuir, 2014. **30**(22): p. 6534-6543.
12. Mojumdar, E., et al., *The role of ceramide chain length distribution on the barrier properties of the skin lipid membranes.* Biochimica et Biophysica Acta (BBA)-Biomembranes, 2014. **1838**(10): p. 2473-2483.
13. Angelova-Fischer, I., et al., *Distinct barrier integrity phenotypes in filaggrin-related atopic eczema following sequential tape stripping and lipid profiling.* Experimental dermatology, 2011. **20**(4): p. 351-356.
14. Jungersted, J., et al., *Stratum corneum lipids, skin barrier function and filaggrin mutations in patients with atopic eczema.* Allergy, 2010. **65**(7): p. 911-918.
15. Smeden, J., et al., *The importance of free fatty acid chain length for the skin barrier function in atopic eczema patients.* Experimental dermatology, 2014. **23**(1): p. 45-52.
16. Macheleidt, O., K. Sandhoff, and H.W. Kaiser, *Deficiency of epidermal protein-bound ω-hydroxyceramides in atopic dermatitis.* Journal of Investigative Dermatology, 2002. **119**(1): p. 166-173.

17. Descamps, F., et al., *Lamellar Lipid Organization and Ceramide Composition in the Stratum Corneum of Patients with Atopic Eczema.* J Eur Acad Dermatol Venereol. **18**: p. 13-26.

18. Motta, S., et al., *Ceramide composition of the psoriatic scale.* Biochimica et Biophysica Acta (BBA)-Molecular Basis of Disease, 1993. **1182**(2): p. 147-151.

19. Motta, S., et al., *Abnormality of water barrier function in psoriasis.* Arch Dermatol, 1994. **130**(4): p. 452-456.

20. Pilgram, G.S., et al., *Aberrant lipid organization in stratum corneum of patients with atopic dermatitis and lamellar ichthyosis.* Journal of investigative dermatology, 2001. **117**(3): p. 710-717.

21. Lavrijsen, A.P., et al., *Reduced skin barrier function parallels abnormal stratum corneum lipid organization in patients with lamellar ichthyosis.* Journal of Investigative dermatology, 1995. **105**(4): p. 619-624.

22. Paige, D., N. Morse-Fisher, and J. Harper, *Quantification of stratum corneum ceramides and lipid envelope ceramides in the hereditary ichthyoses.* British Journal of Dermatology, 1994. **131**(1): p. 23-27.

23. Van Smeden, J., et al., *Intercellular skin barrier lipid composition and organization in Netherton syndrome patients.* Journal of Investigative Dermatology, 2014. **134**(5): p. 1238-1245.

24. Uchida, Y., et al., *Epidermal sphingomyelins are precursors for selected stratum corneum ceramides.* Journal of lipid research, 2000. **41**(12): p. 2071-2082.

25. Holleran, W.M., et al., *Consequences of beta-glucocerebrosidase deficiency in epidermis. Ultrastructure and permeability barrier alterations in Gaucher disease.* The Journal of clinical investigation, 1994. **93**(4): p. 1756-1764.

26. Bellew, S. and J.Q. Del Rosso, *Overcoming the barrier treatment of ichthyosis: a combination-therapy approach.* The Journal of clinical and aesthetic dermatology, 2010. **3**(7): p. 49.

27. Vavrova, K., et al., *Ceramide analogue 14S24 selectively recovers perturbed human skin barrier.* British Journal of Dermatology, 2007. **157**(4): p. 704-712.

28. Mao-Qiang, M., et al., *Optimization of physiological lipid mixtures for barrier repair.* Journal of Investigative Dermatology, 1996. **106**(5): p. 1096-1101.

29. Sahle, F.F., et al., *Polyglycerol fatty acid ester surfactant–based microemulsions for targeted delivery of ceramide AP into the stratum corneum: Formulation, characterisation, in vitro release and penetration investigation.* European Journal of Pharmaceutics and Biopharmaceutics, 2012. **82**(1): p. 139-150.

30. Sahle, F.F., J. Wohlrab, and R.H. Neubert, *Controlled penetration of ceramides into and across the stratum corneum using various types of microemulsions and formulation associated toxicity studies.* European Journal of Pharmaceutics and Biopharmaceutics, 2014. **86**(2): p. 244-250.

31. Kato, E. and N. Takahashi, *Improvement by sodium dl-α-tocopheryl-6-O-phosphate treatment of moisture-retaining ability in stratum corneum through increased ceramide levels.* Bioorganic & medicinal chemistry, 2012. **20**(12): p. 3837-3842.

32. Jin, K., et al., *Analysis of beta-glucocerebrosidase and ceramidase activities in atopic and aged dry skin.* Acta dermato-venereologica, 1994. **74**(5): p. 337-340.

33. Lundborg, M., et al., *Human skin barrier structure and function analyzed by cryo-EM and molecular dynamics simulation.* Journal of Structural Biology, 2018.

34. Groen, D., G. Gooris, and J. Bouwstra, *New insights into the stratum corneum lipid organization by X-ray diffraction analysis.* Biophysical journal, 2009. **97**(8): p. 2242-2249.

35. Van Smeden, J., et al., *The important role of stratum corneum lipids for the cutaneous barrier function.* Biochimica et Biophysica Acta (BBA)-Molecular and Cell Biology of Lipids, 2014. **1841**(3): p. 295-313.

36. Björklund, S., et al., *Characterization of stratum corneum molecular dynamics by natural-abundance 13C solid-state NMR.* PloS one, 2013. **8**(4): p. e61889.

37. Champagne, A.M., et al., *Presence and persistence of a highly ordered lipid phase state in the avian stratum corneum.* Journal of Experimental Biology, 2018. **221**(11): p. jeb176438.

38. Täuber, A. and C.C. Müller-Goymann, *In vitro model of infected stratum corneum for the efficacy evaluation of poloxamer 407-based formulations of ciclopirox olamine against Trichophyton rubrum as well as differential scanning calorimetry and stability studies.* International journal of pharmaceutics, 2015. **494**(1): p. 304-311.

39. Ring, J., et al., *Guidelines for treatment of atopic eczema (atopic dermatitis) Part II.* Journal of the European Academy of Dermatology and Venereology, 2012. **26**(9): p. 1176-1193.

40. Rubel, D., et al., *Consensus guidelines for the management of atopic dermatitis: An Asia–Pacific perspective.* The Journal of dermatology, 2013. **40**(3): p. 160-171.

41. Proksch, E. and J.M. Lachapelle, *The management of dry skin with topical emollients–recent perspectives.* JDDG: Journal der Deutschen Dermatologischen Gesellschaft, 2005. **3**(10): p. 768-774.

42. Giam, Y.C., et al., *A review on the role of moisturizers for atopic dermatitis.* Asia Pacific Allergy, 2016. **6**(2): p. 120-128.

43. Lynde, C., *Moisturizers for the treatment of inflammatory skin conditions.* Journal of drugs in dermatology: JDD, 2008. **7**(11): p. 1038-1043.

44. Anderson, P.C. and J.G. Dinulos, *Are the new moisturizers more effective?* Current opinion in pediatrics, 2009. **21**(4): p. 486-490.

45. Winsor, T. and G.E. Burch, *Differential roles of layers of human epigastric skin on diffusion rate of water.* Archives of Internal Medicine, 1944. **74**(6): p. 428-436.

46. Elias, P.M., *Epidermal lipids, barrier function, and desquamation.* Journal of Investigative Dermatology, 1983. **80**.

47. Weerheim, A. and M. Ponec, *Determination of stratum corneum lipid profile by tape stripping in combination with high-performance thin-layer chromatography.* Archives of dermatological research, 2001. **293**(4): p. 191-199.

48. Zhang, Z. and D.J. Lunter, *Confocal Raman microspectroscopy as an alternative method to investigate the extraction of lipids from stratum corneum by emulsifiers and formulations.* European Journal of Pharmaceutics and Biopharmaceutics, 2018. **127**: p. 61-71.

49. Tfayli, A., et al., *Thermal dependence of Raman descriptors of ceramides. Part I: effect of double bonds in hydrocarbon chains.* Analytical and bioanalytical chemistry, 2010. **397**(3): p. 1281-1296.

50. Narishetty, S.T.K. and R. Panchagnula, *Effect of l-menthol and 1,8-cineole on phase behavior and molecular organization of SC lipids and skin permeation of zidovudine.* Journal of Controlled Release, 2005. **102**(1): p. 59-70.

51. Mendelsohn, R., C.R. Flach, and D.J. Moore, *Determination of molecular conformation and permeation in skin via IR spectroscopy, microscopy, and imaging.* Biochimica et Biophysica Acta (BBA) - Biomembranes, 2006. **1758**(7): p. 923-933.

52. Raman, C.V. and K.S. Krishnan, *A new type of secondary radiation.* Nature, 1928. **121**(3048): p. 501.

53. Dieing, T., O. Hollricher, and J. Toporski, *Confocal raman microscopy*. Vol. 158. 2011: Springer Science & Business Media.

54. Holleran, W.M., et al., *Sphingolipids are required for mammalian epidermal barrier function. Inhibition of sphingolipid synthesis delays barrier recovery after acute perturbation.* The Journal of clinical investigation, 1991. **88**(4): p. 1338-1345.

55. Holleran, W.M., et al., *Regulation of epidermal sphingolipid synthesis by permeability barrier function.* Journal of Lipid Research, 1991. **32**(7): p. 1151-1158.

56. Menon, G.K., K.R. Feingold, and P.M. Elias, *Lamellar body secretory response to barrier disruption.* Journal of investigative dermatology, 1992. **98**(3): p. 279-289.

57. Arzneimittel-Codex, D., *Deutscher Arzneimittel Codex/Neues Rezeptur-Formularium (DAC/NRF).* 2016.

58. *German Pharmacopoeia (Deutsches Arzneibuch DAB)* 2015.

59. Wollenweber, C., et al., *Adsorption of hydroxypropyl methylcellulose at the liquid/liquid interface and the effect on emulsion stability.* Colloids and Surfaces A: Physicochemical and Engineering Aspects, 2000. **172**(1): p. 91-101.

60. Söderlind, E., M. Wollbratt, and C. von Corswant, *The usefulness of sugar surfactants as solubilizing agents in parenteral formulations.* International journal of pharmaceutics, 2003. **252**(1): p. 61-71.

61. Pagnoni, A., A. Kligman, and T. Stoudemayer, *Pyranine, a fluorescent dye, detects subclinical injury to sodium lauryl sulfate.* Journal of the Society of Cosmetic Chemists, 1998. **49**(1): p. 33-38.

62. Egawa, M., T. Hirao, and M. Takahashi, *In vivo estimation of stratum corneum thickness from water concentration profiles obtained with Raman spectroscopy.* Acta dermato-venereologica, 2007. **87**(1): p. 4-8.

63. Wallach, D.F., S.P. Verma, and J. Fookson, *Application of laser Raman and infrared spectroscopy to the analysis of membrane structure.* Biochimica et Biophysica Acta (BBA)-Reviews on Biomembranes, 1979. **559**(2-3): p. 153-208.

64. Choe, C., J. Lademann, and M.E. Darvin, *A depth-dependent profile of the lipid conformation and lateral packing order of the stratum corneum in vivo measured using Raman microscopy.* Analyst, 2016. **141**(6): p. 1981-1987.

65. Choe, C., et al., *In vivo confocal Raman microscopic determination of depth profiles of the stratum corneum lipid organization influenced by application of various oils.* Journal of Dermatological Science, 2017.

66. Bouwstra, J., et al., *Thermodynamic and structural aspects of the skin barrier.* Journal of Controlled Release, 1991. **15**(3): p. 209-219.

67. Silva, C., et al., *Study of human stratum corneum and extracted lipids by thermomicroscopy and DSC.* Chemistry and physics of lipids, 2006. **140**(1): p. 36-47.

68. Mitriaikina, S. and C. Muller-Goymann, *Synergetic effects of isopropyl alcohol (IPA) and isopropyl myristate (IPM) on the permeation of betamethasone-17-valerate from semisolid Pharmacopoeia bases.* Journal of Drug Delivery Science and Technology, 2007. **17**(5): p. 1-8.

69. Zhang, Z. and D.J. Lunter, *Confocal Raman microspectroscopy as an alternative to differential scanning calorimetry to detect the impact of emulsifiers and formulations on stratum corneum lipid conformation.* European Journal of Pharmaceutical Sciences, 2018. **121**: p. 1-8.

70. Winkler, A. and C.C. Müller-Goymann, *The influence of topical formulations on the permeation of 5-aminolevulinic acid and its n-butyl ester through excised human stratum corneum.* European journal of pharmaceutics and biopharmaceutics, 2005. **60**(3): p. 427-437.

71. Brinkmann, I. and C. Müller-Goymann, *An attempt to clarify the influence of glycerol, propylene glycol, isopropyl myristate and a combination of propylene glycol and isopropyl myristate on human stratum corneum.* Die Pharmazie-An International Journal of Pharmaceutical Sciences, 2005. **60**(3): p. 215-220.

72. Zhang, Z., et al., *Reinforcement of barrier function – skin repair formulations to deliver physiological lipids into skin.* International Journal of Cosmetic Science, 2018.

73. Chamlin, S.L., et al., *Ceramide-dominant barrier repair lipids alleviate childhood atopic dermatitis: changes in barrier function provide a sensitive indicator of disease activity.* Journal of the American Academy of Dermatology, 2002. **47**(2): p. 198-208.

74. Mao-Qiang, M., et al., *Exogenous nonphysiologic vs physiologic lipids: divergent mechanisms for correction of permeability barrier dysfunction.* Archives of Dermatology, 1995. **131**(7): p. 809-816.

6. Appendix: Publications incorporated in this study

6.1 Publication 1

Confocal Raman microspectroscopy as an alternative method to investigate the extraction of lipids from stratum corneum by emulsifiers and formulations

Ziwei Zhang, Dominique Lunter *

European Journal of Pharmaceutics and Biopharmaceutics

Volume 127, Pages 61-71. Published on 8 February 2018.

European Journal of Pharmaceutics and Biopharmaceutics 127 (2018) 61–71

Contents lists available at ScienceDirect

European Journal of Pharmaceutics and Biopharmaceutics

journal homepage: www.elsevier.com/locate/ejpb

Research paper

Confocal Raman microspectroscopy as an alternative method to investigate the extraction of lipids from stratum corneum by emulsifiers and formulations

Ziwei Zhang, Dominique Jasmin Lunter*

University of Tuebingen, Pharmaceutical Technology, Tuebingen, Germany

ARTICLE INFO

Keywords:
Skin lipids content
Stratum corneum thickness
Confocal Raman microscopy
High-performance thin-layer chromatography
Lipid extraction

ABSTRACT

The purpose of this study was to investigate the impact of emulsifiers and formulations on intercellular lipids of porcine stratum corneum (SC) and evaluate confocal Raman microscopy (CRM) as an alternative method in this research context. To this end, four different formulations were used: three conventional creams that contained ionic and/or non-ionic emulsifiers and one surfactants-free emulsion stabilized by a polymeric emulsifier. Additionally, all emulsifiers were tested in aqueous solution/dispersion in the respective concentrations as present in the formulations. CRM and HPTLC were used to analyse changes in SC lipid content after treatment. Furthermore, lipid extraction was visualized by fluorescence staining and SC thickness was measured by CRM and light microscopy. Various emulsifiers and emulsifier mixtures showed different impact on SC lipid content and SC thickness, while none of the tested formulations had any effect on SC lipids. Emulsifiers and their mixtures that reduced the lipids content also reduced SC thickness, indicating lipid extraction is the reason for SC thinning. Results from CRM and conventional methods showed a strong positive correlation for both lipid content and SC thickness measurements. With easy sample preparation and fast analytical readout, CRM has the potential to be a standardized analytical method for skin lipids investigation.

1. Introduction

Stratum cornuem (SC) is the outermost layer of the skin and constitutes an effective barrier against environmental influences (e.g. chemical, physical, and microbiological invasion) as well as to prevent excessive water loss from the body. Typically, SC structure is described as the biphasic “mortar and bricks” model, in which mortar is a mixture of lipids and glues corneocytes together [1]. Undoubtedly, the better and stronger the mortar is, the better and stronger the barrier becomes. Normal human skin lipids are highly organized in the form of lamellar bilayers and mainly consist of free fatty acids (FFA), ceramides (CER) and cholesterol (CHOL) in an approximately equimolar ratio [2]. As the only continuous domain in SC, intercellular lipids play an important role in a competent skin barrier. However, undesired lipid extraction or depletion leads to an impaired skin barrier function, which may cause further skin problems. Conversely, many skin diseases such as atopic dermatitis, psoriasis and lamellar ichthyosis are associated with abnormalities in epidermal skin lipid composition, especially the decreased level of SC lipids [3]. Therefore, skin lipid analysis is of paramount importance in dermatological diagnosis and treatment.

Emulsifiers, owing to their intrinsic surface activity, are widely used in cosmetic or dermatological preparations as either stabilizers for emulsions [4–8] or penetration enhancers [9–14] to promote drug absorption into the skin. However, studies have shown that frequent exposure to emulsifiers may affect the composition of SC lipids and consequently induce skin damage or irritation. Researchers demonstrated sodium lauryl sulfate (SLS) perturbs the SC integrity by removing sebaceous and epidermal lipids [15–18]. The mechanism whereby emulsifiers elicit such action has been explained by a two-step process: penetration of the emulsifier monomeric entity and insertion in the lipid bilayer followed by micellar solubilization of lipids [15]. Thus, cutaneous application of emulsifiers incorporated in formulations might also lead to changes in SC lipid composition. To quantify such lipid changes, reliable and effective lipid analytical techniques are in need.

Research on lipid composition goes back to 1959, when Reinertson and Wheatley [19] published the chemical composition of human epidermal lipids. From then on, further studies on lipid content/concentration in skin have improved rapidly along with the great development of analytical methods, including gas chromatography (GC), liquid chromatography (LC), mass spectrometry (MS), high

* Corresponding author at: Department of Pharmaceutical Technology, Faculty of Science, University of Tuebingen, Auf der Morgenstelle 8, 72076 Tuebingen, Germany.
E-mail address: dominique.lunter@uni-tuebingen.de (D.J. Lunter).

https://doi.org/10.1016/j.ejpb.2018.02.006
Received 14 December 2017; Received in revised form 5 February 2018; Accepted 6 February 2018
Available online 08 February 2018
0939-6411/

Table 1
Examples of conventional techniques in skin lipid analysis.

Methods	Principle	Advantages	Drawbacks	Reference
Gas chromatography coupled with mass spectrometry (GC–MS)	Separation of volatile compounds with a carrier gas. Detection often achieved with mass spectrometry	Quick and efficient. Highly established in fatty acid analysis. Highly sensitive – analytes of low amount can be identified	Analytes need to be volatile. Derivatization of samples are necessary	[20–23]
Liquid chromatography coupled with mass spectrometry (LC–MS)	Separation, identification and quantification on a stationary phase under high pressure by elution with different solvents	High-quality separations are achievable. Coupling with MS is well established	Time consuming compared to GC	[24–27]
High performance thin layer chromatography (HPTLC)	Separation on a stationary phase (normally silica gel) due to polarity differences of the analytes	Variations of mobile phase enable separation of even complex mixtures. More sensitive than TLC	Time consuming for development of silica gel plates. Commonly destructive staining followed by charring needs to be done for quantification. Lower sensitivity than LC- or GC–MS	[2,28,29]

performance thin layer chromatography (HPTLC) and most commonly a combination of two of them. Table 1 provides examples of conventional instrumental methods so far applied in skin lipid analysis. All of these experimental methods are invasive, as they require lipid extraction from SC with various organic solvents. Moreover, for GC, lipid extracts need to be further derivatized so that they become sufficiently volatile to be eluted at reasonable temperatures without thermal decomposition. Hence, by means of all these conventional methods, samples undergo different levels of preliminary treatment before the actual analysis. This might lead to risks of loss, contamination or even chemical alteration of analytes. Besides, the whole analytical process, sample preparation in particular, is time-consuming. Therefore, a non-invasive and time-efficient method for skin lipid analysis is of exceptional interest.

Confocal Raman microscopy (CRM) is increasingly used in the field of pharmaceutical research in general [29], and in particular in skin research [30] due to the fact that it is a non-destructive and non-invasive analytical method. It can provide chemical information by peaks/bands at specific wavenumber in the recorded Raman spectrum. Besides, due to the linear dependency of Raman scattering on molecule amount, relative concentration of certain substances (e.g. SC lipids) can be determined by their contribution to the Raman bands. Furthermore, skin samples can be measured directly in 3-D dimensions without complex pre-treatment. In addition, CRM measurement takes relatively short time (several seconds to minutes). Based on these advantages, CRM is - – to the best of our knowledge - – firstly employed in the present study to detect endogenous lipid changes after emulsifiers treatment.

The aim of this study is to investigate the impact of emulsifiers and formulations on SC lipids. To this end, four different formulations were used: a total of three conventional creams that contained ionic and/or non-ionic emulsifiers and one surfactants free emulsion stabilized by a polymeric emulsifier. Additionally, all emulsifiers were tested in aqueous solution/dispersion in the respective concentrations as present in the formulations. CRM and HPTLC were employed to analyse changes in SC lipid concentration after treatment. Furthermore, lipid extraction was visualized by fluorescence staining and SC thickness was measured by light microscopy and CRM. Correlation between CRM and HPTLC results was conducted. This was done to assess if CRM can be used as a reliable and beneficial method in the application of skin lipid analysis. With easy sample preparation and immediate analytical readout, CRM has the potential to be a standardized analytical method for skin lipids investigation. Our work provides a foundation for the establishment of skin lipids analytical routines by CRM.

2. Materials and methods

2.1. Materials

Different materials used and their manufacturer information are as follows: cholesterol and palmitic acid (CHOL and PA; Alfa Aesar GmbH & Co KG, Karlsruhe, Germany), polysorbate 60, polyoxyethylene-20-glycerol monostearate, glycerol monostearate and cetyl stearyl alcohol (PS 60, PEG-20-GMS, GMS and CSA; Caesar & Loretz GmbH, Hilden, Germany), sodium lauryl sulfate (SLS; Cognis GmbH & Co. KG, Düsseldorf, Germany), cetearyl alcohol (and) sodium cetearyl sulfate (CA-SLS; BASF SE, Ludwigshafen, Germany), hydroxypropyl methyl cellulose (HPMC 2208; Metolose 90 SH 100 SR, Shin Etsu Chemical Co. Ltd, Tokyo, Japan), medium chain triglyceride (MCT; Myritol 318, BASF, Ludwigshafen, Germany), liquid paraffin (Hansen & Rosenthal KG, Hamburg, Germany), trypsin type II-S (lyophilized powder) and trypsin inhibitor (lyophilized powder) (Sigma-Aldrich Chemie GmbH, Steinheim, Germany), pyranine (Thermo Fisher (Kandel) GmbH, Karlsruhe, Germany), safranin (Carl Roth GmbH & Co. KG, Karlsruhe, Germany), Parafilm® (Bemis Company Inc., Oshkosh, Wis., USA), NEG-50™ (Thermo Fisher Scientific, Inc., US MA Waltham). Ceramide NP

Table 2
Formulations and emulsifiers that are used in this study.

Formulations	Emulsifiers	Abbreviation	Concentrations
Basic cream	Polyoxyethylene-20-glycerol monostearate	PEG-20-GMS	7%
	Glycerol monostearate	GMS	4%
Non-ionic cream	Polysorbate 60	PS 60	5%
	Cetylstearyl alcohol	CSA	10%
Anionic cream	Cetearyl alcohol (and) sodium cetearyl sulfate	CA-SLS	9%
HPMC-MCT emulsion	Hydroxypropyl methyl cellulose 2208 (Metolose 90 SH 100 SR)	HPMC	2.5%
Positive control	Sodium lauryl sulfate	SLS	1%

was kindly donated by Evonik Goldschmidt GmbH, Essen, Germany. Sodium chloride, disodium hydrogen phosphate, potassium dihydrogen phosphate, potassium chloride, and potassium hydroxide were of European Pharmacopoeia grade. Pig ears (German land race; age: 15 to –30 weeks; weight: 40 to –65 kg) were supplied by the Department of Experimental Medicine at the University of Tuebingen.

2.2. Methods

2.2.1. Preparation of formulations and emulsifier dispersions

Basic cream (Basiscreme DAC) was prepared according to instructions of German Drug Codex/New German Formulary (Deutscher Arzneimittel Codex/Neues Rezeptur Formularium, DAC/NRF) 2016. Anionic cream (Anionische hydrophile Creme) and non-ionic cream (Nichtionische Hydrophile Creme) were prepared according to the instructions of the German Pharmacopoeia (Deutsches Arzneibuch, DAB) 2015. HPMC stabilized emulsion was formulated according to Wollenweber et al. [31]. Composition and preparation methods of investigated formulations are provided in the appendix. Emulsifiers within these formulations were dissolved or dispersed in water and their concentrations remained the same as in formulations (Table 2). Water and SLS were used as negative and positive control.

2.2.2. Preparation of dermatomed pig ear skin

Fresh pig ears were washed with isotonic saline. After excision, the postauricular skin sheets were cleaned with isotonic saline by cotton swabs, blotted dry with tissue, wrapped in aluminium foil and stored at −30 °C. On the day of experiment, skin sheets were thawed to room temperature, cut into strips of 3 cm width and fixed to a block of Styrofoam (wrapped with aluminium foil) with pins. The hair was trimmed to approximately 0.5 mm with electric clippers (QC5115/15, Philips, Netherlands). Subsequently, the skin was dermatomed to a thickness of 1 mm (Dermatom GA 630, Aesculap AG & Co. KG, Tuttlingen, Germany) and cut with a circular hole punch to a diameter of 25 mm [32].

2.2.3. Tape stripping

Frozen pig ear skin was treated under the same procedures (as above) until hair being trimmed to 0.5 mm. Polyvinyl chloride adhesive tape (Tesafilm 4124 PV1, Beiersdorf, Hamburg, Germany), 3 cm wide and 10 cm long, was used. The tape was applied to the skin, rubbed lightly to assure adhesion, and then pulled off with one fluent and decisive movement. This procedure was repeated 10 times and each time was conducted with a new piece of tape [33]. Thereafter, the skin was dermatomed to a thickness of 1 mm (Dermatom GA 630, Aesculap AG & Co. KG, Tuttlingen, Germany) and cut with a circular hole punch to a diameter of 15 mm.

2.2.4. Incubation of pig ear skin in Franz diffusion cells

Incubation of pig ear skin was conducted using dermatomed skin and modified Franz diffusion cells (Gauer Glas, Püttlingen, Germany) with a receptor of 12 mL. Phosphate buffered saline pH 7.4 (PBS, Ph. Eur. 8.0) was used as receptor fluid. Degassed, prewarmed (32 °C) receptor medium was filled into Franz diffusion cells. Subsequently, cells were fitted with dermatomed pig ear skin (thickness: 1 mm, diameter: 25 mm) and donor compartments. Franz diffusion cells were mounted in a water bath heated to 32 °C. After a brief equilibrium period of 30 min, 1 mL of each emulsifier dispersion or formulation was applied to each skin sample. The cells were capped with Parafilm® to prevent evaporation of water. The stirring speed of the receptor fluid was 500 rpm [32]. After 4 h the skin samples were removed from the Franz diffusion cells. To remove remaining emulsifiers or formulations, cleaning procedure was done by gentle wiping using isotonic saline solution and cotton swabs for 30 times. The actual involved area (15 mm in diameter) of pig ear skin was patted dry and punched out for further study. All experiments were performed in triplicate.

2.2.5. Preparation of isolated stratum corneum (SC)

Isolated SC was obtained by incubating the samples at room temperature overnight following a modified protocol of Kligman et al. [34]. The dermatomed skin was placed dermal side down on filter paper soaked with a 0.2% trypsin and phosphate buffer saline solution (pH 7.4). Digested material was peeled off with a blunt pair of tweezers. The isolated SC was immersed in a 0.05% trypsin inhibitor solution for 1 min and subsequently washed with fresh demineralised water for five times. Cleaned SC sheets were dried and stored above silica gel in a desiccator for at least three days before analysis.

2.2.6. Confocal Raman microscopy (CRM) analysis

CRM measurements on isolated SC sheets were conducted immediately after samples had been taken out of the desiccator. Dried SC sheets were deposited on glass slides and spectra were recorded. Raman spectra were acquired with an α 500R confocal Raman microscope (WITec GmbH, Ulm, Germany) equipped with a 532-nm excitation laser source and UHTS 300 spectrometer. A 100 × objective (numerical aperture 0.9, EC Epiplan-neofluor, Carl Zeiss, Germany) was used to focus the light on SC and to collect scattered light. Backscattered light from the samples was dispersed by an optical grating and projected on a charge-coupled device, DV401-BV CCD detector, and cooled to −60 °C. The laser intensity was adjusted to 10 mW, measured as intensity before the objective using an optical power meter (PM100D, Thorlabs GmbH, Dachau, Germany).

Each single spectrum was recorded using a 100 × objective (numerical aperture 0.9) with a grating of 1800 g/mm, an exposure time of 2 s, and 20 accumulations in each spot. A depth resolution of 800 nm was achieved. The spectral range covered the “fingerprint region” between 710 and 1820 cm^{-1}. Cosmic ray removal and spectral background subtraction were performed by the WITec Project Plus software (WITec GmbH, Ulm, Germany). The peak areas of selected peaks were calculated as the area under the curve by trapezoidal method using WiTec Project 4 software. The peaks of interest were the δ(CH_2, CH_3)-mode at 1425–1495 cm^{-1} and the ν(C═O)-mode at 1630–1714 cm^{-1}. The δ(CH_2, CH_3)-mode arises from lipids and proteins and is referred to as the “lipids-peak” [35–37]. Thus, it was chosen to detect lipid changes in SC. The ν(C═O)-mode at 1630–1714 cm^{-1} is attributed to amide I according to literature [35–37]. In preliminary experiments, this peak showed the least variation within one donor as well as among different donors, thus Raman signals were normalized to this peak prior to further comparison (data not shown). Normalized δ(CH_2, CH_3)-mode value was calculated using the following equation:

$$Normalized\delta(CH_2,\ CH_3)=\frac{AUC\delta(CH_2,\ CH_3)}{AUC\nu(C=O)} \quad (1)$$

where AUC is the integrated area under specified peak in a single CRM spectrum.

For each sample, CRM measurements were conducted after emulsifiers or formulations treatment and after lipid extraction.

The thickness of SC was determined using the keratin signal ($\nu(CH_3)$, 2800–3000 cm^{-1}) by moving focus point from under a SC sheet (−50 μm) to above (50 μm) with a step size of 1 μm. The area under the keratin signal was extracted and plotted against the depth. Full width at half maximum of this curve peak was calculated and regarded as the SC thickness (see Appendix). For each treatment three SC sheets were used and spectra were recorded at three random spots for each SC sheet, resulting in a total of nine measurements.

2.2.7. Lipid extraction

The isolated SC sheets (pre-treated with emulsifiers or formulations) were extracted by ethyl acetate:methanol (20:80, v/v) [2] for 3 h under stirring at room temperature. Thereafter, delipidised SC sheets were dried at room temperature and stored in a desiccator for at least three days before subjected to CRM analysis. On the other hand, extracted lipids mixture in organic solvent was evaporated under nitrogen flow. Dried lipid powder was re-dissolved in chloroform:methanol (2:1, v/v) mixture and stored at −20 °C for further high-performance thin-layer chromatography (HPTLC) study.

2.2.8. High-performance thin-layer chromatography (HPTLC)

HPTLC silica gel plates, 10 × 20 cm (Macherey-Nagel GmbH & Co. KG, Düren, Germany) were firstly cleaned once by development with chloroform : methanol (2:1, v/v) [27]. Lipid extracts and a series of standard lipid mixtures of appropriate quantities were applied under a flow of air on the HPTLC plates using Linomat V (CAMAG, Muttenz, Switzerland). The chromatograms were developed twice in a saturated developing tank (CAMAG, Muttenz, Switzerland) with the mobile phase of dichloromethane : methanol : acetic acid (66:2.7:0.075, v/v/v) up to 6 cm migration distance from the starting line. This is a modified procedure originally described by Wertz et al. [38]. The HPTLC plates were air-dried, dipped into 7.5% copper acetate and 2.5% copper sulfate in 8% phosphoric acid (w/w) solution for 20 s and charred at 180 °C for 20 min. After cooling down to room temperature, images of TLC plates were taken by a digital camera (DSC-RX100M3, Sony, Tokyo, Japan) in a closed box where light was evenly distributed. Images were sequentially quantified by ImageJ bundled with Java 1.6.0_24 (https://imagej.nih.gov/ij/). Quantification of lipid fractions was based on the calibration of lipid standards. The intercept of calibration curves was used to perform LOD and LOQ calculation (Table 3) [39]. Quantitative results of all ceramides were related to ceramide NP, and all free fatty acids to palmitic acid. Apart from that, to each HPTLC plate at least one mixture of lipid standards was applied to correct variations in HPTLC resolution.

2.2.9. Histology study

Actual experimental area of pig ear skin was punched out, patted dry with cotton swabs and quickly frozen in liquid nitrogen. The frozen biopsies were partially placed in an aluminium foil cylinder and processed by fixation in NEG-50™ at −60 °C. Samples (thickness 16 μm) were sliced perpendicular to the skin surface with a cryotome (HM 560 Cryo-Star, Thermo Fisher Scientific Inc., Langenselbold, Germany), and the cuts were transferred to glass slides [40,41]. After fixation in cold acetone (4 °C), the sections were stained for 1 min with a 1% (w/v) aqueous safranin solution. Subsequently, the sections were washed with deionized water for 30 s. To allow the corneocytes to swell, a 2% (w/v) potassium hydroxide aqueous solution was applied to the samples during 20 min [42]. Safranin produces clear reddened intensification of the intercellular portions of the SC even in the presence of potassium hydroxide solution. Visualization was performed using a light microscope combined with a digital camera (Microscope Axio Imager Z1, Carl Zeiss, Jena, Germany). The method for determination of the number of cell layers in the SC was based on that reported by Christophers and Kligman [43] in principle and was a modification of that described by Blair [44]. Visualization was done within 10 min to avoid evaporation of water and re-crystallization of potassium hydroxide. The number of corneocytes layers was counted at 18 different locations, avoiding the sites of sweat pores and follicular ostia.

In order to observe the lipid matrix between corneocytes, pyranine was used to stain the cross-section. Dry SC samples were agitated in a 3 mg/mL pyranine aqueous solution for 60 s and subsequently washed in deionized water for 5 min to remove unbound pyranine [45]. Thereafter, samples were deposited on a glass slide and allowed to dry for three days. Examinations of fluorescence were performed by illuminating samples with blue light (450–490 nm) using a microscope (Microscope Axio Imager Z1, Carl Zeiss, Jena, Germany) with a 20 × objective (numerical aperture 0.8, Plan-Apochromat, Carl Zeiss, Jena, Germany).

Table 3
HPTLC calibration of lipid standards.

Compounds	Range	r^2	LOD	LOQ
Cholesterol	2.38–11.9 μg	0.9942	0.58 μg	1.76 μg
Ceramides[1]	1.95–11.7 μg	0.9979	0.42 μg	1.29 μg
Free fatty acids[2]	1.3–7.8 μg	0.9984	0.30 μg	0.92 μg

[1] Related to ceramide NP.
[2] Related to palmitic acid.

2.3. Statistical analysis

Data were acquired from repeated experiments (n ≥ 3). Diagrams show arithmetic mean ± standard deviation (mean ± SD). Statistical differences were determined by a one-way ANOVA followed by the Student-Newman-Keuls (SNK) test or pairwise *t*-test ($p < 0.05$), which were performed using GraphPad Prism 4.0 (GraphPad Software Inc, La Jolla, CA, USA). Data that are significantly different are marked with an asterisk (*).

3. Results

In order to get an insight into the influence of emulsifiers and formulations treatment on SC, common methods, such as HPTLC and fluorescent staining techniques, were performed to evaluate the lipid compositional changes. As an alternative, non-destructive CRM was firstly employed in the present study to assess such effects with easy sample preparation and immediate analytical readout in contrast to aforementioned conventional methods.

3.1. Lipid analysis utilizing CRM

Fig. 1 illustrates a typical CRM spectrum in the full region from 0 to 3800 cm^{-1} for water treated SC. The $\delta(CH_2, CH_3)$-mode at 1425–1495 cm^{-1} and the $\nu(C{=}O)$-mode at 1630–1714 cm^{-1} are marked. In this study, SC treated with water, different emulsifiers and formulations generated Raman peaks in the same range and height, emphasising good reproducibility of CRM measurement. The $\nu(C{=}O)$-mode at 1630–1714 cm^{-1} (amide I-mode) had shown the least variation within one donor as well as among different donors, thus Raman signals were normalized to this peak prior to further comparison. The $\delta(CH_2, CH_3)$-mode arises from lipids and proteins and is referred to as the “lipids-peak” [35–37]. Thus, it was chosen to detect lipid changes in SC.

The normalized $\delta(CH_2, CH_3)$-signals after water and various emulsifiers treatment are shown in Fig. 2A. Water treated SC presented a normalized $\delta(CH_2, CH_3)$-mode value of 0.76. Compared to the reference, PS 60, CSA and their mixture treated SC showed no significant changes in $\delta(CH_2, CH_3)$-signal, indicating they had no obvious effects on intercellular lipid domains in SC. Whereas in other emulsifiers treated SC samples, significant decreases in $\delta(CH_2, CH_3)$-mode could be seen. The $\delta(CH_2, CH_3)$-mode was reduced by GMS, PEG-20-GMS and

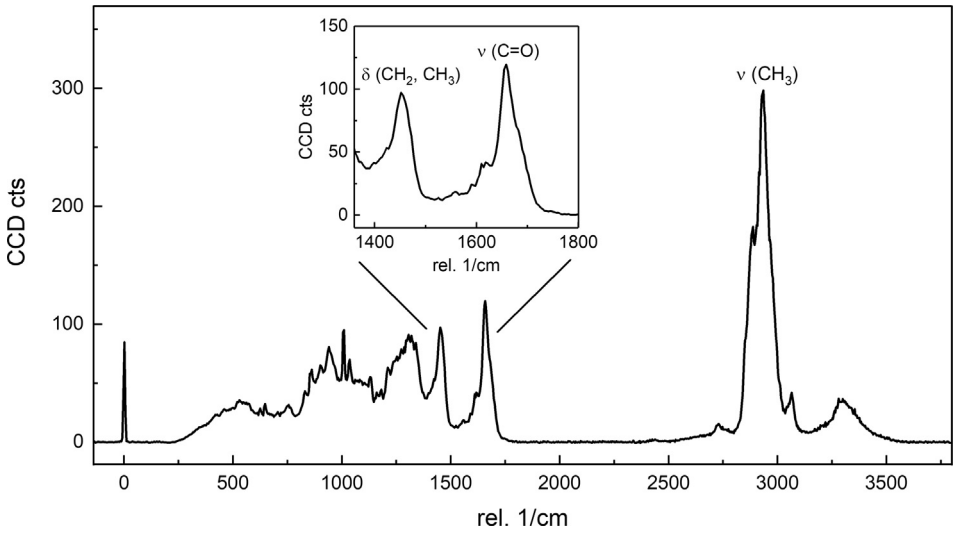

Fig. 1. A typical CRM spectrum in the region from 0 to 3800 cm^{-1} for water treated porcine SC, inserted chart: zoomed-in CRM spectrum in the range between 1300 and 1800 cm^{-1}.

their mixture as well as HPMC to a similar extent, from 5 to 8%. For ionic CA-SLS, a more pronounced reduction of 11% was found. SLS, as the positive control, lead to the most substantial reduction by 25% for δ(CH_2, CH_3)-mode (Table 4). These results indicate a decrease of lipid content in intercellular region of SC after treatment with various emulsifiers.

Lipid extraction can be explained by the nature of solubility-enhancement of emulsifiers [46,47]. During the incubation period in Franz diffusion cells, surface-active emulsifiers, serving as solubilizer, improve the solubility of lipids in the donor compartment. In other words, they facilitate lipid extraction from SC. Therefore, we can conclude that, various kinds of emulsifiers have different capabilities to extract lipids from the stratum corneum.

Fig. 2B shows normalized δ(CH_2, CH_3)-signals after water and formulations treatment. It can be seen that there were no significant changes in normalized δ(CH_2, CH_3)-mode, indicating no significant effects on lipid amount in SC for all studied formulations.

To further characterise the skin lipids and in an attempt to validate the CRM results lipids were extracted from the SC sheets after treatment with formulations or emulsifiers. The extract was subjected to HPTLC analysis and the delipidised SC sheets were subjected to another CRM investigation. Results showed lower normalized peak areas for delipidised SC sheets (Fig. 2). This remaining value of the δ(CH_2, CH_3)-signal corresponds to the signal which results from protein and covalently bond lipids that are impossible to be extracted [36]. A normalized δ(CH_2, CH_3)-mode value of around 0.57 was thus regarded as an indication of effective lipid extraction. All emulsifiers or formulations treated SC sheets gave higher values than 0.57. This indicates that none

Table 4
Characteristics of emulsifiers and their impact on SC lipid reduction, mean, n = 9, $p < 0.05$.

Emulsifier/-mixture	Concentration	HLB value	Reduction of SC lipids by
PEG-20-GMS	7%	16	4.3%*
GMS	4%	7	6.8%*
PS 60	5%	15	n.s.
CSA	10%	1	n.s.
CA-SLS			11%*
Consists of	9%		
> 80% CA	> 7.2%	4	
> 7% SLS	> 0.63%		
HPMC	2.5%	n.a.	5.6%*
SLS	1%	40	25%*

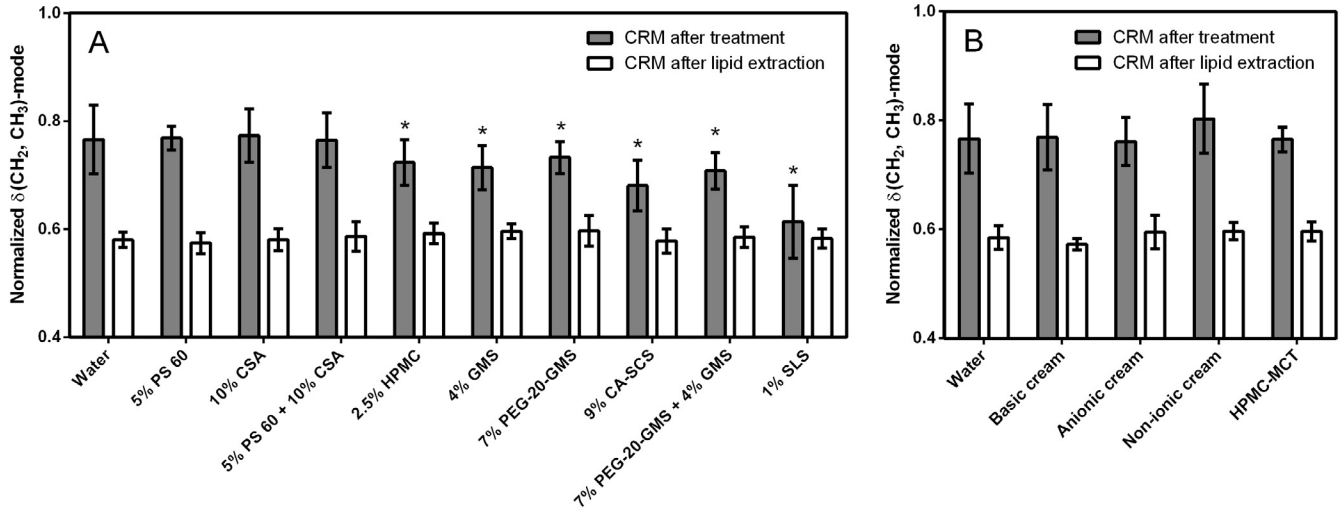

Fig. 2. Normalized δ (CH2, CH3)-signal at 1425–1495 cm^{-1} after treatment and after lipid extraction, A: emulsifiers treated SC, B: formulations treated SC, mean ± SD, n = 9, *significant difference (ANOVA, SNK; $p < 0.05$).

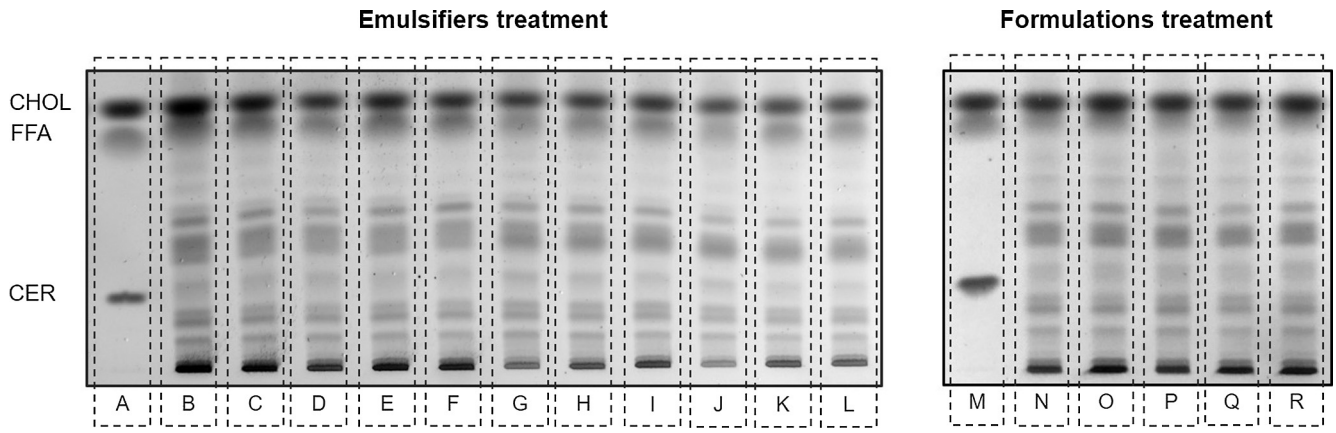

Fig. 3. Representative HPTLC plates of lipids extracted from SC after treatment with emulsifiers (left) and formulations (right), A: lipid standards, B: water, C: PS 60, D: CSA, E: PS 60 + CSA, F: HPMC, G: water, H: GMS, I: PEG-20-GMS, J: CA-SLS, K: PEG-20-GMS + GMS, L: SLS, M: lipid standards, N: water, O: basic cream, P: anionic cream, Q: non-ionic cream and R: HPMC-MCT. From B to F, G to L, M to R are samples from one donor, respectively.

of the formulations or emulsifiers was capable of withdrawing all lipids from the SC.

3.2. HPTLC study

As results from CRM suggested lipid extraction from SC by different emulsifiers, an HPTLC study of SC lipid extracts was carried out. Results are given in Figs. 3 and 4.

Compared with the reference (water treated), all studied formulations, PS 60, CSA, as well as their mixture showed no obvious distinction in any extract levels, indicating no lipid extraction by any treatment. However, HPMC, GMS, PEG-20-GMS and their mixture presented differently decreased levels of lipids, values ranging from 5% to 10%. This trend is more obvious in CA-SLS treated SC. Besides, as a positive control, SLS treated SC exhibited the most substantial reduction of lipid extracts by 27%. These results demonstrated decreases in the remaining lipid content post incubation with various emulsifiers, implying lipid withdrawal during emulsifiers treatment in Franz cells. This conclusion is consistent with those of CRM analysis. Thus, in this point of view, CRM can be proven to be a potential assessing method for lipid content in dermatology field.

More interestingly, if we take a further look at each lipid fraction, it was found that free fatty acids decreased to a higher extent than cholesterol and ceramides. Weerheim and Ponec [2] showed that the levels of free fatty acids were the highest in the uppermost SC layers. They are thus assumed to be easily extracted by emulsifiers in our study as they are in direct contact during the experiment.

3.3. Fluorescent imaging

In order to additionally evaluate the barrier disruption of SC by emulsifiers and formulations treatment, a tissue staining technique with pyranine was conducted. This method was previously used to estimate in vivo subclinical injury caused by SLS [45]. SC with less barrier integrity is stained more intensely compared to normal SC, which is nowadays believed as pyranine binds to keratin filaments that are exposed to the dye as intercellular lipids are extracted [45]. In our study, SLS treated SC (Fig. 5J) showed a markedly increase intensity in contrast with the reference (Fig. 5A), which complies with reported literature [45]. Other investigated emulsifiers and formulations exhibited different extent of increased fluorescent intensity, indicating different abilities of lipid extraction and barrier impairment (Figs. 5 and 6).

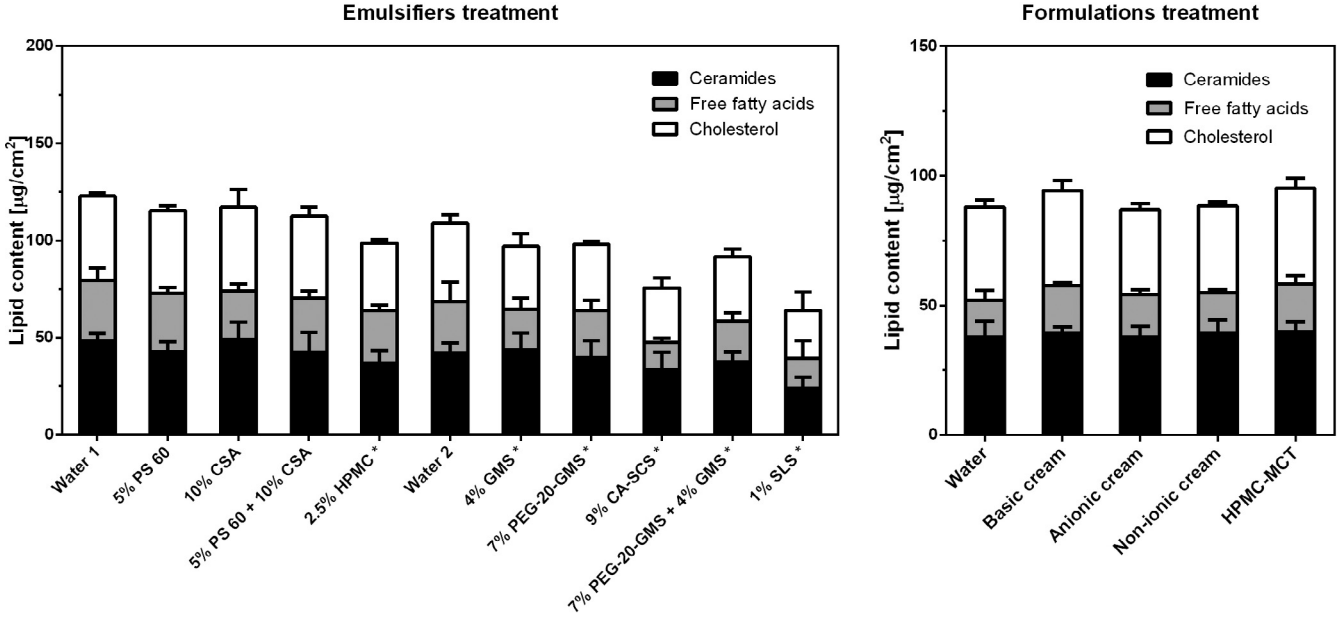

Fig. 4. Levels of major stratum corneum lipids, ceramides, free fatty acids and cholesterol following lipid extraction and high-performance thin-layer chromatography separation. In emulsifiers treatment study, water 1 to HPMC are samples from one donor and water 2 to SLS are from another donor, mean ± SD, n = 3.

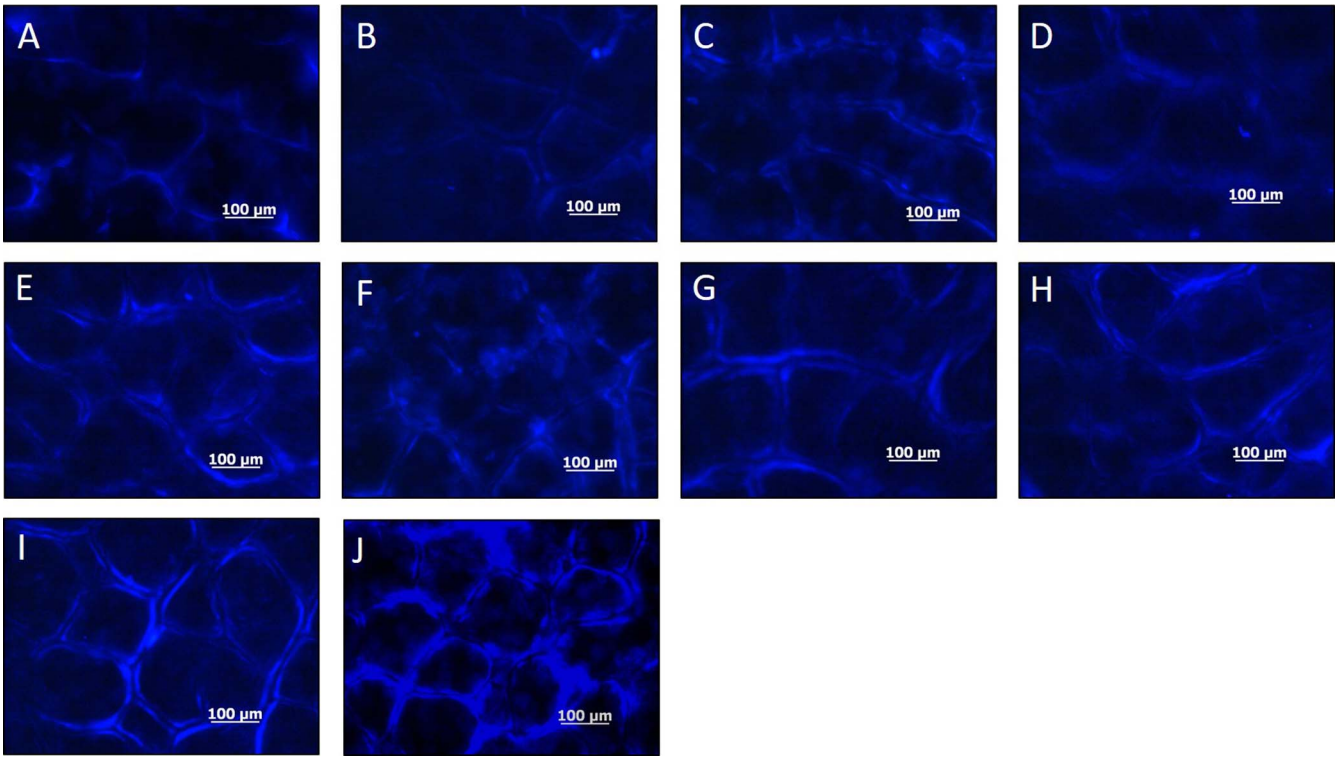

Fig. 5. Microscopic image of pyranine stained porcine skin after the treatment of A: water, B: PS 60, C: CSA, D: PS 60 + CSA, E: GMS, F: PEG-20-GMS, G: PEG-20-GMS + GMS, H: HPMC, I: CA-SLS and J: SLS.

Specifically, CA-SLS (Fig. 5I) caused the most intense fluorescence, followed by GMS, PEG-20-GMS and their mixture as well as HPMC (Fig. 5E–H) in a similar level. PS 60, CSA, their mixture (Fig. 5B–D) as well as formulations (Fig. 6) showed no increases. These results are in accordance with those of HPTLC and CRM results and give further proof of the assumption that CA-SLS, GMS, PEG-20-GMS and their mixture withdraw lipids from SC while other emulsifiers and formulations do not.

3.4. Thickness estimation utilizing CRM

Visual inspection of SC sheets after treatment with different emulsifiers gave clear hints that some sheets were thinner compared to the reference. It thus appeared reasonable to raise the question whether the emulsifiers-induced lipid extraction also affected SC thickness. This hypothesis was assessed utilizing CRM. Fig. 7 presents SC thickness after treatment with water, emulsifiers and formulations.

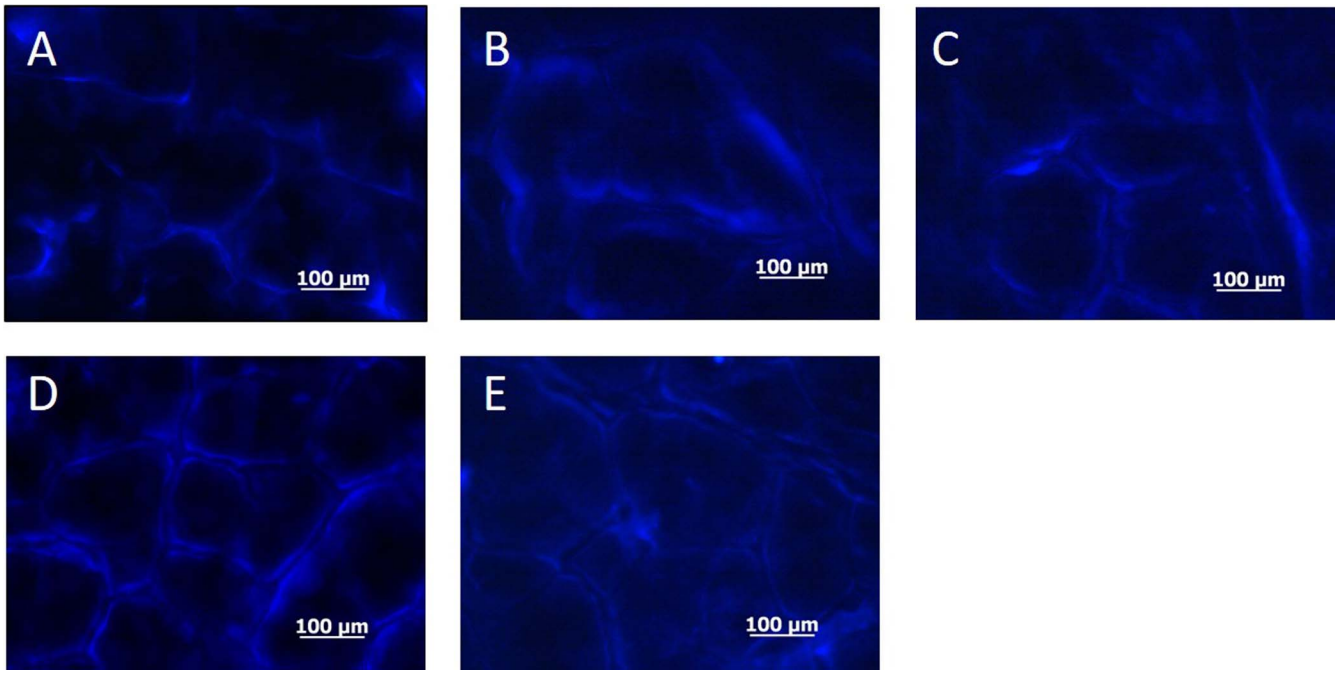

Fig. 6. Microscopic image of pyranine stained porcine skin by the treatment of formulations, A: water, B: non-ionic cream, C: anionic cream, D: basic cream and E: HPMC-MCT emulsion.

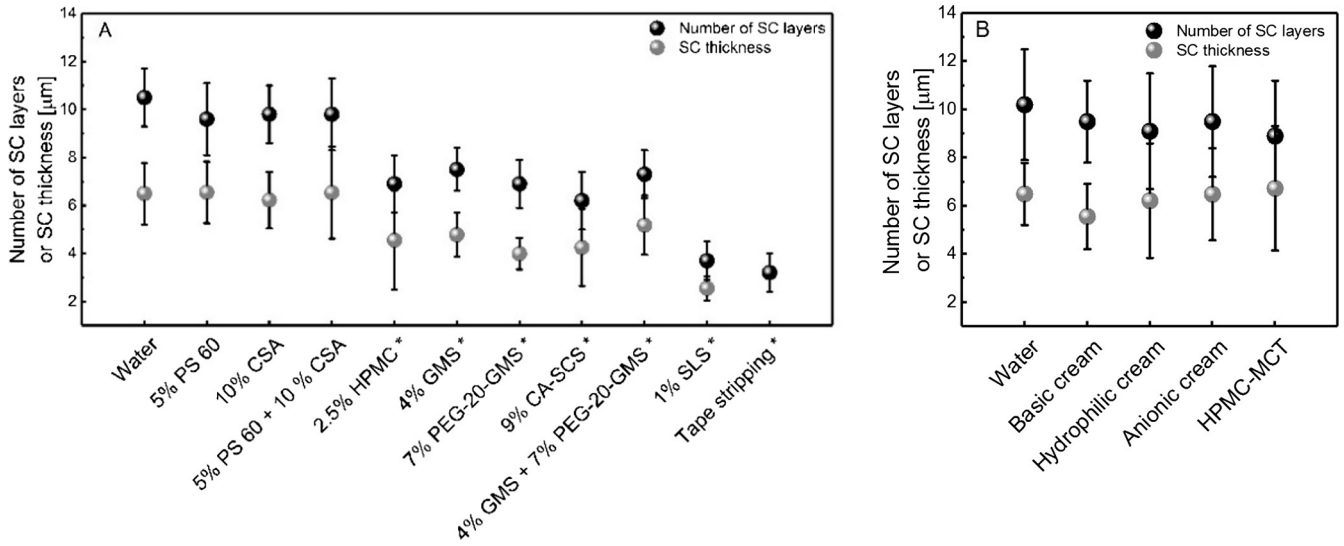

Fig. 7. Corneocytes layers and thickness of SC after treatment with emulsifiers (A) and formulations (B), mean ± SD, n = 9 or 18, $p < 0.05$.

Water treated SC exhibited an average thickness of 6.5 ± 1.29 µm. The measured thickness here corresponds to dried SC thickness and is smaller compared to that of native SC [48]. This is due to that native SC contains a certain amount of water, and corneocytes are swollen and larger in volume. All formulations, PS 60, CSA and their mixture treated SC samples showed no obvious difference in contrast with the reference. Whereas, all the rest of the investigated emulsifiers showed significantly reduced thickness of SC: GMS, PEG-20-GMS and their mixture, as well as HPMC exhibited an average thickness of approximately 4 µm, respectively; SLS showed the trend to an even more pronounced reduction of SC thickness of 2.6 µm. It can therefore be said that SC barrier was evidently disrupted by various emulsifiers but not by formulations treatment. This SC barrier damage trend is in accordance with the results of normalized δ (CH_2, CH_3)-signal (see Fig. 2), implying the reduced SC thickness resulted from the decrease of lipid content. However, SC membrane does not solely consist of lipids but contains corneocytes that are embedded in the lipid lamellar regions, which is widely described as a "brick and mortar" model [1]. Now, another question rises whether the decreased SC thickness comes from lipid extraction solely or a synchronous removal of corneocytes. Results of thickness measurement after tape stripping indicate that the latter might be the case as tape stripped skin and SLS treated skin show similar thickness. A histology study was performed for further visual observation.

3.5. Histology study

The histological features of safranin stained cross-sections of porcine skin are depicted in Fig. 8. For comparison, tape-stripping exhibited a pronounced reduction of SC layers (Fig. 8K). Interestingly, a lower number of corneocytes layers were also observed after treatment with different emulsifiers. The comparison of the number of corneocytes layers after emulsifiers treatment is shown in Fig. 7A. It can be seen that there were approximately 10 corneocytes layers in water treated porcine postauricular ear skin (Fig. 7A), whereas after incubation with various emulsifiers, significant amount of corneocytes layers were removed. The results are thus in line with the findings of SC thickness measurement by CRM.

Figs. 7B and 9 describe corneocytes layers after formulations treatment. Corneoctytes layers are well maintained. Meanwhile, no significant reduction of δ(CH_2, CH_3)-signal after formulations treatment (Fig. 2B) was found. These results indicate all investigated formulations do not have an influence on lipid and corneocytes amount.

4. Discussion

We investigated different types of emulsifiers that are used in conventional creams on their ability to extract lipids from the SC. We used non-ionic as well as ionic emulsifiers and one polymeric emulsifier. Obviously, lipid extraction from the SC depends on the type of emulsifier used. We found that the different emulsifiers and emulsifier mixtures had different effects on SC lipids content and SC thickness. Interestingly, emulsifiers and emulsifier mixtures that reduced the lipids content also reduced SC thickness. It could be shown that the reduction of SC thickness is not only due to lipid extration, but also due to corneocytes removal. Our hypothetical explanation is, as lipids were withdrawn from SC during incubation, cohesion of the top layers of corneocytes is impaired. Consequently, certain amount of corneocytes are removed with cotton swabs in cleaning procedures. However, the reduction of SC lipids seems to be the underlying cause of the destabilization of the SC matrix.

It could have been expected that the ability to extract lipids would correlate with the HLB-value of the emulsifier. Our experiments only partially comply with this assumption. SLS which exhibits the highest HLB-value of about 40 extracts the highest amount of lipids from the skin. CSA which exhibits the lowest HLB-value extracts the least lipids. GMS with a HLB-value of 7 extracts less lipids from the skin than PEG-20-GMS with a HLB-value of 16. CA-SLS consists of min. 7% SLS and min. 80% CA (according to European Pharmacopoeia). It reduces the lipids peak by 11% whereas SLS decreases it by 25%. SLS was used in 1% concentration whereas CA-SLS was used in 9% concentration which makes a concentration of 0.63% regarding SLS. The decreased level of lipids extraction can thus be explained by a reduced concentration of SLS which is the main lipid extracting component of the CA-SLS mixture. Interestingly, PS 60 with a HLB-value of 15 does not affect SC lipids content. This cannot be explained by its concentration which is 5% and therefore in the same range as that of PEG-20-GMS (7%) that exhibits a similar HLB-value and does extract lipids from the skin. A possible explanation might be that the size and shape of PS 60 is too large to effectively penetrate the SC in order to extract lipids from it. The fact that HPMC extracts lipids from the skin in a range similar to that of PEG-20-GMS and CA-SLS is somewhat unexpected as polymeric emulsifiers are commonly believed to be less harmful to the skin compared to pegylated and ionic emulsifiers. From another side of view, the lipid extraction ability would probably correlate with the solubilization potential of different emulsifier systems. If this were the case, skin lipids showed distinct behaviours in different emulsifier systems. This might explain why PS 60 dispersion does not affect SC

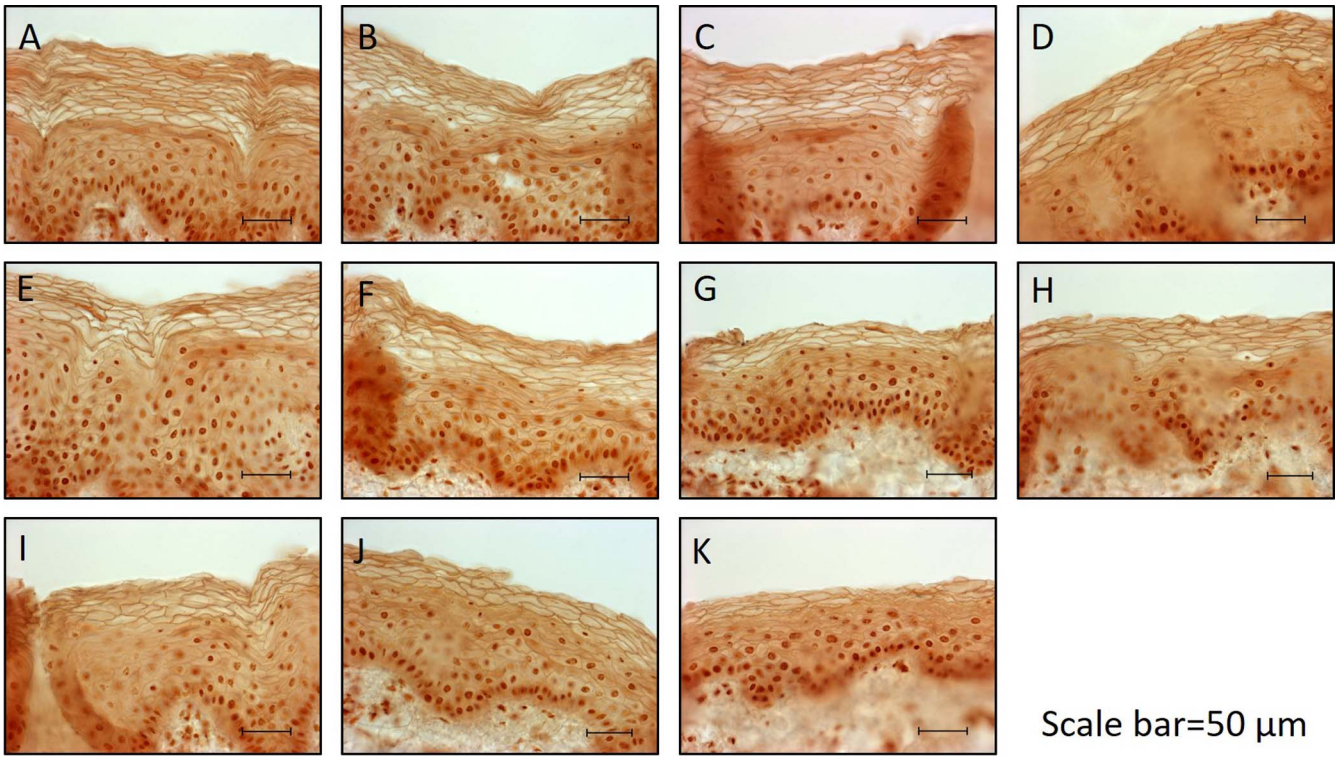

Fig. 8. Microscopic image of safranin stained porcine skin after the treatment of A: water, B: PS 60, C: CSA, D: PS 60 + CSA, E: GMS, F: PEG-20-GMS, G: PEG-20-GMS + GMS, H: HPMC, I: CA-SLS, J: SLS and K: tape stripping.

lipid content whereas unexpectedly the polymeric emulsifier HPMC does. However, further experiments should be done to verify this assumption. Therefore, a systematic and in-depth investigation is of great interest.

In contrast to the single emulsifiers, none of the tested formulations had any effect on lipids content of the SC although formulations contained the emulsifiers in the same concentration as the emulsifier solutions. This indicates that the emulsifiers are bound to the interfacial layers in the creams or emulsions. Interactions with the oil phase of the formulations are strong enough to saturate all binding sites and therefore emulsifiers cannot engage in interactions with the SC lipids.

As the major aim of this study was to investigate the capability of CRM to evaluate the impact of emulsifiers and formulations treatment on SC lipids, we measured SC lipids content as well as SC thickness by CRM and by the conventional methods HPTLC and light microscopy, respectively. To establish a correlation we plotted results from CRM against results from conventional methods (Figs. 10 and 11).

CRM led to similar results as the conventional methods. From the

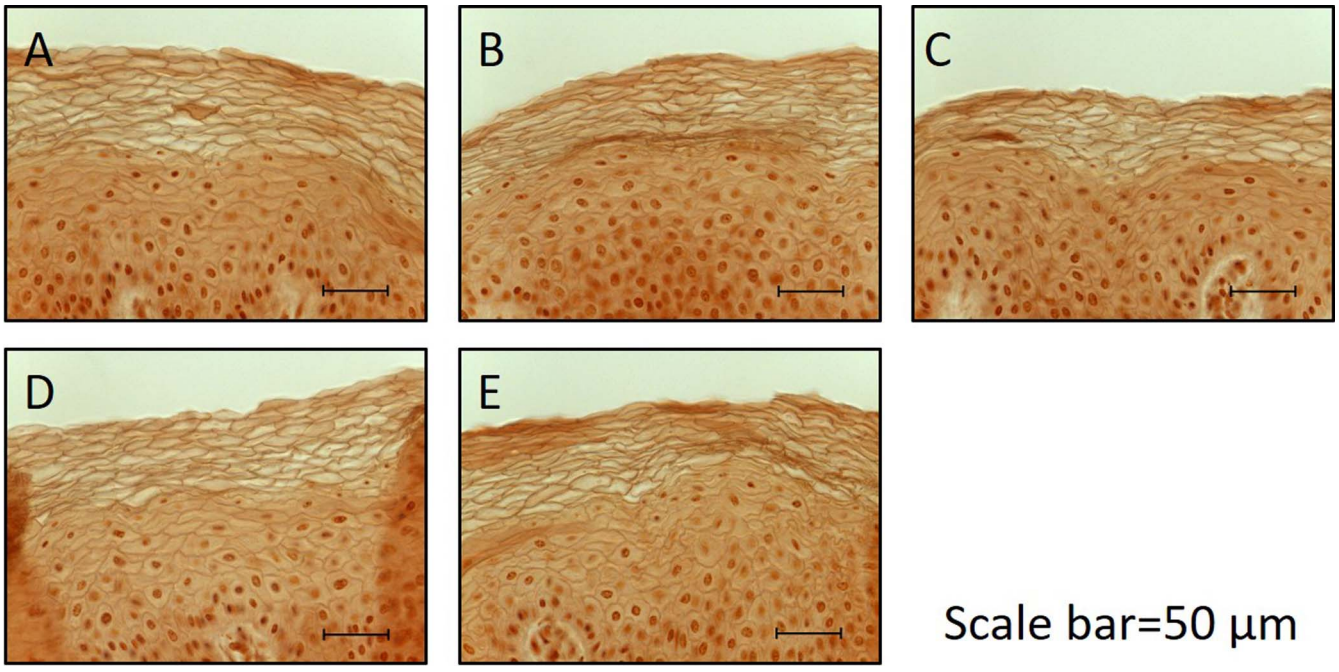

Fig. 9. Microscopic image of safranin stained porcine skin by the treatment of formulations, A: water, B: non-ionic cream, C: anionic cream, D: basic cream and E: HPMC-MCT emulsion.

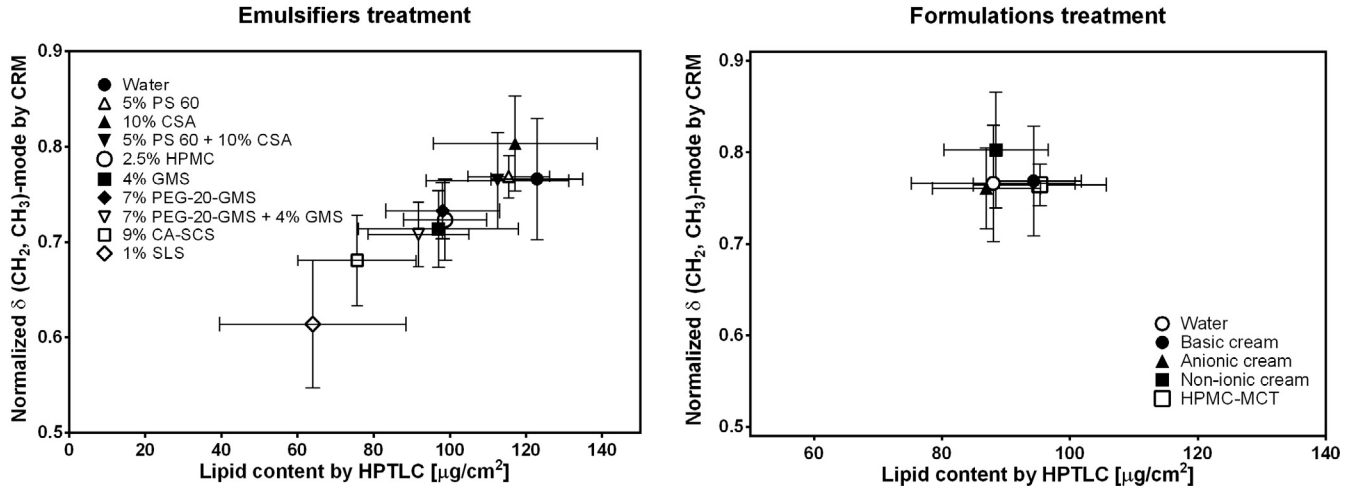

Fig. 10. Correlation plot of SC lipids content measured by CRM (y-axis) and HPTLC (pooled ceramides, cholesterol and free fatty acids content; x-axis); left: after emulsifiers treatment, right: after formulations treatment.

correlation plots, it can clearly be seen that there is a strong positive correlation between CRM and conventional methods both for lipids content and SC thickness measurements. This further proves the excellent correlation and shows that CRM can be used as an alternative technique to measure lipid content and SC thickness. Its ease of handling with no sample preparation, extraction or staining needed and short measurement times make it a versatile tool for SC investigation. Nevertheless, if a more detailed analysis of SC lipids (e. g. separate analysis of ceramides, cholesterol or free fatty acids) is aimed for, HPTLC remains the preferable method. For more detailed analyses still more sophisticated methods are required.

5. Conclusion

This study elucidates the influence of emulsifiers and formulations on porcine SC by means of CRM, HPTLC and histological staining. Lipids were withdrawn by emulsifier dispersions during incubation period, leading to decreased lipid-related signal in Raman spectra. Likewise, the latter was confirmed by HPTLC results. In contrast, the same emulsifiers incorporated in respective formulations were shown not to affect lipids content. CRM, HPTLC and pyranine staining experiments lead to a similar conclusion on lipid extraction from the skin. It was further shown that lipid extraction is the reason for SC thinning caused by different emulsifiers. Quantification of lipids extraction from CRM measurements correlate very well with results from HPTLC-analysis which can be regarded as one of the standard techniques in SC lipid quantification. CRM can thus be used as an alternative to HPTLC if the lipid content of SC samples is to be investigated.

This work may therefore serve as a basis for a systematic evaluation of the effects of emulsifiers and formulations on SC lipids. This would be of interest to develop formulations for patients suffering from skin problems, especially those that are characterized by impaired barrier function of SC, e.g. non-lesional skin atopic eczema, psoriasis and lamellar ichthyosis [27].

Acknowledgements

PD Dr. Martin Schenk is acknowledged for the donation of pig ears. This project was supported by the European Social Fund and by the Ministry of Science, Research and the Arts Baden-Wuerttemberg and the China Scholarship Council. Evonik Goldschmidt GmbH, Essen, Germany was kindly thanked for donating ceramide NP. We would like to thank Luis Quintairos for his work in pyranine staining.

Statement of ethics

Pig ears were received from the Department of Experimental Medicine of the University Hospital Tuebingen. The live animals were

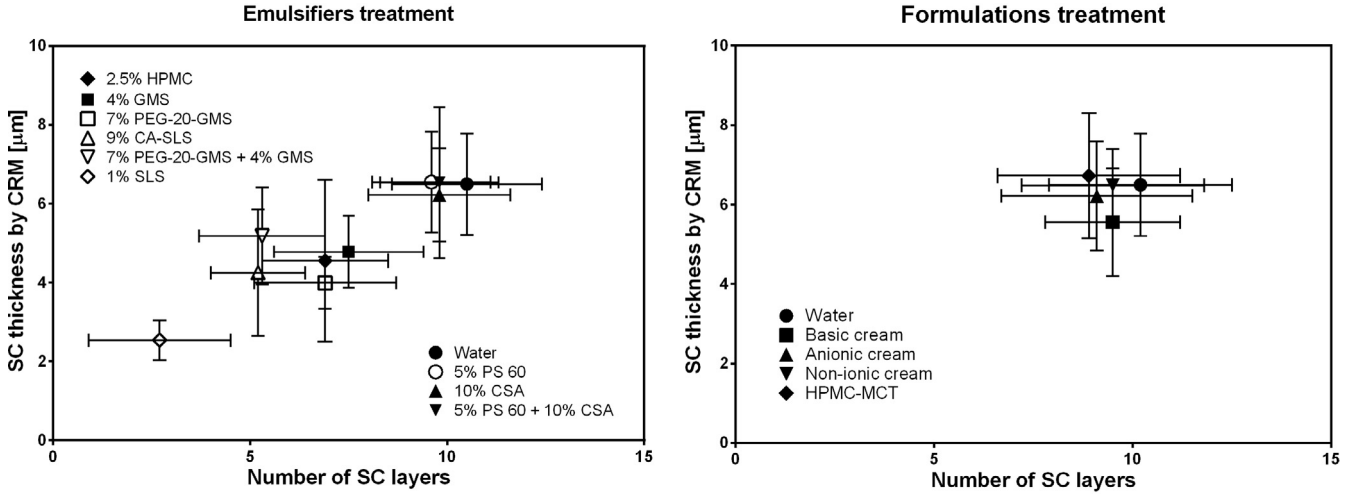

Fig. 11. Correlation plot of SC thickness measured by CRM (y-axis) and light microscopy after safranin staining; left: after emulsifiers treatment, right: after formulations treatment.

kept at the Department of Experimental Medicine and were sacrificed in the course of their experiments, with the approval of the Ethics Committee of the University Hospital Tubingen. The ears were received directly after the death of the animals. The Department of Pharmaceutical Technology is registered for the use of animal products at the District Office of Tuebingen (registration number: DE 08 416 1052 21).

Disclosure statement

The authors report no conflicts of interest.

Appendix A. Supplementary material

Supplementary data associated with this article can be found, in the online version, at https://doi.org/10.1016/j.ejpb.2018.02.006.

References

[1] P.M. Elias, Epidermal lipids, barrier function, and desquamation, J. Invest. Dermatol. 80 (1983).
[2] A. Weerheim, M. Ponec, Determination of stratum corneum lipid profile by tape stripping in combination with high-performance thin-layer chromatography, Arch. Dermatol. Res. 293 (2001) 191–199.
[3] F.F. Sahle, T. Gebre-Mariam, B. Dobner, J. Wohlrab, R.H. Neubert, Skin diseases associated with the depletion of stratum corneum lipids and stratum corneum lipid substitution therapy, Skin Pharmacol. Physiol. 28 (2015) 42–55.
[4] B.P. Binks, J.A. Rodrigues, W.J. Frith, Synergistic interaction in emulsions stabilized by a mixture of silica nanoparticles and cationic surfactant, Langmuir 23 (2007) 3626–3636.
[5] R.N. Gursoy, S. Benita, Self-emulsifying drug delivery systems (SEDDS) for improved oral delivery of lipophilic drugs, Biomed. Pharmacother. 58 (2004) 173–182.
[6] S. Tcholakova, N. Denkov, A. Lips, Comparison of solid particles, globular proteins and surfactants as emulsifiers, Phys. Chem. Chem. Phys. 10 (2008) 1608–1627.
[7] A. Nesterenko, A. Drelich, H. Lu, D. Clausse, I. Pezron, Influence of a mixed particle/surfactant emulsifier system on water-in-oil emulsion stability, Colloids Surf. Physicochem. Eng. Aspects 457 (2014) 49–57.
[8] N.I. Politova, S. Tcholakova, S. Tsibranska, N.D. Denkov, K. Muelheims, Coalescence stability of water-in-oil drops: effects of drop size and surfactant concentration, Colloids Surf. Physicochem. Eng. Aspects 531 (2017) 32–39.
[9] P.P. Sarpotdar, J.L. Zatz, Evaluation of penetration enhancement of lidocaine by nonionic surfactants through hairless mouse skin in vitro, J. Pharm. Sci. 75 (1986) 176–181.
[10] P.p. Sarpotdar, J.L. Zatz, Percutaneous absorption enhancement by nonionic surfactants, Drug Dev. Ind. Pharm. 12 (1986) 1625–1647.
[11] C.-W. Cho, J.-S. Choi, S.-C. Shin, Enhanced local anesthetic action of mepivacaine from the bioadhesive gels, Pak. J. Pharm. Sci. 24 (2011) 87–93.
[12] A. Fini, V. Bergamante, G.C. Ceschel, C. Ronchi, C.A.F. De Moraes, Control of transdermal permeation of hydrocortisone acetate from hydrophilic and lipophilic formulations, AAPS PharmSciTech 9 (2008) 762–768.
[13] L.B. Lopes, N. Murphy, A. Nornoo, Enhancement of transdermal delivery of progesterone using medium-chain mono and diglycerides as skin penetration enhancers, Pharm. Dev. Technol. 14 (2009) 524–529.
[14] B. Magnusson, S. Cross, G. Winckle, M.S. Roberts, Percutaneous absorption of steroids: determination of in vitro permeability and tissue reservoir characteristics in human skin layers, Skin Pharmacol. Physiol. 19 (2006) 336–342.
[15] E. Lemery, S. Briançon, Y. Chevalier, T. Oddos, A. Gohier, O. Boyron, M.-A. Bolzinger, Surfactants have multi-fold effects on skin barrier functionSurfactants have multi-fold effects on skin barrier function, Eur. J. Dermatol. 25 (2015) 424–435.
[16] G. Mao, C. Flach, R. Mendelsohn, R. Walters, Imaging the distribution of sodium dodecyl sulfate in skin by confocal Raman and infrared microspectroscopy, Pharm. Res. 29 (2012) 2189–2201.
[17] G. Imokawa, S. Akasaki, Y. Minematsu, M. Kawai, Importance of intercellular lipids in water-retention properties of the stratum corneum: induction and recovery study of surfactant dry skin, Arch. Dermatol. Res. 281 (1989) 45–51.
[18] H. Törmä, M. Lindberg, B. Berne, Skin barrier disruption by sodium lauryl sulfate-exposure alters the expressions of involucrin, transglutaminase 1, profilaggrin, and kallikreins during the repair phase in human skin in vivo, J. Invest. Dermatol. 128 (2008) 1212–1219.
[19] R.P. Reinertson, V.R. Wheatley, Studies on the chemical composition of human epidermal lipids11from the section of dermatology (Dr. Stephen Rothman, Chief of Service), Department of Medicine, The University of Chicago, Chicago, Illinois, J. Invest. Dermatol. 32 (1959) 49–59.
[20] R. Michael-Jubeli, J. Bleton, A. Baillet-Guffroy, High-temperature gas chromatography-mass spectrometry for skin surface lipids profiling, J. Lipid Res. 52 (2011) 143–151.
[21] L. Norlén, I. Nicander, A. Lundsjö, T. Cronholm, B. Forslind, A new HPLC-based method for the quantitative analysis of inner stratum corneum lipids with special reference to the free fatty acid fraction, Arch. Dermatol. Res. 290 (1998) 508–516.
[22] M. Ponec, A. Weerheim, P. Lankhorst, P. Wertz, New acylceramide in native and reconstructed epidermis, J. Invest. Dermatol. 120 (2003) 581–588.
[23] J. van Smeden, L. Hoppel, R. van der Heijden, T. Hankemeier, R.J. Vreeken, J.A. Bouwstra, LC/MS analysis of stratum corneum lipids: ceramide profiling and discovery, J. Lipid Res. 52 (2011) 1211–1221.
[24] H. Farwanah, J. Wohlrab, R.H. Neubert, K. Raith, Profiling of human stratum corneum ceramides by means of normal phase LC/APCI–MS, Anal. Bioanal. Chem. 383 (2005) 632–637.
[25] Y. Masukawa, H. Narita, H. Sato, A. Naoe, N. Kondo, Y. Sugai, T. Oba, R. Homma, J. Ishikawa, Y. Takagi, Comprehensive quantification of ceramide species in human stratum corneum, J. Lipid Res. 50 (2009) 1708–1719.
[26] R. t'Kindt, L. Jorge, E. Dumont, P. Couturon, F. David, P. Sandra, K. Sandra, Profiling and characterizing skin ceramides using reversed-phase liquid chromatography–quadrupole time-of-flight mass spectrometry, Anal. Chem. 84 (2011) 403–411.
[27] O. Bleck, D. Abeck, J. Ring, U. Hoppe, J.-P. Vietzke, R. Wolber, O. Brandt, V. Schreiner, Two ceramide subfractions detectable in Cer (AS) position by HPTLC in skin surface lipids of non-lesional skin of atopic eczema, J. Invest. Dermatol. 113 (1999) 894–900.
[28] J. Jungersted, H. Scheer, M. Mempel, H. Baurecht, L. Cifuentes, J. Høgh, L. Hellgren, G. Jemec, T. Agner, S. Weidinger, Stratum corneum lipids, skin barrier function and filaggrin mutations in patients with atopic eczema, Allergy 65 (2010) 911–918.
[29] L.A. Nafie, Recent advances in linear and nonlinear Raman spectroscopy. Part VI, J. Raman Spectrosc. 43 (2012) 1845–1863.
[30] M. Förster, M.-A. Bolzinger, G. Montagnac, S. Briançon, Confocal Raman microspectroscopy of the skin, Eur. J. Dermatol. 21 (2012) 851–863.
[31] C. Wollenweber, A. Makievski, R. Miller, R. Daniels, Adsorption of hydroxypropyl methylcellulose at the liquid/liquid interface and the effect on emulsion stability, Colloids Surf. Physicochem. Eng. Aspects 172 (2000) 91–101.
[32] D.J. Lunter, M. Rottke, R. Daniels, Oil-in-oil-emulsions with enhanced substantivity for the treatment of chronic skin diseases, J. Pharm. Sci. 103 (2014) 1515–1519.
[33] A. Färber, R. Daniels, Ex vivo skin permeation of betulin from water-in-oil foams, Skin Pharmacol. Physiol. 29 (2016) 250–256.
[34] A.M. Kligman, E. Christophers, Preparation of isolated sheets of human stratum corneum, Arch. Dermatol. 88 (1963) 702–705.
[35] S.M. Ali, F. Bonnier, A. Tfayli, H. Lambkin, K. Flynn, V. McDonagh, C. Healy, T.C. Lee, F.M. Lyng, H.J. Byrne, Raman spectroscopic analysis of human skin tissue sections ex-vivo: evaluation of the effects of tissue processing and dewaxing, J. Biomed. Opt. 18 (2013) 061202 061202-061202.
[36] A.N. Anigbogu, A.C. Williams, B.W. Barry, H.G. Edwards, Fourier transform Raman spectroscopy of interactions between the penetration enhancer dimethyl sulfoxide and human stratum corneum, Int. J. Pharm. 125 (1995) 265–282.
[37] M. Gąsior-Głogowska, M. Komorowska, J. Hanuza, M. Mączka, A. Zając, M. Ptak, R. Będziński, M. Kobielarz, K. Maksymowicz, P. Kuropka, FT-Raman spectroscopic study of human skin subjected to uniaxial stress, J. Mech. Behav. Biomed. Mater. 18 (2013) 240–252.
[38] P.W. Wertz, M.C. Miethke, S.A. Long, J.S. Strauss, D.T. Downing, The composition of the ceramides from human stratum corneum and from comedones, J. Invest. Dermatol. 84 (1985) 410–412.
[39] I.H.T. Guideline, Validation of analytical procedures: text and methodology, Q2 (R1), 1, 2005.
[40] M.H. Oudshoorn, R. Rissmann, D. Van Der Coelen, W.E. Hennink, M. Ponec, J.A. Bouwstra, Development of a murine model to evaluate the effect of vernix caseosa on skin barrier recovery, Exp. Dermatol. 18 (2009) 178–184.
[41] M.H. Oudshoorn, R. Rissmann, D. Van Der Coelen, W.E. Hennink, M. Ponec, J.A. Bouwstra, Effect of synthetic vernix biofilms on barrier recovery of damaged mouse skin, Exp. Dermatol. 18 (2009) 695–703.
[42] G. Grubauer, K.R. Feingold, P.M. Elias, Relationship of epidermal lipogenesis to cutaneous barrier function, J. Lipid Res. 28 (1987) 746–752.
[43] E. Christophers, A.M. Kligman, Visualization of the cell layers of the stratum corneum, J. Invest. Dermatol. 42 (1964) 407–409.
[44] C. Blair, Morphology and thickness of the human stratum corneum, Br. J. Dermatol. 80 (1968) 430–436.
[45] A. Pagnoni, A. Kligman, T. Stoudemayer, Pyranine, a fluorescent dye, detects subclinical injury to sodium lauryl sulfate, J. Soc. Cosmet. Chem. 49 (1998) 33–38.
[46] S.H. Yalkowsky, Solubilization by Surfactants, American Chemical Society, New York, 1999.
[47] E. Söderlind, M. Wollbratt, C. von Corswant, The usefulness of sugar surfactants as solubilizing agents in parenteral formulations, Int. J. Pharm. 252 (2003) 61–71.
[48] M. Egawa, T. Hirao, M. Takahashi, In vivo estimation of stratum corneum thickness from water concentration profiles obtained with Raman spectroscopy, Acta Derm. Venereol. 87 (2007) 4–8.

Supporting information to

Confocal Raman microspectroscopy as an alternative method to investigate the extraction of lipids from stratum corneum by emulsifiers and formulations

Ziwei Zhang, Dominique Jasmin Lunter *

Department of Pharmaceutical Technology, University of Tuebingen, Tuebingen, Germany

1. Composition and preparation of studied formulations

Four kinds of formulations are investigated in this study. Except for HPMC-MCT emulsion, other formulations are either from German Pharmacopoeia (Deutsches Arzneibuch, DAB) 2015 or German Drug Codex/New German Formulary (Deutscher Arzneimittel Codex/Neues Rezeptur Formularium, DAC/NRF) 2016. To clarify, their composition and preparation methods are provided in Table A.1.

Table A.1 Composition and preparation of studied formulations.

Formulations	Official names	Composition		Preparation
Basic cream	Basiscreme DAC	Glycerol monostearate (GMS) Cetyl alcohol Medium chain triglyceride Polyoxyethylene-20-glycerol monostearate (PEG-20-GMS) Propylene glycol Soft paraffin Water	4.0 g 6.0 g 7.5 g 7.0 g 10.0 g 25.5 g 40.0 g	Medium chain triglyceride, soft paraffin, cetyl alcohol and GMS mixture was melted at 70 °C. PEG-20-GMS and propylene glycol was dissolved in water at the same temperature. The aqueous phase was incorporated into the oily phase by mixing until room temperature.
Anionic cream	Anionische hydrophile Creme DAB	Cetearyl alcohol (and) sodium cetearyl sulfate (CA-SLS) Liquid paraffin Soft paraffin Water	9.0 g 10.5 g 10.5 g 70.0 g	Paraffin, CA-SLS and soft paraffin mixture was melted at 70 °C. The cream was made by incorporating hot water into oily phase by mixing until room temperature.
Non-ionic cream	Nichtionische Hydrophile Creme DAB	Polysorbate 60 (PS 60) Cetyl stearyl alcohol (CSA) Soft paraffin Glycerol Water	5.0 g 10.0 g 25.0 g 10.0 g 50.0 g	PS 60, CSA and soft paraffin was melted at 70 °C. Glycerol was dissolved in distilled water at the same temperature. Subsequently the aqueous phase was added into oily phase. The cream was prepared by stirring the mixture until room temperature.
HPMC-MCT emulsion	HPMC stabilized Emulsion	Hydroxypropyl methyl cellulose (HPMC) Water Medium chain triglycerides (MCT)	2.0 g 78.0 g 20.0 g	2.5 % HPMC aqueous solution was prepared by dispersing the polymer in pure water at 80 °C. Emulsion was prepared by mixing HPMC solution and MCT at 40 °C and homogenizing for 5 min at 15000 rpm using an Ultra Turrax.

2. Selection of appropriate lipid extraction solvent

Classically, lipid was extracted with a mixture of chloroform : methanol (CHLO : MeOH, 2:1, v/v) [1-3]. Due to the toxicity of chloroform, we tried to replace it with dichloromethane (DCM), which has a similar chemical structure and properties to chloroform but less toxicity. Some literature also reported ethyl acetate : methanol (EA : MeOH, 20:80, v/v) as an effective mixture to extract lipids. These three mixtures were tested to seek the most suitable extraction solvent. CRM was utilized to compare δ(CH_2, CH_3)-mode after extraction, which is a signal for lipid content. The lower this signal is, the more effectively the solvent acts. Fig. A.1 shows integrated Raman signals before and after extraction with three kinds of mixtures. Compared to before extraction, CHLO : MeOH (2:1, v/v) and EA : MeOH (20:80, v/v) showed a more pronounced reduction of δ(CH_2, CH_3)-signal than DCM : MeOH (2:1, v/v). However, there was no significant difference between these two methods. Thus, EA : MeOH (20:80, v/v), with less toxicity and comparable effectiveness, can act as a suitable solvent for lipid extraction. Furthermore, a lower δ(CH_2, CH_3)-signal could not be seen even if the extraction time was extended. Therefore, normalized δ(CH_2, CH_3)-mode value of around 0.57 was regarded as an indication of effective lipid extraction.

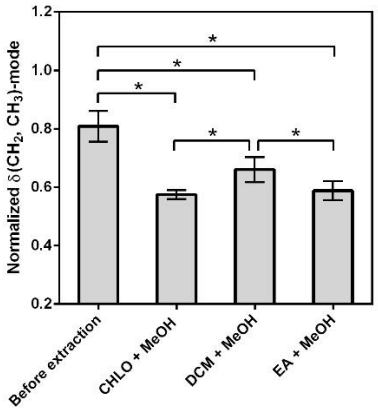

Fig. A.1 Comparison of normalized δ(CH_2, CH_3)-signal at 1425 - 1495 cm^{-1} before and after lipid extraction with different solvents, mean ± SD, n = 9, $p < 0.05$.

3. Determination of SC thickness

This part gives supplementary information with regard to the data acquisition of SC thickness in the course of CRM measurement. Pre-treated SC was dried and deposited on a glass slide. Firstly, laser focus point was moved from under sample (-50 µm) to above SC (50 µm) with a step size of 1 µm (Fig. A.2). Thus, a series of Raman spectra along a line were recorded. For example, five representative spectra (at 40, 47, 50, 52 and 60 µm) are illustrated in the inserted chart of Fig. A.3. Subsequently, area under the peak of the keratin signal (ν(CH_3)-mode, 2800

- 3000 cm^{-1}) was extracted and plotted as a function of depth in Fig. A.3, which showed the area under the keratin peak across the SC sample. Full width at half maximum of this peak curve was calculated by the WITec Project Plus software (WITec GmbH, Ulm, Germany) and regarded as the SC thickness. In other words, it is the width of the keratin peak curve between those two points (x_1 and x_2 in Fig. A.3) on the vertical (z) axis which are half the maximum amplitude. The described procedure is a typical method to measure the thickness of a sample by CRM [4].

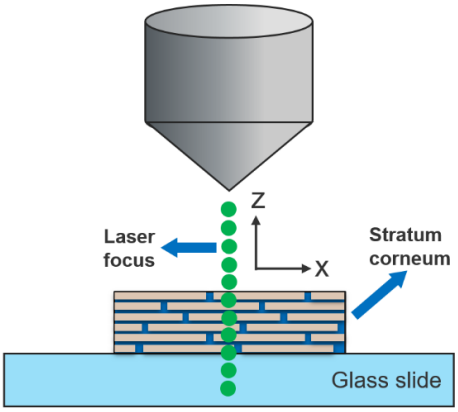

Fig. A.2 Schematic drawing of line scanning of stratum corneum (SC) using confocal Raman microscopy (CRM).

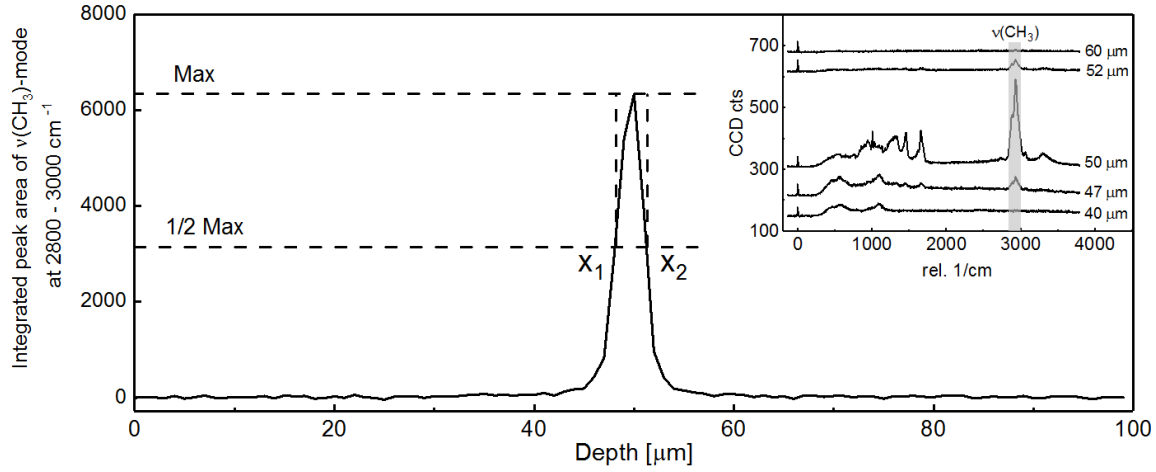

Fig. A. 3 Profile of integrated Raman signal intensity (ν(CH_3)-mode, 2800 - 3000 cm^{-1}) through SC along the path indicated by the dash green line in Fig. A.2, inserted chart: five representative single Raman signals at different depths.

4. References

[1] E.G. Bligh, W.J. Dyer, A rapid method of total lipid extraction and purification, Can. J. Biochem. Physiol., 37 (1959) 911-917.

[2] H. Tanojo, J.A. Bouwstra, H.E. Junginger, H.E. Boddé, Subzero thermal analysis of human stratum corneum, Pharm. Res., 11 (1994) 1610-1616.
[3] O. Bleck, D. Abeck, J. Ring, U. Hoppe, J.-P. Vietzke, R. Wolber, O. Brandt, V. Schreiner, Two ceramide subfractions detectable in Cer (AS) position by HPTLC in skin surface lipids of non-lesional skin of atopic eczema, J. Invest. Dermatol., 113 (1999) 894-900.
[4] K. Wormuth, Springer series in optical sciences, Springer, Heidelberg, 2010.

6.2 Publication 2

Confocal Raman microspectroscopy as an alternative to differential scanning calorimetry to detect the impact of emulsifiers and formulations on stratum corneum lipid conformation

Ziwei Zhang, Dominique Lunter *

European Journal of Pharmaceutical Sciences

Volume 121, Pages 1-8. Published on 23 May 2018.

European Journal of Pharmaceutical Sciences 121 (2018) 1–8

Contents lists available at ScienceDirect

European Journal of Pharmaceutical Sciences

journal homepage: www.elsevier.com/locate/ejps

Confocal Raman microspectroscopy as an alternative to differential scanning calorimetry to detect the impact of emulsifiers and formulations on stratum corneum lipid conformation

Ziwei Zhang, Dominique Jasmin Lunter*

University of Tuebingen, Pharmaceutical Technology, Tuebingen, Germany

ARTICLE INFO

Keywords:
Stratum corneum
Lipid conformation
Confocal Raman microscopy
Differential scanning calorimetry
Emulsifier

ABSTRACT

The purpose of this study was to investigate the impact of emulsifiers and formulations on stratum corneum (SC) lipid conformation and evaluate confocal Raman microspectroscopy (CRM) as an alternative method to differential scanning calorimetry (DSC) in this research context. To this end, four different formulations were used: three conventional creams that contained ionic and/or non-ionic emulsifiers and one surfactants-free emulsion stabilized by a polymeric emulsifier. Additionally, all emulsifiers were tested in aqueous solutions/dispersions in the respective concentrations as present in the formulations. In this study, emulsifiers and formulations were applied onto excised porcine skin during incubation in Franz diffusion cells. Subsequently, SC was isolated, dried and subjected to CRM and DSC measurement to analyse lipid structural changes after treatment. In CRM measurement, 1080 cm^{-1}/(1130 cm^{-1} + 1070 cm^{-1}) peak ratio, which represents the C-C skeleton vibration and *trans-gauche* conformation order of lipids, was investigated. Various emulsifiers and formulations showed different impact on SC lipid conformation. Specifically, cetearyl alcohol and sodium cetearyl sulfate mixture dispersion showed the strongest ability among all studied emulsifiers, followed by glycerol monostearate, polyoxyethylene-20-glycerol monostearate as well as their mixture. Polysorbate 60, cetyl stearyl alcohol and their mixture did not affect SC lipid structure. The results of CRM and DSC correlated very well, indicating CRM, as an alternative to DSC, can be a reliable method to investigate SC lipid conformation.

1. Introduction

The uppermost layer in skin is stratum corneum (SC), which provides a very effective barrier function for the human body. SC comprises flattened corneocytes embedded in intercellular lipids. Researchers have proven that SC lipids are mainly composed of non-polar ceramides, free fatty acids and cholesterol at a molar ratio of approximately 1:1:1 (Weerheim and Ponec, 2001). The intercellular lipids are highly arranged in lamellar phases oriented approximately parallel to the surface of corneocytes. This unique structure is considered to be crucial in assuring an effective protection. Conversely, lipid structural changes could dramatically influence the condition of the skin. The lipid packing states tend to be less ordered and lead to a compromised skin barrier. Furthermore, many skin diseases, e.g. lamellar ichthyosis, psoriasis, atopic dermatitis, are associated with impaired barrier function (Walters et al., 2012). Therefore, analyses of the state of the cutaneous lipids are important for both healthy skin screening and therapy control.

Emulsifiers can cause barrier damage, increases in trans-epidermal water loss, skin dryness and irritation. In our previous research, it was found that various emulsifiers extracted intercellular lipids from SC at different extent and thus lead to disruptive skin integrity (Zhang and Lunter, 2018). However, changes in lipid organization also cannot be ignored during the interaction between emulsifiers and SC. Depending on their abilities to enter the skin, emulsifiers can reform the lipid organization as being a penetration enhancer and consequently alter the skin barrier (Ananthapadmanabhan et al., 2013; Barel et al., 2014; Mao et al., 2012; Seweryn, 2018). By means of infrared spectroscopy, researchers have demonstrated that after treated with sodium lauryl sulfate, lipid matrix was modified towards a more fluid state whereas there was no change in the protein regions (Walters et al., 2012). Therefore, investigation of intercellular lipid structure is of great importance to comprehensively study the effects of emulsifiers on SC.

In the past, a number of studies have been carried out to explore the lipid arrangement in SC by means of various of methods, including but not limited to electron microscopy (Iwai et al., 2012; Lundborg et al., 2018), small angle and wide angle X-ray scattering (Groen et al., 2009; Van Smeden et al., 2014), NMR spectroscopy (Björklund et al., 2013),

* Corresponding author at: Department of Pharmaceutical Technology, Faculty of Science, University of Tuebingen, Auf der Morgenstelle 8, 72076 Tuebingen, Germany.
E-mail address: dominique.lunter@uni-tuebingen.de (D.J. Lunter).

https://doi.org/10.1016/j.ejps.2018.05.013
Received 7 March 2018; Received in revised form 9 May 2018; Accepted 14 May 2018

Fourier transform infrared (FTIR) spectroscopy (Champagne et al., 2018; Mack Correa et al., 2014) as well as differential scanning calorimetry (DSC) (Mitriaikina and Muller-Goymann, 2007; Täuber and Müller-Goymann, 2015; Wang et al., 2018). Thanks to these technologies, more comprehensive knowledge on the sophisticated lipid structure was obtained. However, these methods can only provide information on intercellular lipid organization, but are not capable of analysing lipid composition. As a promising approach, confocal Raman microspectroscopy (CRM) is increasingly used as a powerful non-invasive tool, offering the capability to analyse the physico-chemical properties of the SC lipids. Contrary to DSC or FTIR, very few reports using Raman spectroscopy to study SC lipids were published (Choe et al., 2016; Choe et al., 2017; Vyumvuhore et al., 2013). In fact, CRM is very sensitive to scattering by non-polar groups (e.g., C-C) (Tfayli et al., 2010). It has a high potential for studying conformational changes in hydrocarbon backbones and is therefore applicable to the study of lipid thermal transitions. In the present study, CRM was employed to measure C-C skeleton conformational order of SC lipids. The *trans-gauche* conformational value was determined by the Raman band intensities and is closely related to lipid crystallographic properties (Guillard et al., 2011). Furthermore, as experimentally proved in our earlier research, CRM spectra also provide information regarding the lipid content of SC (Zhang and Lunter, 2018). In conjunction with this, lipid concentration and conformational information can be obtained simultaneously in a single CRM measurement. Therefore, skin lipids changes can be comprehensively investigated by CRM in both aspects of composition and organization.

The aim of the study is to investigate the impact of emulsifiers and formulations on SC lipids. To this end, four different formulations were used: a total of three conventional creams that contained ionic and/or non-ionic emulsifiers and one emulsion stabilized by a polymeric emulsifier. Additionally, all emulsifiers were analysed in aqueous solutions/dispersions in similar concentrations as present in the formulations. The creams investigated are frequently used by dermatologists and pharmacies to prepare individualised medications for patients. They are applied onto diseased skin with a potential lack of barrier properties. It is thus pivotal for the therapy to prevent further barrier impairment by the medication itself. We therefore chose to investigate exactly these three creams in our study. The emulsion was used as polymeric emulsifiers are deemed to be less harmful to the skin compared to classical emulsifiers. The validity of this assumption should be investigated in the course of the study.

CRM was used to detect the lipid conformational alterations after treatment. DSC studies were performed in parallel to investigate the thermal behaviour changes of SC lipids. Correlation between CRM and DSC results were conducted. This was done to assess if CRM can be a reliable analytical technique to study SC lipid structural alterations after emulsifiers treatment. Moreover, combined with our previous findings, SC lipid composition and conformation can be simultaneously analysed in one single CRM measurement. Based on the advantages of easy sample preparation, immediate analytical readout and low data variability, CRM could be utilized as an advantageous and powerful instrument for skin lipids investigation. This work may also serve as a basis for clinical use such as healthy skin screening and therapy control.

2. Materials and methods

2.1. Materials

Different materials used and their manufacturer information are as follows: polysorbate 60, polyoxyethylene-20-glycerol monostearate, glycerol monostearate and cetyl stearyl alcohol (PS 60, PEG-20-GMS, GMS and CSA; Caesar & Loretz GmbH, Hilden, Germany), sodium lauryl sulfate (SLS; Cognis GmbH & Co. KG, Düsseldorf, Germany), cetearyl alcohol (and) sodium cetearyl sulfate (CA-SLS; BASF SE, Ludwigshafen, Germany), hydroxypropyl methyl cellulose (HPMC 2208; Metolose 90 SH 100 SR, Shin Etsu Chemical Co. Ltd., Tokyo, Japan), medium chain triglyceride (MCT; Myritol 318, BASF, Ludwigshafen, Germany), liquid paraffin (Hansen & Rosenthal KG, Hamburg, Germany), trypsin type II-S (lyophilized powder) and trypsin inhibitor (lyophilized powder) (Sigma-Aldrich Chemie GmbH, Steinheim, Germany), Parafilm® (Bemis Company Inc., Oshkosh, Wis., USA). Sodium chloride, disodium hydrogen phosphate, potassium dihydrogen phosphate, and potassium chloride were of European Pharmacopoeia grade. Pig ears (German land race; age: 15 to 30 weeks; weight: 40 to 65 kg) were supplied by the Department of Experimental Medicine at the University of Tuebingen.

2.2. Preparation of formulations and emulsifier dispersions

Basic cream (Basiscreme DAC) was prepared according to instructions of German Drug Codex/New German Formulary (Deutscher Arzneimittel Codex/Neues Rezeptur Formularium, DAC/NRF) 2016. Anionic cream (Anionische hydrophile Creme) and non-ionic cream (Nichtionische Hydrophile Creme) were prepared according to the instructions of the German Pharmacopoeia (Deutsches Arzneibuch, DAB) 2015. HPMC stabilized emulsion was formulated according to Wollenweber et al. (2000). Composition and preparation methods of investigated formulations are provided in the appendix. Emulsifiers within these formulations were dissolved or dispersed in water and their concentrations remained the same as in formulations (Table 1). Water and SLS were used as negative and positive control.

2.3. Preparation of dermatomed pig ear skin

Fresh pig ears were washed with isotonic saline. After excision, the postauricular skin sheets were cleaned with isotonic saline by cotton swabs, blotted dry with tissue, wrapped in aluminium foil and stored at −30 °C. On the day of experiment, skin sheets were thawed to room temperature, cut into strips of 3 cm width and fixed to a block of Styrofoam (wrapped with aluminium foil) with pins. The hair was trimmed to approximately 0.5 mm with electric clippers (QC5115/15, Philips, Netherlands). Subsequently, the skin was dermatomed to a thickness of 1 mm (Dermatom GA 630, Aesculap AG & Co. KG, Tuttlingen, Germany) and cut with a circular hole punch to a diameter of 25 mm (Lunter et al., 2014).

2.4. Incubation of pig ear skin in Franz diffusion cells

Incubation of pig ear skin was conducted using dermatomed skin and modified Franz diffusion cells (Gauer Glas, Püttlingen, Germany) with a receptor of 12 mL. Phosphate buffered saline pH 7.4 (PBS, Ph. Eur. 8.0) was used as receptor fluid. Degassed, prewarmed (32 °C) receptor medium was filled into Franz diffusion cells. Subsequently, cells were fitted with dermatomed pig ear skin (thickness: 1 mm, diameter:

Table 1
Formulations and emulsifiers that are used in this study.

Formulations	Emulsifiers	Abbreviation	Concentrations
Basic cream	Polyoxyethylene-20-glycerol monostearate	PEG-20-GMS	7%
	Glycerol monostearate	GMS	4%
Non-ionic cream	Polysorbate 60	PS 60	5%
	Cetylstearyl alcohol	CSA	10%
Anionic cream	Cetearyl alcohol (and) sodium cetearyl sulfate	CA-SLS	9%
HPMC-MCT emulsion	Hydroxypropyl methyl cellulose 2208 (Metolose 90 SH 100 SR)	HPMC	2.5%
Positive control	Sodium lauryl sulfate	SLS	1%

25 mm) and donor compartments. Franz diffusion cells were mounted in a water bath heated to 32 °C. After a brief equilibrium period of 30 min, 1 mL of each emulsifier solution/dispersion or 1 g of each formulation was applied to each skin sample. The cells were capped with Parafilm® to prevent evaporation of water. The stirring speed of the receptor fluid was 500 rpm (Heck et al., 2016; Lunter and Daniels, 2012; Lunter et al., 2014; Rottke et al., 2014; Zhang and Lunter, 2018). After 4 h the skin samples were removed from the Franz diffusion cells. To remove remaining emulsifiers or formulations, cleaning procedure was done by gentle wiping using isotonic saline solution and cotton swabs for 30 times. The actual involved area (15 mm in diameter) of pig ear skin was patted dry and punched out for further study (Zhang and Lunter, 2018). All experiments were performed in triplicate.

2.5. Preparation of isolated stratum corneum (SC)

Isolated SC was obtained by incubating the samples at room temperature overnight following a modified protocol of Kligman and Christophers (1963) that was adjusted to porcine skin. The dermatomed skin was placed dermal side down on filter paper soaked with a 0.2% trypsin and phosphate buffer saline solution (pH 7.4). Digested material was peeled off with a blunt pair of tweezers. The isolated SC was immersed in a 0.05% trypsin inhibitor solution for 1 min and subsequently washed with fresh demineralised water for five times. Cleaned SC sheets were dried and stored above silica gel in a desiccator for at least three days before analysis (Zhang and Lunter, 2018).

2.6. Differential scanning calorimetry (DSC)

Hydrated SC samples were prepared by equilibrating dry SC sheets for 24 h at room temperature in a closed vessel above 27% sodium bromide aqueous solution to obtain a water content of 20% (Tanojo et al., 1999). DSC thermograms were collected by a DSC 820 calorimeter (Mettler-Toledo GmbH, Giessen, Germany). Samples of SC sheets weighing 3–5 mg were encapsulated in 40 µL aluminium crucibles (Mettler-Toledo GmbH, Switzerland) adequate for volatile samples, and an empty crucible was used as reference. The calorimeter was calibrated for temperature with indium, and the onset temperature was 156.6 °C. An 80 mL/min nitrogen purging gas flow was used. Typically, after equilibration for 3 min at 0 °C, the temperature ramps in the range of 0–100 °C were performed with a heating rate of 5 °C/min. Measurements were conducted in triplicate.

2.7. Lipid conformation measurement by CRM

The intercellular lipid structure of SC is directly linked to skin barrier function. In the present study, lipid conformation was measured with dried porcine SC sheets using CRM. Raman spectra were acquired with an α 500R confocal Raman microscope (WITec GmbH, Ulm, Germany) equipped with a 532-nm excitation laser source and UHTS 300 spectrometer. A 100 × objective (numerical aperture 0.9, EC Epiplan-neofluor, Carl Zeiss, Germany) was used to focus the light on SC and to collect scattered light. Backscattered light from the samples was dispersed by an optical grating of 1800 g/mm and projected on a charge-coupled device, DV401-BV CCD detector, cooled to −60 °C. The laser intensity was adjusted to 10 mW, measured as intensity before the objective using an optical power meter (PM100D, Thorlabs GmbH, Dachau, Germany).

For each measuring position on the skin, spectra of the fingerprint region (between 710 and 1820 cm^{-1}) were obtained at the following spatial settings. Raman spectra were recorded starting from −50 µm under the SC surface to above 50 µm in 1 µm increment. Each single spectrum was calculated by recording 4 spectra at an exposure time of 2 s and subsequent calculation of the average spectrum (Zhang and Lunter, 2018). Principle component analysis (PCA) was used to remove the minor variations in the dataset from the spectra. PCA is a classical feature extraction and data representation technique which is widely used to reduce the dimensionality and seek the correlation between variables. It was achieved by employing the first three principal components (PCs) for the reconstruction of the Raman spectra, as the remaining PCs contain less essential information (Choe et al., 2016). In the fingerprint region, three peaks at the wavelength of 1070 cm^{-1}, 1080 cm^{-1} and 1130 cm^{-1} are relevant to the C-C skeleton stretching mode for long-chain hydrocarbons and are very sensitive to their *trans-gauche* conformation order (Tfayli et al., 2012; Vyumvuhore et al., 2013). Vyumvuhore et al. (2013) showed the first peak appeared at 1060 cm^{-1}, but in our experiment it shifted to 1070 cm^{-1}. This is explained by the difference between human and porcine skin. The peak areas of selected peaks were calculated as the area under the curve using WiTec Project Plus 4 software.

2.8. Statistical analysis

Data were acquired from repeated experiments ($n \geq 3$). Diagrams show arithmetic mean ± standard deviation (mean ± SD). Statistical differences were determined by a one-way ANOVA followed by the Student-Newman-Keuls test or pairwise *t*-test ($p < 0.05$), which were performed using GraphPad Prism 4.0 (GraphPad Software Inc., La Jolla, CA, USA). Data that are significantly different are marked with an asterisk (*).

3. Results

In order to get an insight into the influence of emulsifiers and formulations treatment on SC DSC and CRM were performed to evaluate the lipid structural and componential changes. CRM was firstly employed in the present study to assess such effects with easy sample preparation and immediate analytical readout in contrast to conventional methods, like DSC. Furthermore, CRM results were proven in our previous set of experiments to be consistent with those of HPTLC and histological study with better reproducibility and lower data variability (Zhang and Lunter, 2018). We therefore set out to investigate if even more information could be obtained from the CRM measurement.

3.1. Lipid conformation measurement by CRM

To investigate the impact of emulsifiers and formulations treatment on SC lipid packing, we firstly studied the influence of each single emulsifier and emulsifier mixtures in the same concentrations as used in formulations, and in the second step evaluated the effects of formulations themselves.

Fig. 1 highlights three peaks relevant to C-C skeleton stretching in the fingerprint region. The peaks at 1070 cm^{-1} and 1130 cm^{-1} are highly linked to the *all-trans* chain segments in lipids, while the peak at 1080 cm^{-1} corresponds to the *gauche* conformation only. Intercellular lipids have prominent peaks at 1070 cm^{-1} and 1080 cm^{-1} and a very strong peak at 1130 cm^{-1}. Since keratin contributes very little to the peaks at 1070 cm^{-1} and 1080 cm^{-1}, these two peaks can be assumed as originating from lipids. However, keratin has a weak peak at 1125 cm^{-1}, and this contribution cannot be ignored (Edwards et al., 1998). In order to eliminate the influence of the keratin peak at 1125 cm^{-1}, an adequate integration area was selected when calculating the area at 1130 cm^{-1} (Choe et al., 2016). According to previous findings, during the lipid transformation from order to disorder, the peak at 1070 cm^{-1} becomes lower and sharper, whereas the peak at 1080 cm^{-1} gets broader and shifts towards the lower wavenumbers. In order to calculate the *trans-gauche* conformation of intercellular lipids in the fingerprint region from the viewpoint of the C-C skeleton vibration, the conformational value was introduced as follows:

$$\text{Comformational value} = \frac{AUC_{1080}}{AUC_{1130} + AUC_{1070}} \quad (1)$$

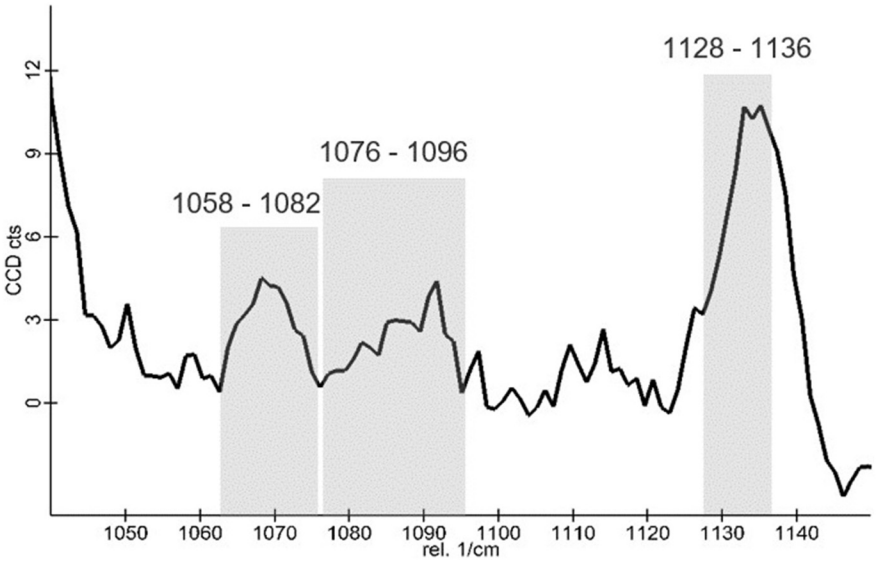

Fig. 1. Lipid-related Raman spectrum of porcine stratum corneum in the region of 1040–1150 cm^{-1} post-PCA-based noise reduction procedure with appropriated integration ranges.

where AUC is the integrated area under the specified peak.

This ratio indicates the *gauche* conformation order of the lipids, i.e., a high value represents a tendency towards *gauche* conformation order (less-ordered lateral packing state of lipids), and low value means a prevalence of *trans* conformation order (higher-ordered lateral packing state of lipids) from the viewpoint of C-C skeleton vibration. A detailed description of this procedure has been published (Choe et al., 2016).

Fig. 2A shows the conformational values of intercellular lipids after treatment with various kinds of emulsifiers. We can clearly see that the values of HPMC, CA-SLS, GMS, PEG-20-GMS and their mixture treated samples were significantly higher than the reference (water treated samples), indicating that the total intercellular lipids conformation changed to more *gauche* (disordered) states. Furthermore, this result is most obvious for the positive control, SLS treatment, as the ratio increased twice higher than the reference. Whereas for PS 60, CSA as well as their mixture, the calculated conformational values were statistically insignificant compared to the water treated samples, which means the lipid structural arrangement remained to be ordered.

Fig. 2B shows the conformational values of skin lipids post treatment with different formulations. Among all investigated formulations, basic cream, anionic cream and HPMC-MCT emulsion showed significantly elevated ratios than the reference, indicating the intercellular lipids have more *gauche*-conformation (more disordered state) and a lower ratio of the orthorhombic/hexagonal structures (Choe et al., 2017). Whereas for non-ionic cream the calculated conformational value showed no significant difference in contrast with the reference, implying no obvious influence on the lateral lipids ordering. Therefore, comparison among the formulations applied on the skin showed that HPMC-MCT emulsion has the most apparent effect, while non-ionic cream has the lowest impact on the lipid conformational order of the SC. This might due to MCT in the emulsion, as it can dramatically influence intercellular lipid structure (Täuber and Müller-Goymann, 2015).

3.2. DSC study

To correlate the findings of the CRM experiment, DSC studies were performed. DSC is conventionally used to analyse the lipid conformation in SC. Typically, DSC thermograms of excised porcine SC show two main characteristic endothermic transitions between 0 and 100 °C. The

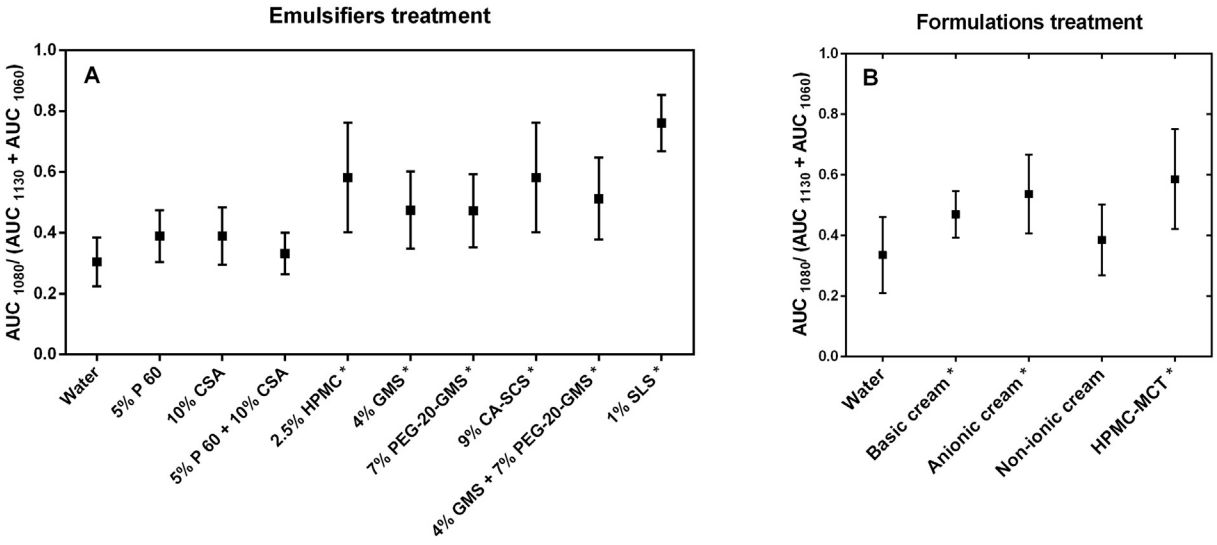

Fig. 2. Comparison of lipid conformational values of porcine skin after treated with emulsifiers (A) and formulations (B), mean ± SD, $n = 9$.

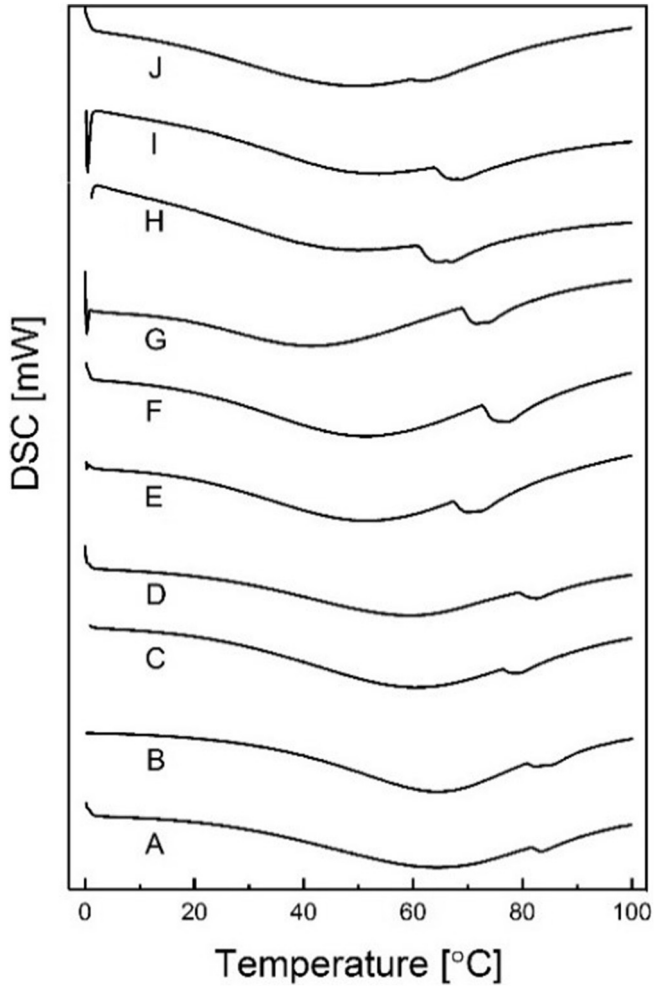

Fig. 3. Thermal profiles of emulsifiers treated SC, A: water, B: PS 60, C: CSA, D: PS 60 + CSA, E: HPMC, F: GMS, G: PEG-20-GMS, H: CA-SLS, I: PEG-20-GMS + GMS, and J: SLS.

Table 2
Peak minimum temperature of the first (T1) and second (T2) phase transitions of stratum corneum after treatment with emulsifiers, mean ± SD, $n = 3$, $p < 0.05$.

SC treated with	T1 [°C]	T2 [°C]
Water	63.0 ± 2.6	81.0 ± 2.4
5% PS 60	63.7 ± 2.5	81.5 ± 1.5
10% CSA	61.5 ± 1.9	79.4 ± 1.7
5% PS 60 + 10% CSA	62.8 ± 1.2	81.2 ± 2.6
2.5% HPMC	53.7 ± 1.3*	73.8 ± 2.5*
4% GMS	54.6 ± 2.5*	76.8 ± 2.3*
7% PEG-20-GMS	53.8 ± 3.1*	72.1 ± 1.5*
9% CA-SLS	52.3 ± 2.4*	66.8 ± 1.9*
7% PEG-20-GMS + 4% GMS	55.7 ± 2.3*	70.0 ± 2.8*
1% SLS	50.4 ± 1.7*	62.5 ± 1.2*

* Statistically different data.

first transition (T1) appears near 60 °C and the second (T2) near 80 °C, both are considered by several investigators to represent a phase transition related to lipids (Bouwstra et al., 1991). In Golden's work, there is a third peak occurring at 95 °C, which is due to the thermal denaturation of intracellular keratin (Golden et al., 1987). In contrast to T1 and T2, the third peak is too small to be detectable in some cases (Mitriaikina and Muller-Goymann, 2007; Schubert and Muller-Goymann, 2004). Therefore, only the transitions of T1 and T2 near 60 °C and 80 °C were determined in present study, respectively. Since the determination of onset temperature was difficult in this case, the peak minima of profiles were chosen instead (Mitriaikina and Muller-Goymann, 2007; Silva et al., 2006). The thermal behaviour of emulsifiers treated SC is shown in Fig. 3. Table 2 lists the peak minimum temperature of the first (T1) and second (T2) phase transitions of SC after treatment with water and emulsifiers. Water treated SC (reference) showed two phase transitions. The first one with peak minimum (T1) at 63 °C represents the thermal transition of the intercellular lipids, and the second one (T2) at 81 °C exhibits endothermic characteristic of both proteins and lipids (Golden et al., 1987). However, various kinds of emulsifiers showed distinct abilities of shifting phase transition temperature. As a positive control, SLS treatment shifted peak temperature the most by reducing T1 by 12.6 °C and T2 by 18.5 °C (average mean value), indicating the least intercellular lipid order in SC. Among all studied emulsifiers, anionic CA-SLS treated SC showed the most significant shifts of 10.7 °C and 14.2 °C for T1 and T2, yet both were not as obvious as SLS alone. This is due to the fact that, CA-SLS just contains min. 7% sodium cetearyl sulfate (SLS) and min. 80% cetearyl alcohol (according to European Pharmacopoeia). SC treated with GMS and PEG-20-GMS showed phase transitions lowered by 8.4 °C and 9.2 °C for T1 and 4.2 °C and 8.9 °C for T2. Whereas, PEG-20-GMS and GMS mixture exhibited even stronger ability in contrast with either component by shifting thermal transitions to lower temperature by 7.3 °C for T1 and 11 °C for T2. Presumably, there is a molecular cooperative interaction between these two emulsifiers and thereby leads to a more disordered lipid conformation. PS 60, CSA and their mixture did not shift phase transition significantly in contrast to the reference. These results suggest that they do not affect SC structure. Thus, except for PS 60, CSA and their mixture, other investigated emulsifiers perturb lipid lamellae packing to different extent, resulting in impaired SC integrity.

Fig. 4 and Table 3 reveal peak minima temperature changes after formulations treatment. The shifts were 7.5 °C (T1) and 9.9 °C (T2) for HPMC-MCT emulsion, 8.0 °C (T1) and 4.8 °C (T2) for basic cream, 7.2 °C (T1) and 2.2 °C (T2) for anionic cream, and 1.3 °C (T1) and 1.1 °C (T2) for non-ionic cream. For non-ionic cream, such a small shift is considered to be insignificant ($p > 0.05$) (Winkler and Müller-Goymann, 2005). Thus, it yields no significant structural changes in SC. Whereas, for other investigated formulations, they produced obvious alteration of lipid structure in SC. Therefore, barrier properties of SC, which relate to certain composition, complex structural arrangement of lipids, are decreased after treatment with basic cream, anionic cream and HPMC-MCT emulsion. A comparison among all the formulations suggests HPMC-MCT emulsion is the most effective in terms of increasing fluidity of SC. This may due to the component of MCT, as Müller-Goymann' group also found that MCT incorporated in formulations lead to an increased lipid mobility and a less compact microstructure by showing decreased T1 and T2 in DSC thermograms (Täuber and Müller-Goymann, 2015).

Interestingly, for both emulsifiers and formulations treatment the conclusions are in fully consistent with the results of the CRM measurements.

4. Discussion

It was expected that emulsifiers/formulations of different composition, concentration, viscosity, HLB values as well as pH values may show distinct abilities to affect lipid conformation in SC. In our study, the concentration of emulsifiers remained the same as present in the model formulations. This was done to easily compare the effects of emulsifiers on skin lipid conformation either in the form of solutions/dispersion or in the form of formulations. Regarding the effect of emulsifier concentration on the impact on SC lipids ordering our results show a clear trend. We used SLS as a positive control in 1% concentration whereas CA-SLS was used in 9% concentration. As CA-SLS contains approximately 7% SLS, this gives a concentration of 0.63% of

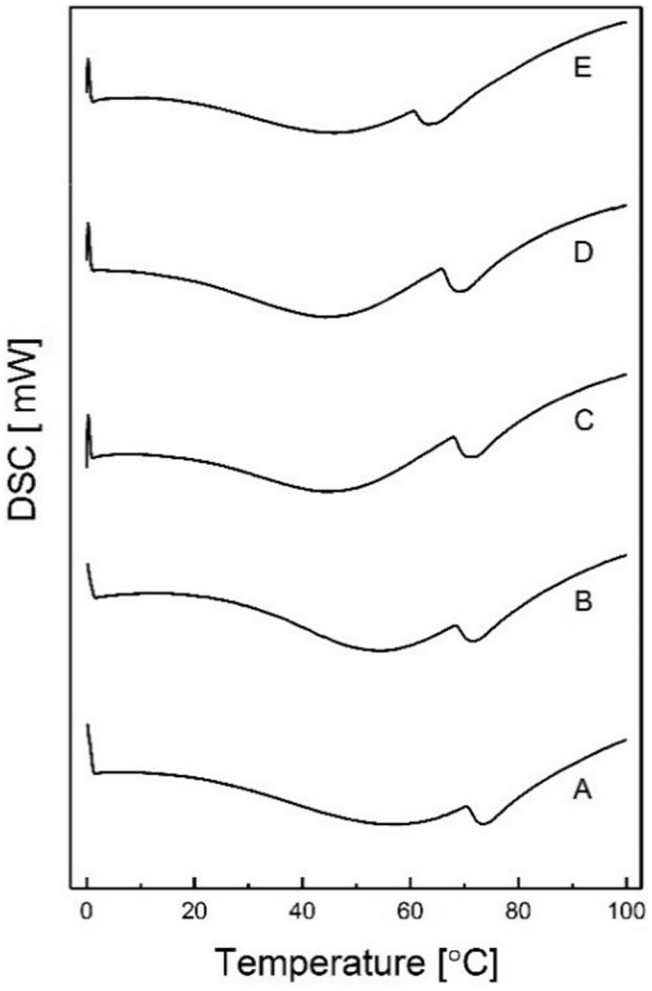

Fig. 4. Thermal profiles of formulations treated SC, A: water, B: non-ionic cream, C: anionic cream, D: basic cream and E: HPMC-MCT emulsion.

Table 3
Peak minimum temperature of the first (T1) and second (T2) phase transitions of stratum corneum after treatment with formulations, mean ± SD, $n = 3$, $p < 0.05$.

SC treated with	T1 [°C]	T2 [°C]
Water	59.8 ± 1.6	77.4 ± 2.5
Non-ionic cream	58.5 ± 2.4	76.3 ± 1.9
Anionic cream	52.6 ± 3.1*	75.2 ± 1.2*
Basic cream	51.8 ± 2.7*	72.6 ± 2.1*
HPMC-MCT emulsion	52.3 ± 2.2*	67.5 ± 2.6*

* Statistically different data.

SLS in the CA-SLS dispersion. CA-SLS impacts SC lipids conformation to a lower extent compared to SLS alone. This reflects the lower concentration of SLS in the CA-SLS-dispersion. It could also have been expected that the ability to change lipid conformation would correlate with the HLB-value of the emulsifiers. Our experiments only partially comply with this assumption. SLS which exhibits the highest HLB-value of 40 leads to the most prominent conformational change in skin lipids. CSA which has the lowest HLB-value results in the least changes in lipid conformation. PEG-20-GMS with a HLB-value of 16 shows intermediate effects on the skin lipid structure. However, PS 60 with a HLB-value of 15 does not affect SC lipids organization significantly. A possible explanation might be that the size and structure of PS 60 is too large to effectively penetrate the SC in order to lead to lipid conformational changes. Still, further comprehensive studies will have to be conducted to clarify the impact of formulation variables in SC lipids conformation.

In DSC thermal profiles, phase transition temperature shifts indicate changes in the intercellular lipid ordering based on thermodynamic theory. Likewise, conformational values calculated from CRM spectra also represent lipid conformation, but from the viewpoint of the C-C skeleton vibration. Therefore, they can both reflect the structural arrangement of intercellular lipids and profile the changes of lipid ordering state. CRM can thus be used as an alternative to DSC to obtain information on conformational ordering of SC lipids. As we already showed that CRM can be used to determine SC lipid content reliably (Zhang and Lunter, 2018), it is deemed more advantageous to perform one CRM analysis which can provide information on both aspects (concentration and conformation) than to separately perform DSC plus HPTLC (or other chromatographic quantification of lipids) investigations which are notoriously time consuming and suffer from more extensive sample preparation. To investigate this issue further, results from CRM lipid conformation analysis and DSC lipid ordering study were correlated in Fig. 5.

As can be seen from Fig. 5 there is a strong negative correlation between the results of CRM and those of DSC. This shows that the higher conformational values of the lipids (tendency towards *gauche* conformation) correlate very well with lowered phase transition temperature in the cases of both emulsifiers and formulations treated SC. This could be explained as follows: after emulsifiers treatment, SC intercellular lipids conformation changed to more *gauche* state (see Fig. 2), leading to a less ordered structural arrangement. Such increased lipid mobility and less compact microstructure were detected by DSC by showing decreased phase transition temperature in thermograms. Higher mobility leads to less ordered packing and as a result to increased values in conformational order as detected by CRM.

DSC is an approved method to characterize the intercellular lipids of SC in detail (Brinkmann and Müller-Goymann, 2005). Nevertheless, it is relatively time-consuming (depending on the heating rate). In addition, samples are destroyed during the measuring process and thus not possible to be further analysed by other instruments. Furthermore, lipid composition cannot be investigated by means of DSC. In contrast, CRM can counter the abovementioned drawbacks. CRM measurement takes relatively shorter time (several seconds to minutes) and it is non-destructive to samples. As we have already shown in a previous publication, CRM spectra also provide information regarding lipid content of the SC (Zhang and Lunter, 2018). To be more precise, CA-SLS, GMS, PEG-20-GMS and their mixture showed potent abilities to extract lipids from SC, while other investigated emulsifiers did not. The present study shows that the same emulsifiers also have a significant impact on SC lipids conformation. In combination, we can conclude that emulsifiers that extract lipids also show a tendency to cause lipid conformational changes. Impact of emulsifiers on lipid conformational order and lipid extraction from the SC are highly likely to be two sides of the same story. Their extraction by emulsifiers from SC might facilitate the shift towards less ordered state of SC lipids. On the other hand, less ordered structure may likewise facilitate lipid extraction from the SC. In conjunction with the previous findings this means lipid concentration and conformational information could be obtained simultaneously in a single CRM measurement. CRM has the great potential to be an alternative to DSC to detect the impact of emulsifiers and formulations on SC lipid conformation.

5. Conclusion

The results of this work elucidate the influence of emulsifiers and formulations on porcine SC lipids by means of CRM and DSC. Both emulsifiers and formulations treatment lead to phase transition shifts in SC recorded by DSC profiles and increased lipid disorder measured by Raman spectra. This contributes to disordered lipid systems in SC and consequently a damaged SC barrier. CRM was employed as an efficient and useful methodology. It provides advantageous features like fast,

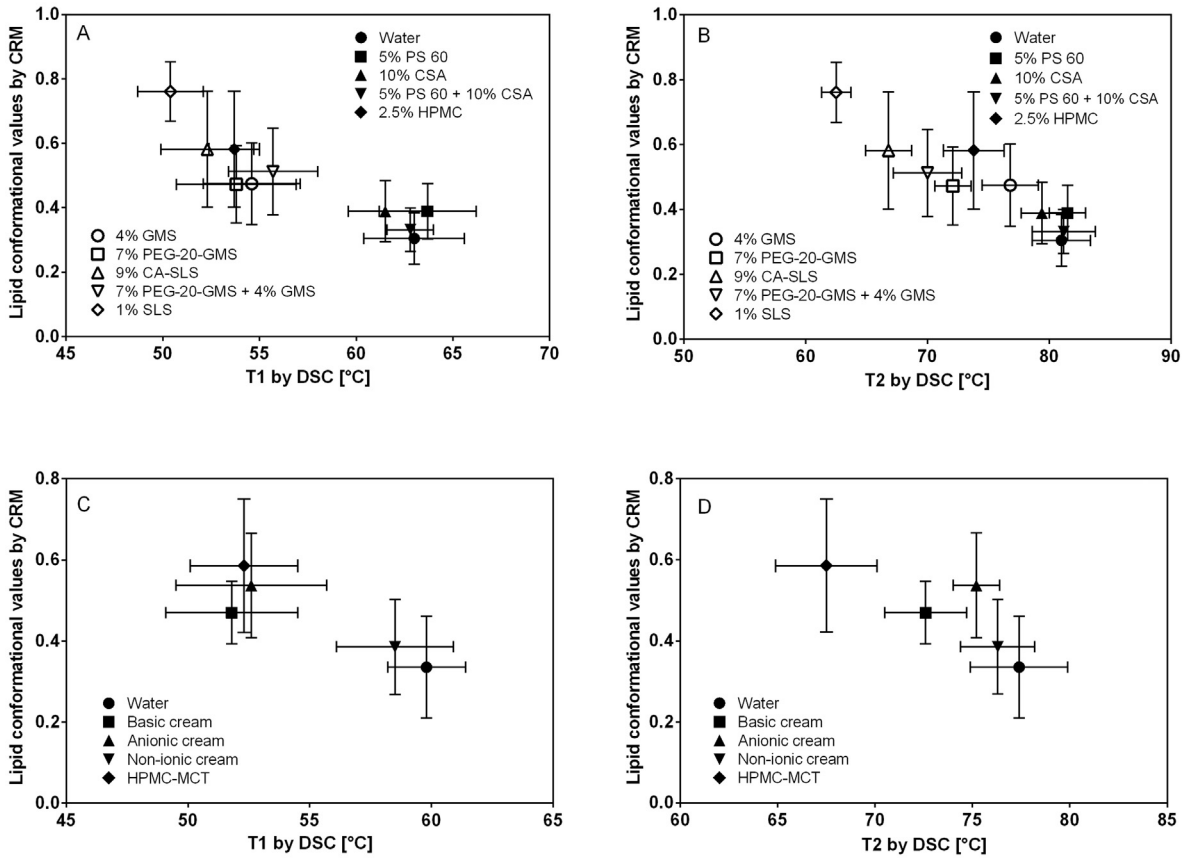

Fig. 5. Correlation between lipid conformational values (by CRM) and lipid phase transition temperature (T1 and T2 in DSC), A and B: emulsifiers treated SC, C and D: formulations treated SC, mean ± SD, $n = 9$.

non-destructive, contact- and label-free measurement on SC to give reliable and reproducible conformational information of SC based on its highly chemical selectivity. The results of CRM and DSC correlate very well, indicating CRM can be an alternative method to DSC in terms of lipid conformation analysis. By means of CRM, samples are easy to prepare and undergo non-destructive measurement compared to conventional methods, and thus can be subjected to other characterization analysis subsequently.

In summary, it is demonstrated that various emulsifiers and emulsifiers incorporated in formulations can affect SC lipids arrangement at different levels. This work may therefore serve as a basis for investigating effects of emulsifiers incorporated in formulations on patients suffering from skin problems, especially those that are characterized by impaired barrier function of SC, e.g. non-lesional skin atopic eczema. Furthermore, confocal Raman microscopy (CRM) can be utilized as an advantageous and powerful instrument to provide molecular structure-based parameters for exploring composition and structure changes in skin.

Acknowledgements

PD Dr. Martin Schenk is acknowledged for the donation of pig ears. This project was supported by the European Social Fund and by the Ministry of Science, Research and the Arts Baden-Wuerttemberg and the China Scholarship Council.

Statement of ethics

Pig ears were received from the Department of Experimental Medicine of the University Hospital Tuebingen. The live animals were kept at the Department of Experimental Medicine and were sacrificed in the course of their experiments, with the approval of the Ethics Committee of the University Hospital Tubingen. The ears were received directly after the death of the animals. The Department of Pharmaceutical Technology is registered for the use of animal products at the District Office of Tuebingen (registration number: DE 08 416 1052 21).

Disclosure statement

The authors report no conflicts of interest.

Appendix A. Supplementary data

Supplementary data to this article can be found online at https://doi.org/10.1016/j.ejps.2018.05.013.

References

Ananthapadmanabhan, K., Mukherjee, S., Chandar, P., 2013. Stratum corneum fatty acids: their critical role in preserving barrier integrity during cleansing. Int. J. Cosmet. Sci. 35, 337–345.
Barel, A.O., Paye, M., Maibach, H.I., 2014. Handbook of Cosmetic Science and Technology. CRC Press.
Björklund, S., Nowacka, A., Bouwstra, J.A., Sparr, E., Topgaard, D., 2013. Characterization of stratum corneum molecular dynamics by natural-abundance ^{13}C solid-state NMR. PLoS One 8, e61889.
Bouwstra, J., De Vries, M., Gooris, G., Bras, W., Brussee, J., Ponec, M., 1991. Thermodynamic and structural aspects of the skin barrier. J. Control. Release 15, 209–219.
Brinkmann, I., Müller-Goymann, C., 2005. An attempt to clarify the influence of glycerol, propylene glycol, isopropyl myristate and a combination of propylene glycol and isopropyl myristate on human stratum corneum. Die pharmazie-an international. J. Pharm. Sci. 60, 215–220.
Champagne, A.M., Pigg, V.A., Allen, H.C., Williams, J.B., 2018. Presence and persistence of a highly ordered lipid phase state in the avian stratum corneum. J. Exp. Biol (jeb.

176438, in press).
Choe, C., Lademann, J., Darvin, M.E., 2016. A depth-dependent profile of the lipid conformation and lateral packing order of the stratum corneum in vivo measured using Raman microscopy. Analyst 141, 1981–1987.
Choe, C., Schleusener, J., Lademann, J., Darvin, M.E., 2017. In vivo confocal Raman microscopic determination of depth profiles of the stratum corneum lipid organization influenced by application of various oils. J. Dermatol. Sci. 183–191.
Edwards, H., Hunt, D., Sibley, M., 1998. FT-Raman spectroscopic study of keratotic materials: horn, hoof and tortoiseshell. Spectrochim. Acta A Mol. Biomol. Spectrosc. 54, 745–757.
Golden, G.M., Guzek, D.B., Kennedy, A., McKie, J.E., Potts, R.O., 1987. Stratum corneum lipid phase transitions and water barrier properties. Biochemistry 26, 2382–2388.
Groen, D., Gooris, G., Bouwstra, J., 2009. New insights into the stratum corneum lipid organization by X-ray diffraction analysis. Biophys. J. 97, 2242–2249.
Guillard, E., Tfayli, A., Manfait, M., Baillet-Guffroy, A., 2011. Thermal dependence of Raman descriptors of ceramides. Part II: effect of chains lengths and head group structures. Anal. Bioanal. Chem. 399, 1201–1213.
Heck, R., Hermann, S., Lunter, D.J., Daniels, R., 2016. Film-forming formulations containing porous silica for the sustained delivery of actives to the skin. Eur. J. Pharm. Biopharm. 108, 1–8.
Iwai, I., Han, H., Den Hollander, L., Svensson, S., Öfverstedt, L.-G., Anwar, J., Brewer, J., Bloksgaard, M., Laloeuf, A., Nosek, D., 2012. The human skin barrier is organized as stacked bilayers of fully extended ceramides with cholesterol molecules associated with the ceramide sphingoid moiety. J. Investig. Dermatol. 132, 2215–2225.
Kligman, A.M., Christophers, E., 1963. Preparation of isolated sheets of human stratum corneum. Arch. Dermatol. 88, 702–705.
Lundborg, M., Narangifard, A., Wennberg, C.L., Lindahl, E., Daneholt, B., Norlén, L., 2018. Human skin barrier structure and function analyzed by Cryo-EM and molecular dynamics simulation. J. Struct. Biol (in press).
Lunter, D.J., Daniels, R., 2012. New film forming emulsions containing Eudragit® NE and/or RS 30D for sustained dermal delivery of nonivamide. Eur. J. Pharm. Biopharm. 82, 291–298.
Lunter, D.J., Rottke, M., Daniels, R., 2014. Oil-in-oil-emulsions with enhanced substantivity for the treatment of chronic skin diseases. J. Pharm. Sci. 103, 1515–1519.
Mack Correa, M.C., Mao, G., Saad, P., Flach, C.R., Mendelsohn, R., Walters, R.M., 2014. Molecular interactions of plant oil components with stratum corneum lipids correlate with clinical measures of skin barrier function. Exp. Dermatol. 23, 39–44.
Mao, G., Flach, C., Mendelsohn, R., Walters, R., 2012. Imaging the distribution of sodium dodecyl sulfate in skin by confocal Raman and infrared microspectroscopy. Pharm. Res. 29, 2189–2201.
Mitriaikina, S., Muller-Goymann, C., 2007. Synergetic effects of isopropyl alcohol (IPA) and isopropyl myristate (IPM) on the permeation of betamethasone-17-valerate from semisolid pharmacopoeia bases. J. Drug Delivery Sci. Technol. 17, 1–8.
Rottke, M., Lunter, D.J., Daniels, R., 2014. In vitro studies on release and skin permeation of nonivamide from novel oil-in-oil-emulsions. Eur. J. Pharm. Biopharm. 86, 260–266.
Schubert, M., Muller-Goymann, C., 2004. Novel colloidal delivery systems for dermal application. J. Drug Delivery Sci. Technol. 14, 423–434.
Seweryn, A., 2018. Interactions between surfactants and the skin–theory and practice. Adv. Colloid Interf. Sci (in press).
Silva, C., Nunes, S., Eusebio, M., Sousa, J., Pais, A., 2006. Study of human stratum corneum and extracted lipids by thermomicroscopy and DSC. Chem. Phys. Lipids 140, 36–47.
Tanojo, H., Junginger, H., Boddé, H., 1999. Thermal analysis studies on human skin and skin barrier modulation by fatty acids and propylene glycol. J. Therm. Anal. Calorim. 57, 313–322.
Täuber, A., Müller-Goymann, C.C., 2015. In vitro model of infected stratum corneum for the efficacy evaluation of poloxamer 407-based formulations of ciclopirox olamine against *Trichophyton rubrum* as well as differential scanning calorimetry and stability studies. Int. J. Pharm. 494, 304–311.
Tfayli, A., Guillard, E., Manfait, M., Baillet-Guffroy, A., 2010. Thermal dependence of Raman descriptors of ceramides. Part I: effect of double bonds in hydrocarbon chains. Anal. Bioanal. Chem. 397, 1281–1296.
Tfayli, A., Guillard, E., Manfait, M., Baillet-Guffroy, A., 2012. Raman spectroscopy: feasibility of in vivo survey of stratum corneum lipids, effect of natural aging. EJD. Eur. J. Dermatol. 22, 36–41.
Van Smeden, J., Janssens, M., Gooris, G., Bouwstra, J., 2014. The important role of stratum corneum lipids for the cutaneous barrier function. Biochim. Biophys. Acta, Mol. Cell Biol. Lipids 1841, 295–313.
Vyumvuhore, R., Tfayli, A., Duplan, H., Delalleau, A., Manfait, M., Baillet-Guffroy, A., 2013. Effects of atmospheric relative humidity on stratum corneum structure at the molecular level: ex vivo Raman spectroscopy analysis. Analyst 138, 4103–4111.
Walters, R.M., Mao, G., Gunn, E.T., Hornby, S., 2012. Cleansing formulations that respect skin barrier integrity. Dermatol. Res. Pract. 2012.
Wang, C., Zhu, J., Zhang, D., Yang, Y., Zheng, L., Qu, Y., Yang, X., Cui, X., 2018. Ionic liquid–microemulsions assisting in the transdermal delivery of Dencichine: preparation, in-vitro and in-vivo evaluations, and investigation of the permeation mechanism. Int. J. Pharm. 535, 120–131.
Weerheim, A., Ponec, M., 2001. Determination of stratum corneum lipid profile by tape stripping in combination with high-performance thin-layer chromatography. Arch. Dermatol. Res. 293, 191–199.
Winkler, A., Müller-Goymann, C.C., 2005. The influence of topical formulations on the permeation of 5-aminolevulinic acid and its n-butyl ester through excised human stratum corneum. Eur. J. Pharm. Biopharm. 60, 427–437.
Wollenweber, C., Makievski, A., Miller, R., Daniels, R., 2000. Adsorption of hydroxypropyl methylcellulose at the liquid/liquid interface and the effect on emulsion stability. Colloids Surf. A Physicochem. Eng. Asp. 172, 91–101.
Zhang, Z., Lunter, D.J., 2018. Confocal Raman microspectroscopy as an alternative method to investigate the extraction of lipids from stratum corneum by emulsifiers and formulations. Eur. J. Pharm. Biopharm. 127, 61–71.

Supporting information to

Confocal Raman microspectroscopy as an alternative to differential scanning calorimetry to detect the impact of emulsifiers and formulations on stratum corneum lipid conformation

Ziwei Zhang, Dominique Jasmin Lunter *

Department of Pharmaceutical Technology, University of Tuebingen, Tuebingen, Germany

Composition and preparation of studied formulations

Four kinds of formulations are investigated in this study. Except for HPMC-MCT emulsion, other formulations are either from German Pharmacopoeia (Deutsches Arzneibuch, DAB) 2015 or German Drug Codex/New German Formulary (Deutscher Arzneimittel Codex/Neues Rezeptur Formularium, DAC/NRF) 2016. To clarify, their composition and preparation methods are provided in Table A. 1.

Table A. 1 Composition and preparation of studied formulations.

Formulations	Official names	Composition		Preparation
Basic cream	Basiscreme DAC	Glycerol monostearate (GMS) Cetyl alcohol Medium chain triglyceride Polyoxyethylene-20-glycerol monostearate (PEG-20-GMS) Propylene glycol Soft paraffin Water	4.0 g 6.0 g 7.5 g 7.0 g 10.0 g 25.5 g 40.0 g	Medium chain triglyceride, soft paraffin, cetyl alcohol and GMS mixture was melted at 70 °C. PEG-20-GMS and propylene glycol was dissolved in water at the same temperature. The aqueous phase was incorporated into the oily phase by mixing until room temperature.
Anionic cream	Anionische hydrophile Creme DAB	Cetearyl alcohol (and) sodium cetearyl sulfate (CA-SLS) Liquid paraffin Soft paraffin Water	9.0 g 10.5 g 10.5 g 70.0 g	Paraffin, CA-SLS and soft paraffin mixture was melted at 70 °C. The cream was made by incorporating hot water into oily phase by mixing until room temperature.
Non-ionic cream	Nichtionische Hydrophile Creme DAB	Polysorbate 60 (PS 60) Cetyl stearyl alcohol (CSA) Soft paraffin Glycerol Water	5.0 g 10.0 g 25.0 g 10.0 g 50.0 g	PS 60, CSA and soft paraffin was melted at 70 °C. Glycerol was dissolved in distilled water at the same temperature. Subsequently the aqueous phase was added into oily phase. The cream was prepared by stirring the mixture until room temperature.

HPMC-MCT emulsion	HPMC stabilized Emulsion	Hydroxypropyl methyl cellulose (HPMC)	2.0 g	2.5 % HPMC aqueous solution was prepared by dispersing the polymer in pure water at 80 °C. Emulsion was prepared by mixing HPMC solution and MCT at 40 °C and homogenizing for 5 min at 15000 rpm using an Ultra Turrax.
		Water	78.0 g	
		Medium chain triglycerides (MCT)	20.0 g	

6.3 Publication 3

Reinforcement of barrier function – skin repair formulations to deliver physiological lipids into skin

Ziwei Zhang, Milica Lukic, Snezana Savic and Dominique Lunter *

International Journal of Cosmetic Science

Volume 40, Pages 494-501. Published on 1 September 2018.

International Journal of
Cosmetic Science

International Journal of Cosmetic Science, 2018, **40**, 494–501 doi: 10.1111/ics.12491

Reinforcement of barrier function – skin repair formulations to deliver physiological lipids into skin

Z. Zhang*, M. Lukic†, S. Savic† and D. J. Lunter*
*Department of Pharmaceutical Technology, University of Tuebingen, Tuebingen, Germany and †Department of Pharmaceutical Technology and Cosmetology, University of Belgrade-Faculty of Pharmacy, Belgrade, Serbia

Received 4 July 2018, Accepted 28 August 2018

Keywords: skin repair, physiological lipids, lipid delivery, barrier function, Raman

Abstract

OBJECTIVE: The aim of the study was to develop formulations to deliver physiological lipids into skin in an attempt to repair defective barrier function.

METHODS: Physiological cholesterol and linoleic acid were incorporated into basic cream and non-ionic cream to prepare skin repair formulations. Homogeneity and storage stability of the developed creams were examined by polarized light microscopy. *Ex vivo* evaluation was conducted using lipid-deficient skin samples and confocal Raman microspectroscopy. A 7-day *in vivo* study was performed on volunteers to study the repairing efficacy.

RESULTS: Homogeneous texture was seen in the prepared skin repair formulations. The application of the creams led to substantially increased lipid levels compared to the reference in the lipid-deficient skin in *ex vivo* study. Twice-a-day application of the skin repair creams provided a reinforcement of the skin barrier as transepidermal water loss (TEWL) was significantly decreased.

CONCLUSION: The skin repair creams showed excellent efficacy in skin recovery. They have great potentials for treating impaired skin barrier associated with depletion of lipids in stratum corneum.

Résumé

OBJECTIF: l'objectif de l'étude était de développer des formulations pour délivrer des lipides physiologiques dans la peau dans le but de réparer une fonction barrière défectueuse.

MÉTHODES: du cholestérol et de l'acide linoléique physiologiques ont été incorporés dans une crème basique et une crème non-ionique afin de réaliser des formulations pour la réparation de la peau. L'homogénéité et la stabilité au cours de la conservation des crèmes développées ont été examinées par microscopie en lumière polarisée. Une évaluation *ex vivo* a été réalisée en utilisant des échantillons de peau délipidée et la microspectroscopie confocale Raman. Une étude *in vivo* de 7 jours a été réalisée sur des volontaires pour étudier l'efficacité de la réparation.

RÉSULTATS: une texture homogène a été observée dans les formulations préparées pour réparation cutanée. L'application des crèmes a conduit à une augmentation substantielle des taux de lipides par rapport au témoin dans l'étude *ex vivo* sur la peau délipidée. Une application deux fois par jour des crèmes réparatrices cutanées a permis de renforcer la barrière cutanée, car la perte d'eau transépidermique (transepidermal water loss, TEWL) a été significativement diminuée.

CONCLUSION: les crèmes réparatrices cutanées ont montré une excellente efficacité au niveau de la régénération de la peau. Elles possèdent des potentiels élevés pour traiter une altération de la barrière cutanée associée à un appauvrissement en lipides de la couche cornée.

Correspondence: Dominique Jasmin Lunter, Department of Pharmaceutical Technology, Faculty of Science, University of Tuebingen, Auf der Morgenstelle 8, 72076 Tuebingen, Germany. Tel.: +49 (0) 7071 74558; fax: +49 (0) 7071-29 5531; e-mail: dominique.lunter@uni-tuebingen.de

Introduction

Skin protects human body as a barrier against external environmental influences. The main barrier function is located in stratum corneum (SC), which is the topmost layer in skin. SC consists of flattened corneocytes as well as intercellular lipid lamellae. As the only continuous domain in SC, intercellular lipids play a critical role in ensuring a competent skin barrier function. SC lipids are mainly composed of ceramides, free fatty acids and cholesterol in an approximately equimolar ratio [1]. Literature reported that a reduced lipid level is observed in dry and sensitive skin conditions which are accompanied by impaired barrier function [2]. This can cause skin redness, itchiness, allergy or irritation upon mild stimulation, and has a strong impact on life quality. Therefore, reinforcement of a competent skin barrier is of great importance in the daily care of dry and sensitive skin.

Topical formulations are generally recommended as a key and basic step in improving compromised barrier function [3–5]. The traditional approach is the 'outside-in' approach [6], in which non-physiological lipids of high concentrations are primarily applied onto the skin in order to enhance barrier function, such as petrolatum [7–10]. These products normally show a lower compliance among patients, since they are not easy to spread and leave an oily feeling on the skin. Furthermore, even though they effectively reduce water loss in a short time, they are not able to repair the lipid deficiency [11]. Hence, another therapeutic concept has gained great popularity to restore the lipid content of SC and thus to enhance the skin barrier. Therefore, in the present study this was achieved by introducing physiological lipids in creams and delivering them into skin, which stimulates the intrinsic pathways in the epidermis to promote the production of intercellular lipids in SC. Compared with traditional methods, this skin repair cream leads to an increase in the total lipid amount for a longer period and thereby could be considered more effective.

Basic cream (BC) and non-ionic cream (NiC) showed the least impairment of SC in terms of lipid extraction and conformational alteration in our earlier research, as shown in Ref [12, 13]. Thus, in the present study, they both were chosen as base creams to prepare skin repair formulations to replenish lipids in SC. Physiological cholesterol and linoleic acid were chosen as model lipids and incorporated into BC and NiC. Skin repair creams were prepared using a lab mixer and were examined by stability studies. *Ex vivo* evaluation was performed to compare lipid changes by means of confocal Raman microspectroscopy (CRM), which was demonstrated to be a reliable and efficient method to quantify global lipids in SC [12]. In addition, *in vivo* study was conducted to investigate the skin recovery potential of cream samples in the living conditions. The prepared creams improve skin conditions effectively and thus possess a great potential in dry and sensitive skin care as part of maintenance therapy.

Materials and methods

Materials

Different materials used and their manufacturer information were as follows: polysorbate 60, polyoxyethylene-20-glycerol monostearate, glycerol monostearate, cetyl alcohol and cetyl stearyl alcohol (Caesar & Loretz GmbH, Hilden, Germany), cholesterol (Alfa Aesar GmbH & Co KG, Karlsruhe, Germany), linoleic acid and glycerol (Sigma-Aldrich Chemie GmbH, Steinheim, Germany), propylene glycol and medium chain triglyceride (Myritol 318, BASF, Ludwigshafen, Germany), soft paraffin (white, Sasol, Johannesburg, South Africa), sodium lauryl sulphate (Cognis GmbH & Co. KG, Düsseldorf, Germany) and Parafilm® (Bemis Company Inc., Oshkosh, Wis., USA). Pig ears (German land race; age: 15–30 weeks; weight: 40–65 kg) were supplied by the Department of Experimental Medicine at the University of Tuebingen.

Composition and preparation of the skin repair formulations

Composition of the investigated formulations are provided in Table I. Cholesterol and linoleic acid (molar ratio of 1: 1) were incorporated into the base creams. Aqueous and oil phases of the formulations were melted separately in a water bath at the same temperature of 70 °C, and then they were mixed by a lab mixer (Unguator®, Gako International GmbH, Scheßlitz, Germany) following the optimal method in Table II. BC and NiC were also prepared with the same method and used as control formulations [14, 15]. Compositions of BC and NiC are given in the supplementary Table SI.

Table I Composition of investigated formulations and evaluation methods

Lipids incorporated (%)	Base creams	Abbreviations	Evaluation methods		
			Stability study	*Ex vivo* study	*In vivo* study
0	Basic cream	BC	+	+	–
0	Non-ionic cream	NiC	+	+	–
5.0	Basic cream	5% L-BC	+	+	+
5.0	Non-ionic cream	5% L-NiC	+	+	+

Table II An optimal method for preparing creams by a lab mixer (Unguator®)

	Step 1			Step 2		
Parameters	Mixing speed of the motor (rpm)	Lifting speed of the motor (rpm)	Time (min)	Mixing speed of the motor (rpm)	Lifting speed of the motor (rpm)	Time (min)
Values	2000	1500	9	250	800	30

Stability study

After preparation of the formulations, approximately 100 g of the preparations were filled in each closely sealed container. The samples were stored at room temperature of 25°C for 6 months. Samples were taken and characterized by polarized light microscopy (PLM) after storage for 1, 2 and 6 months.

Polarized light microscopy

In order to get first insights of the formulation structures, the prepared creams were observed microscopically. Observation was conducted by using a light microscope combined with a digital camera (Microscope Axio Imager Z1, Carl Zeiss, Jena, Germany) integrated with AxioVision 4.6 computer software. A pin-tip amount of each sample was taken from three separate sites within the formulation and smeared on the microscope glass slide, covered with the cover slip and pressed to make it as thin as possible. PLM visualization was performed in bright field and between crossed polarizers using the photomicroscope with a λ plate (Zeiss, Type III, Oberkochen, Germany).

Ex vivo study with porcine skin

Incubation of pig ear skin was conducted using porcine postauricular skin (thickness: 1 mm) and Franz diffusion cells (Gauer Glas, Püttlingen, Germany) as described in Ref [12, 13]. Water-treated and SLS-treated skin samples served as controls. First, 1 mL of sodium lauryl sulphate (SLS) solution was applied to skin samples to extract lipids from SC. After 1 h, the SLS solution was removed and skin was rinsed with isotonic saline solution. Subsequently, 1 g of each formulation were applied on to skin samples for 3 h. The actual involved skin was cleaned and punched out for further study. All experiments were performed in triplicate.

Preparation of isolated stratum corneum

Isolated SC was obtained by incubating the pig skin with 0.2% trypsin solution overnight as detailed in Ref [12, 13]. Cleaned SC sheets were dried and stored above silica gel in a desiccator for at least 3 days before analysis.

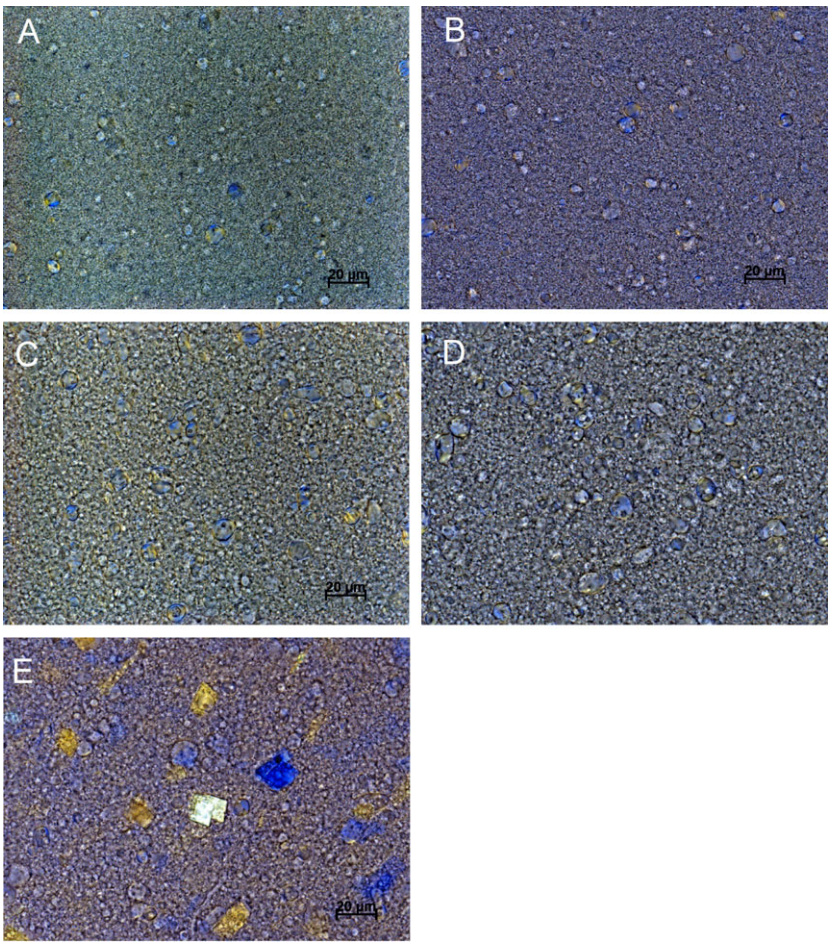

Figure 1 Polarization micrographs of developed creams in stability study, (A) initial image of 5% L-BC (after 24 h of the preparation), (B) 5% L-BC after 6-month storage, (C) initial image of 5% L-NiC (after 24 h of the preparation), (D) 5% L-NiC after 1-month storage and E: 5% L-NiC after 2-month storage.

Confocal Raman microspectroscopy

Dried SC sheets were deposited on glass slides and spectra were recorded by using a confocal Raman microscope (WITec GmbH, Ulm, Germany). As described in Ref [12], normalized lipid signal value was calculated using the following equation:

$$\text{Normalized } \delta(\text{CH}_2, \text{CH}_3) = \frac{\text{AUC } \delta(\text{CH}_2, \text{CH}_3)}{\text{AUC } \nu(\text{C}=\text{O})} \quad (1)$$

where AUC is the integrated area under specified peak in a single CRM spectrum [12].

Water-diluted cream samples were subjected to CRM analysis. The laser intensity of CRM was adjusted to 10 mW. An area of 25 × 25 µm was mapped using a 100× objective (NA 0.9). Colour-coded images were calculated after cosmic ray removal and baseline correction by the software WiTec Project 4 (WITec GmbH, Ulm, Germany). As each spectrum is a fingerprint of the chemical species at a specific image point, the distribution of different components in the cream can be analysed. Using the spectra of each component incorporated into the formulation, the relative amount of each substance at each image point is calculated. By assigning the spectrum of each component to a colour, distribution of the formulation within the examined section can be indicated by giving a colour-coded image of the scanned area.

In vivo skin efficacy study

In vivo study was performed on 11 healthy volunteers (age 25–26) after the written informed consent had been obtained from each volunteer. The study protocol was in accordance to the Declaration of Helsinki and was approved by the local Ethical Committee on Human Research (University of Belgrade, Faculty of Pharmacy, Serbia, No. 2297/2). In order to induce skin barrier impairment, we chose tape stripping instead of SLS treatment because of the following reasons: when SLS is used to induce the (chemical) barrier impairment *in vivo*, it causes epidermal swelling and thus alters the skin hydration [16, 17]. Therefore, in order to get only information which could be contributed to the investigated formulations' effects, and exclude the effect of the SLS on SCH in our 7-day long study,

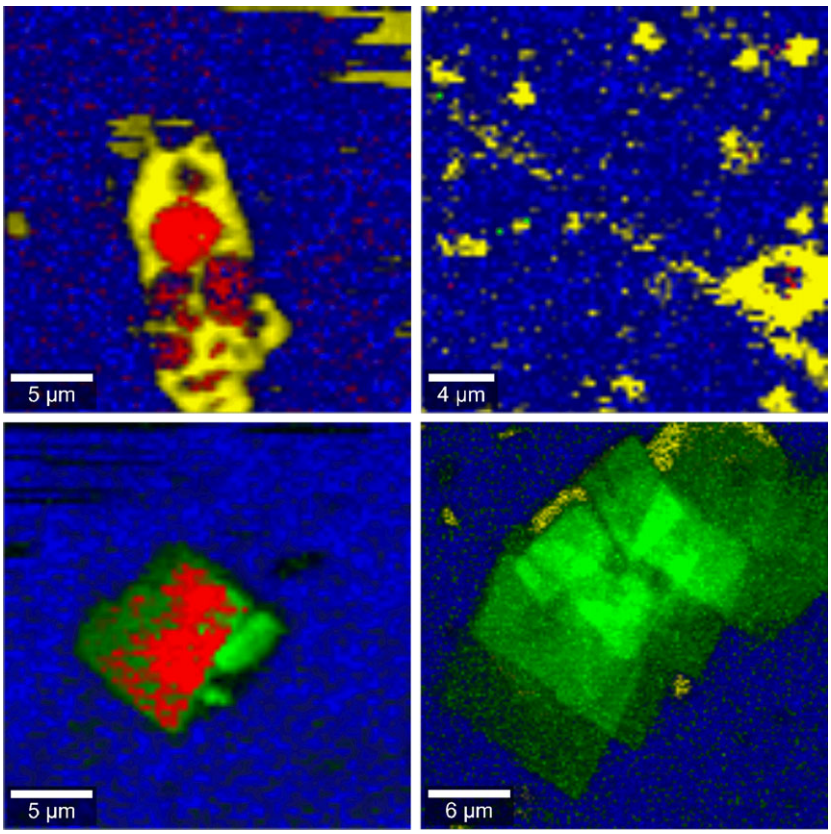

Figure 2 Raman microscopic colour-coded images of water-diluted 5% L-NiC (after 2-month storage at room temperature), blue: water, red: cetylstearyl alcohol, yellow: white soft paraffin and green: cholesterol.

a tape stripping method was used as the barrier impairment method in the *in vivo* study.

Prior to the *in vivo* skin barrier impairment, several preliminary studies were performed in order to standardize the method which would enable barrier impairment without significant irritation after 24 h (erythema and oedema) and without unnecessary inconvenience for volunteers. Regarding the measured biophysical parameters, we wanted to obtain unchanged SCH values and slightly increased TEWL and EI values (compared to values before tape stripping). Therefore, tape stripping was performed on the volar aspects of forearm (4 cm^2). Twelve adhesive D-squame® discs (CuDerm, Dallas, Texas) with constant surface area (3.8 cm^2) were used to remove the superficial SC layers. Each adhesive disc was placed to a defined place on the skin. Twelve tapes were sufficient to obtain desired initial parameters among the most volunteers. In addition, the removal of additional tape (from 13th) was characterized as painful (this was not the case for the previous 12 tapes). After being submitted to uniform pressure (140 g/cm^2) for 10 s, it was removed [18]. After this mechanical impairment, the skin repairing effects of two formulations were investigated in a 7-day long-term study. Transepidermal water loss (TEWL) and stratum corneum moisturization (SCM) were assessed by Tewameter TM210 and Cutometer MPA580 (Courage Khazaka electronic GmbH, Germany). On each arm, there were two investigated sites, one for 5% L-NiC or 5% L-BC and the other for control. Control on one arm was subjected to SC removal (tape-stripped control) and on the other arm was untreated control. Volunteers were acclimatized for 20 min to room conditions (21 ± 1°C, relative humidity 40 ± 5%) prior to measurement.

Initial measurements were performed 24 h after the SC removal. Volunteers were obliged to apply the samples twice a day (in the morning and evening). The first application was after initial measurement and the last was in the evening of the 7th day. Volunteers were not allowed to use any other cosmetic products on the investigated skin sites. Final measurements were performed after 7-day application of the investigated formulations.

Statistical analysis

Data were acquired from repeated experiments ($n \geq 3$). Diagrams show arithmetic mean ± standard deviation (mean ± SD). Statistical differences (except for *in vivo* study) were determined by a one-way ANOVA followed by the Student–Newman–Keuls (SNK) test or pairwise *t*-test ($P < 0.05$), which were performed using GraphPad Prism 4.0 (GraphPad Software Inc, La Jolla, CA, USA). For *in vivo* study, two-way ANOVA was performed on the obtained results. Post hoc Bonferroni *t*-test was conducted where appropriate. Data that are significantly different are marked with an asterisk (*).

Results and discussion

In the present study, we aim at developing skin recovery creams to deliver physiological lipids (cholesterol and linoleic acid) into impaired skin. The creams were characterized by microscopy to evaluate their homogeneity and stability. Further *ex vivo* and *in vivo* studies were performed to assess their efficacy in restoring depleted SC and improve impaired skin conditions.

Storage stability of the skin repair creams

Formulations of BC, NiC, 5% L-BC and 5% L-NiC were prepared following the methods in Table II and stored at room temperature. As shown in Fig. 1A,B, well-distributed character was seen for 5% L-BC. Homogeneous cream texture was maintained even after 6 months, indicating the high stability of 5% L-BC (Fig. 1B). Therefore, the developed 5% L-BC was proved to be highly structurally stable. Figure 1C–E reveal structural changes of 5% L-NiC in stability study. After 1 month, no clear changes were found in the cream texture (Fig. 1D) compared to the initial image (Fig. 1C). However, after 2 months, square crystals appeared and they distributed randomly in the formulation, indicating the instability of 5% L-NiC at room temperature after 2 months (Fig. 1E). To address the question what the crystals are, further investigation in the composition of 5% L-NiC was performed using CRM.

Figure 2 shows the colour-coded image of 5% L-NiC. Different configurations were formed: irregular ovals, needles, squares and layered squares. Irregular ovals were proved to be mixtures of cetylstearyl alcohol and white soft paraffin, whereas needle shapes were pure white soft paraffin. These two substances essentially exist in the base cream of NiC. Crystal squares were found to be cholesterol, which was partly covered by cetylstearyl alcohol. Highly regular layered squares were pure cholesterol, which crystallized during long-term storage. Such crystallization process is as a result of a limited solubility of cholesterol in the formulation, leading to a supersaturated state for cholesterol. This supersaturated state could be attributed to high concentration of cholesterol, low concentration of emulsifiers or weak solubility-enhancing ability of emulsifiers, irrespective which can be a crucial driving force for the formation of crystal lattice. Therefore, in combination with the results of PLM, it was manifested that 5% L-NiC was not stable after 2-month storage at room temperature, as the added cholesterol crystallized under such conditions.

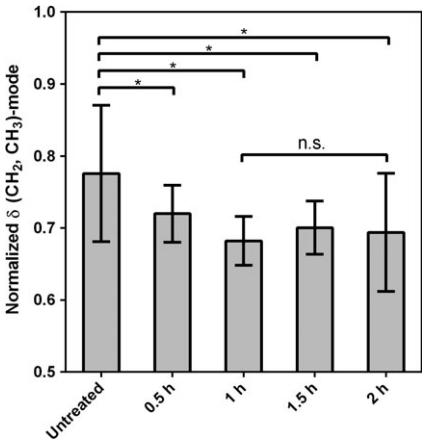

Figure 3 Comparison of lipid content in stratum corneum after SLS treatment for different time periods, $n = 9$, mean ± SD *significant difference (ANOVA, SNK; $p < 0.05$).

Ex vivo evaluation by CRM

Ex vivo experiment was carried out to assess whether the skin repair creams can deliver lipids into SC. For comparison, water-treated skin was used as the reference to simulate non-impaired skin. For the rest of the skin samples, SLS treatment was first conducted to induce lipid deficiency in SC and thus lead to SC impairment. Preliminary experiment was conducted to investigate the lipid residue as a function of time by SLS treatment. Results are given in Fig. 3. Normalized $\delta(CH_2, CH_3)$-mode values represent the relative lipid concentration in SC, and a higher value means more lipid residue in SC after extraction. It was found that after 1 h treatment, the lipid content was significantly reduced by 10% in contrast with untreated SC. Moreover, longer treatment time (up to 2 h) showed insignificant difference compared to 1 h treatment. In addition, even longer treatment results in destroyed SC membrane, which cannot be subjected to further experiment. Thus, 1-h SLS

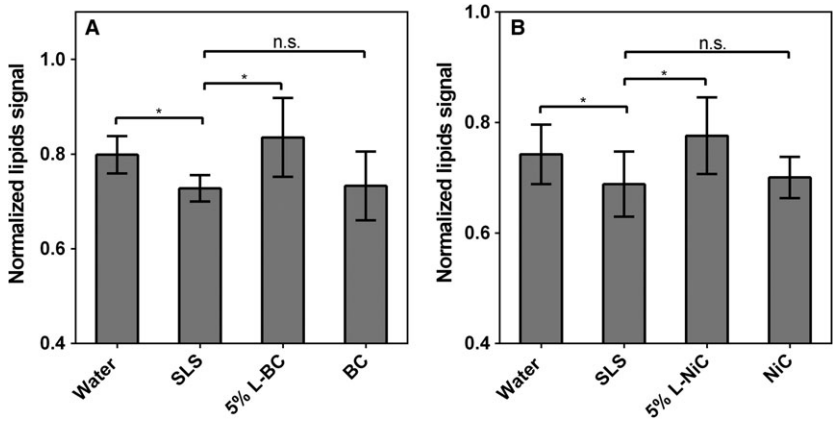

Figure 4 Comparison of lipid content in porcine stratum corneum after treated with (A) BC and 5% L-BC, (B): NiC and 5% L-NiC, $n = 9$, mean ± SD. *significant difference (ANOVA, SNK; $p < 0.05$).

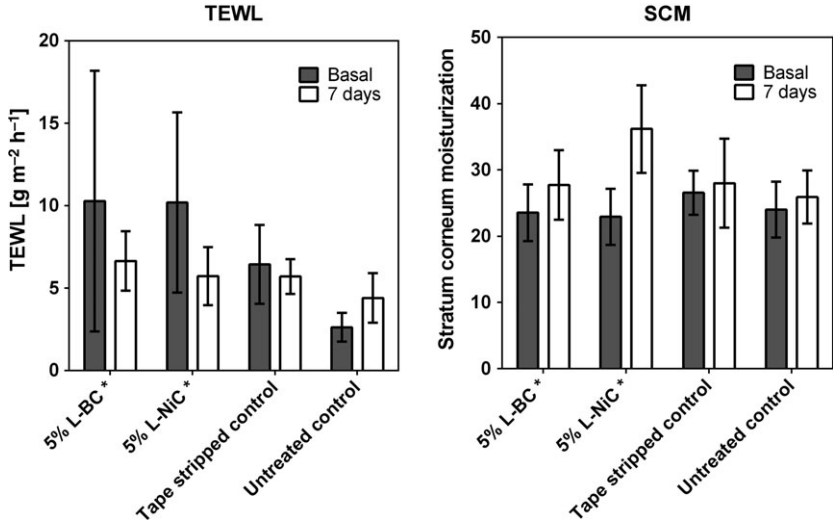

Figure 5 Results of skin efficacy study for investigated creams, left: transepidermal water loss (TEWL) and right: stratum corneum moisturization (SCM). SCM is in arbitrary units, $n = 11$, mean ± SD.

treatment was chosen to induce the lipid-lacking features as they can be observed in many skin diseases.

After SLS treatment, 5% L-BC, 5% L-NiC as well as control formulations of BC and NiC (without lipids) were applied onto the skin respectively. Additionally, SLS-treated skin samples served as a positive control for lipid extraction from SC. Results are shown in Fig. 4. From Fig. 4A, it can be seen that after SLS treatment, the lipid content significantly reduced compared to the reference (water-treated SC). The application of 5% L-BC to SLS-impaired skin led to an increase in the lipid amount in SC, indicating 5% L-BC delivered physiological lipids into the lipid-deficient SC. In contrast, BC-treated SC did not show any changes in lipid content compared with SLS treatment, as the global amount was still significantly lower than water-treated samples. Therefore, 5% L-BC was experimentally proved to be able to deliver lipids into SLS impaired SC, whereas BC was not.

Figure 4B shows the *ex vivo* evaluation results of 5% L-NiC and NiC. Compared to water-treated samples, the lipid content declined significantly after SLS treatment. However, application of 5% L-NiC increased the lipid content in impaired SC prominently. In comparison, NiC treatment did not lead to any change in the lipid amount. This means that 5% L-NiC is capable of delivering lipids into lipid-lacking SC whereas NiC (control formulation) is not. Thus, the developed 5% L-NiC and 5% L-BC were demonstrated to possess a promising ability to restore intercellular lipid composition.

In vivo skin efficacy study

To investigate the skin recovery potential of cream samples in the actual living conditions, *in vivo* study on human volunteers was performed by non-invasive techniques. To induce barrier impairment, designated skin sites were tape stripped. Thereafter, the sites were either not treated (tape-stripped control) or treated with skin repair creams. One site that was not stripped and not treated was used as an untreated control.

As shown in Fig. 5, for initial/basal values (grey bars), TEWL was statistically increased after tape stripping for all sites, indicating skin barrier disruption after tape stripping procedures. However, after 7-day application of 5% L-BC and 5% L-NiC, significant decrease in TEWL was found for both new creams, suggesting skin barrier function was restored. In contrast, decreases in TEWL were not found in tape-stripped control and untreated control. Hence, 5% L-BC and 5% L-NiC were demonstrated to dramatically improve the barrier function of impaired skin by transporting physiological lipids into the depleted SC.

There was no statistical difference among initial SC moisturization levels for all sites (grey bars). After 7 days, SCM was significantly increased after the application of 5% L-NiC and 5% L-BC compared to the initial values. However, this was not seen in tape-stripped control and untreated control. Glycerol in 5% L-NiC and propylene glycol in 5% L-BC are well-known moisturizers. Their humectant properties help to retain water in SC and thus lead to high SCM values in the experiment. However, literature reports that SC lipids are also necessary for water retention within skin and for the integrity of the barrier [19], suggesting delivered lipids played a role in keeping skin moisturized.

Therefore, these improvements in the biophysical parameters proved that 5% L-BC and 5% L-NiC facilitated the skin barrier recovery in volunteers. Such process can be described as follows: physiological lipids in preparations traverse the SC interstices between corneocytes. When reaching the nucleated cell layers, physiological lipids are taken up by keratinocytes and incorporated into nascent lamellar bodies and eventually secreted into SC intercellular lipid regions [11, 20]. Through this process, 5% L-BC and 5% L-NiC replenish lipids in the depleted skin barrier. Thus, both 5% L-BC and 5% L-NiC showed excellent efficacy in skin protection and impaired skin recovery.

Conclusion

Many skin diseases are featured with a reduction in skin lipids and one therapeutic concept is to deliver lipids into the skin. In the present study, two new formulations, 5% L-BC and 5% L-NiC, containing physiological lipids of cholesterol and linoleic acid were developed. In *ex vivo* evaluation experiment, both 5% L-BC and

5% L-NiC showed prominent lipids delivery into SC. Further *in vivo* study demonstrated that 5% L-BC and 5% L-NiC can facilitate the recovery of impaired skin barrier by showing significantly reduced TEWL values after application. Therefore, the new developed 5% L-BC and 5% L-NiC are able to deliver lipids into skin effectively. 5% L-BC was found to be more stable than 5% L-NiC. Because of the higher stability, 5% L-BC has a great potential in clinical use for treating impaired skin barrier associated with depletion of SC lipids. Moreover, it could be an excellent candidate as a base cream to incorporate pharmaceutical actives into the course of an individualized treatment.

Statement of ethics

Pig ears were received from the Department of Experimental Medicine of the University Hospital Tuebingen. The live animals were kept at the Department of Experimental Medicine and were sacrificed in the course of their experiments, with the approval of the Ethics Committee of the University Hospital Tubingen. The ears were received directly after the death of the animals. The Department of Pharmaceutical Technology is registered for the use of animal products at the District Office of Tuebingen (registration number: DE 08 416 1052 21). *In vivo* study was performed on volunteers after the written informed consent had been obtained from each volunteer. The study protocol was in accordance to the Declaration of Helsinki and was approved by the local Ethical Committee on Human Research (University of Belgrade, Faculty of Pharmacy, Serbia, No. 2297/2).

Conflicts of interest

None.

Acknowledgements

The authors thank Dr. Schenk at the University Hospital Tuebingen, Department of Experimental Medicine, for the supply of pig ears. This project was supported by the European Social Fund and Ministry of Science, Research and Arts Baden-Wuerttemberg, China Scholarship Council, German Academic Exchange Service (DAAD, project number 57334785) and Ministry of Education, Science and Technological Development of the Republic of Serbia (grant number 451-03-01766/2014-09/2).

References

1. Weerheim, A. and Ponec, M. Determination of stratum corneum lipid profile by tape stripping in combination with high-performance thin-layer chromatography. *Arch. Dermatol. Res.* **293**(4), 191–199 (2001).
2. Fan, L., Jia, Y., Cui, L., Li, X. and He, C. Analysis of sensitive skin barrier function: basic indicators and sebum composition. *Int. J. Cosmetic Sci.* **40**(2), 117–126 (2018).
3. Lynde, C., Barber, K., Claveau, J., *et al.* Canadian practical guide for the treatment and management of atopic dermatitis. *J. Cutan. Med. Surg.* **8**, 1–9 (2005).
4. Ring, J., Alomar, A., Bieber, T., Deleuran, M., Fink-Wagner, A., Gelmetti, C. *et al.* Guidelines for treatment of atopic eczema (atopic dermatitis) Part II. *J. Eur. Acad. Dermatol. Venereol.* **26**(9), 1176–1193 (2012).
5. Rubel, D., Thirumoorthy, T., Soebaryo, R.W., Weng, S.C., Gabriel, T.M., Villafuerte, L.L. *et al.* Consensus guidelines for the management of atopic dermatitis: an Asia-Pacific perspective. *J. Dermatol.* **40**(3), 160–171 (2013).
6. Proksch, E. and Lachapelle, J.M. The management of dry skin with topical emollients–recent perspectives. *J. Dtsch. Dermatol. Ges.* **3**(10), 768–774 (2005).
7. Giam, Y.C., Hebert, A.A., Dizon, M.V., Van Bever, H., Tiongco-Recto, M., Kim, K.-H. *et al.* A review on the role of moisturizers for atopic dermatitis. *Asia Pac. Allergy.* **6**(2), 120–128 (2016).
8. Ananthapadmanabhan, K., Mukherjee, S. and Chandar, P. Stratum corneum fatty acids: their critical role in preserving barrier integrity during cleansing. *Int. J. Cosmetic Sci.* **35**(4), 337–345 (2013).
9. Rawlings, A., Canestrari, D.A. and Dobkowski, B. Moisturizer technology versus clinical performance. *Dermatol. Ther.* **17**(s1), 49–56 (2004).
10. Lynde, C. Moisturizers for the treatment of inflammatory skin conditions. *J. Drugs Dermatol.* **7**(11), 1038–1043 (2008).
11. Anderson, P.C. and Dinulos, J.G. Are the new moisturizers more effective? *Curr. Opin. Pediatr.* **21**(4), 486–490 (2009).
12. Zhang, Z. and Lunter, D.J. Confocal Raman microspectroscopy as an alternative method to investigate the extraction of lipids from stratum corneum by emulsifiers and formulations. *Eur. J. Pharm. Biopharm.* **127**, 61–71 (2018).
13. Zhang, Z. and Lunter, D.J. Confocal Raman microspectroscopy as an alternative to differential scanning calorimetry to detect the impact of emulsifiers and formulations on stratum corneum lipid conformation. *Eur. J. Pharm. Sci.* **121**, 1–8 (2018).
14. Basiscreme DAC. *German Drug Codex/New German Formulary (Deutscher Arzneimittel Codex/Neues Rezeptur Formularium, DAC/NRF)*. (2016).
15. Nichtionische Hydrophile Creme. *German Pharmacopoeia (Deutsches Arzneibuch, DAB)*. (2015).
16. Döge, N., Avetisyan, A., Hadam, S., Pfannes, E.K.B., Rancan, F., Blume-Peytavi, U. *et al.* Assessment of skin barrier function and biochemical changes of ex vivo human skin in response to physical and chemical barrier disruption. *Eur. J. Pharm. Biopharm.* **116**, 138–148 (2017).
17. Tupker, R., Willis, C., Berardksca, E., Lee, C., Fartasch, M., Atinrat, T. *et al.* Guidelines on sodium lauryl sulfate (SLS) exposure tests: a report from the Standardization Group* of the European Society of Contact Dermatitis. *Contact Dermatitis.* **37**(2), 53–69 (1997).
18. Jaksic, I., Lukic, M., Malenovic, A., Reichl, S., Hoffmann, C., Müller-Goymann, C. *et al.* Compounding of a topical drug with prospective natural surfactant-stabilized pharmaceutical bases: physicochemical and in vitro/in vivo characterization–a ketoprofen case study. *Eur. J. Pharm. Biopharm.* **80**(1), 164–175 (2012).
19. Chamlin, S.L., Kao, J., Frieden, I.J., Sheu, M.Y., Fowler, A.J., Fluhr, J.W. *et al.* Ceramide-dominant barrier repair lipids alleviate childhood atopic dermatitis: changes in barrier function provide a sensitive indicator of disease activity. *J. Am. Acad. Dermatol.* **47**(2), 198–208 (2002).
20. Mao-Qiang, M., Brown, B.E., Wu-Pong, S., Feingold, K.R. and Elias, P.M. Exogenous nonphysiologic vs physiologic lipids: divergent mechanisms for correction of permeability barrier dysfunction. *Arch. Dermatol.* **131**(7), 809–816 (1995).

Supporting Information

Additional supporting information may be found online in the Supporting Information section at the end of the article:

Figure S1. Polarization micrographs of 5% L-BC prepared by Unguator® for screening proper mixing speed of the motor, A: 1000 rpm, B: 1500 rpm, C: 2000 rpm and D: 2500 rpm.

Figure S2. Polarization micrographs of 5% L-BC prepared by Unguator® for screening proper mixing time, A: 3 min, B: 6 min and C: 9 min.

Figure S3. Polarization micrographs of 5% L-BC prepared by Unguator®, A: after 15 min of low-speed mixing, B: after 30 min of low-speed mixing and C: after 45 min of low-speed mixing.

Figure S4. Polarization micrographs of BC in stability study, A: initial image (after 24 h of the preparation), B: after 7 days in AS, C: after 14 days in AS, D: after 1 month in AS and E: after 3 months in LTS.

Figure S5. Polarization micrographs of NiC in stability study, A: initial image (after 24 h of the preparation), B: after 7 days in AS, C: after 14 days in AS, D: after 1 month in AS and E: after 3 months in LTS.

Figure S6. Rheological behaviour of NiC and BC in the stability study. A and C results are from oscillatory test; B and D are calculated viscosity results from flow curves, n = 3.

Figure S7. Rheological behaviour of L-NiC and L-BC in the stability study. A and C results are from oscillatory test; B and D are calculated viscosity results from flow curves, n = 3.

Table S1. Composition and preparation of basic cream and nonionic cream.

Table S2. Operating parameters of Unguator® for screening proper mixing speed.

Table S3. Operating parameters of Unguator® for screening proper mixing time.

Supporting information to

Reinforcement of barrier function – skin repair formulations to deliver physiological lipids into skin

Ziwei Zhang [1], Milica Lukic [2], Snezana Savic [2], Dominique Jasmin Lunter [1*]

[1] *Department of Pharmaceutical Technology, University of Tuebingen, Tuebingen, Germany*

[2] *Department of Pharmaceutical Technology and Cosmetology, University of Belgrade-Faculty of Pharmacy, Belgrade, Serbia*

Abstract

In this supplementary section we report additional results about the skin repair formulations which are designed to deliver physiological lipids into skin. An optimal cream preparation method with Unguator® was developed after screening the mixing speed, mixing time and temperature. Basic cream (BC) and non-ionic cream (NiC) were chosen as base creams and their composition are provided. The stability studies of BC and NiC were conducted and examined by microscopy and rheology. They both showed excellent stability in long-term storage and accelerated stability test. In addition, prior to ex vivo evaluation experiment, stratum corneum was impaired by sodium lauryl sulfate induced lipid extraction. Results showed that 1-h SLS treatment was proper to induce the lipid-lacking features as they can be observed in many skin diseases.

1. Composition and preparation of base creams

Basic cream (Basiscreme DAC) was prepared according to instructions of German Drug Codex/New German Formulary (Deutscher Arzneimittel Codex/Neues Rezeptur Formularium, DAC/NRF) 2016. Non-ionic cream (Nichtionische Hydrophile Creme) was prepared according to the instructions of the German Pharmacopoeia (Deutsches Arzneibuch, DAB) 2015. They were used for comparison in homogeneity and storage stability studies. To clarify, their composition and preparation methods are provided in Table S1.

Table S1 Composition and preparation of basic cream and non-ionic cream

Formulations	Official names	Composition		Preparation
Basic cream	Basiscreme DAC	Glycerol monostearate (GMS)	4.0 g	Medium chain triglyceride, soft paraffin, cetyl alcohol and GMS mixture was melted at 70 °C. PEG-20-GMS and propylene glycol was dissolved in water at the same temperature. The aqueous phase was incorporated into the oily phase by Unguator® mixing until room temperature.
		Cetyl alcohol	6.0 g	
		Medium chain triglyceride	7.5 g	
		Polyoxyethylene-20-glycerol monostearate (PEG-20-GMS)	7.0 g	
		Propylene glycol	10.0 g	
		Soft paraffin	25.5 g	
		Water	40.0 g	
Non-ionic cream	Nichtionische Hydrophile Creme DAB	Polysorbate 60 (PS 60)	5.0 g	PS 60, CSA and soft paraffin was melted at 70 °C. Glycerol was dissolved in distilled water at the same temperature. Subsequently the aqueous phase was added into oily phase. The cream was prepared by Unguator® mixing until room temperature.
		Cetyl stearyl alcohol (CSA)	10.0 g	
		Soft paraffin	25.0 g	
		Glycerol	10.0 g	
		Water	50.0 g	

2. Creams preparation by Unguator®

2.1. Mixing speed

High-speed mixing is of great importance to form a homogeneous and stable cream structure. Hence, in the first step, four rotating speeds of the motor (for mixing) were screened. The speed of the motor for lifting blade was kept at an intermediate value of 1500 rpm. In the second step (cooling step), all the parameters were kept at the lowest values in the Unguator® setting panel (see Table S2). Formulations prepared by each method were characterized by polarized light microscopy (PLM) in order to evaluate the homogeneity.

Table S2 Operating parameters of Unguator® for screening proper mixing speed

	Step 1			Step 2		
No.	Mixing speed of the motor [rpm]	Lifting speed of the motor [rpm]	Time [min]	Mixing speed of the motor [rpm]	Lifting speed of the motor [rpm]	Time [min]
1	1000	1500	3	250	800	15
2	1500	1500	3	250	800	15
3	2000	1500	3	250	800	15
4	2500	1500	3	250	800	15

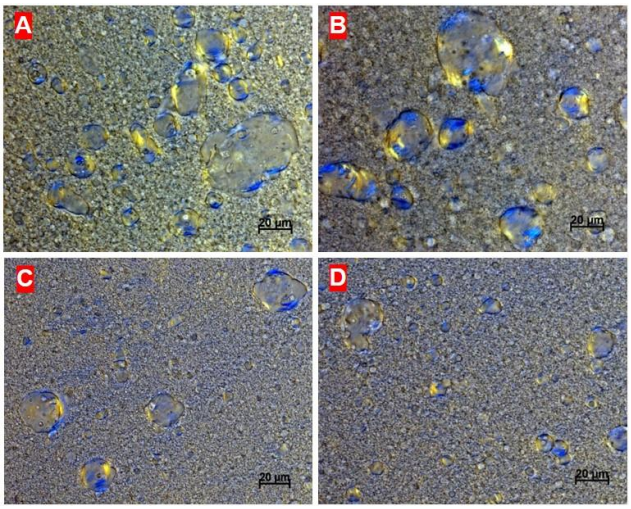

Fig. S1 Polarization micrographs of 5% L-BC prepared by Unguator® for screening proper mixing speed of the motor, A: 1000 rpm, B: 1500 rpm, C: 2000 rpm and D: 2500 rpm.

As shown in Fig. S1A and S1B, at the mixing speed of 1000 and 1500 rpm, anisotropic structures (defined as distorted Maltese crosses) as well as birefringence at the oil droplets border indicated the presence of lamellar structures. Obvious oil droplets in irregular spherical shapes with the size ranging from 10 to 40 µm were seen, implying inhomogeneity of the formulation. In contrast, as the speed increased to 2000 rpm, appearance of the cream was relatively improved, although oil droplets of approximately 20 µm in diameter were observed randomly in the microscopic image (Fig. S1C). However, further increase of the motor speed to 2500 rpm (Fig. S1D) did not alter the appearance of the polarization micrograph when compared to 2000 rpm. Therefore, a proper mixing speed of the motor was chosen to be 2000 rpm, as it gave a relatively better cream texture at an intermediate mixing speed.

2.2 Mixing time

Time for high-speed mixing is also important for the homogeneity of a cream. Appropriate mixing time gives homogeneous cream texture, while too long mixing process may affect the properties of the formulation and damage the machine as well. Thus, three mixing time periods were studied. All the process parameters are shown in Table S3. Formulations prepared by different methods were evaluated by means of PLM.

Table S3 Operating parameters of Unguator® for screening proper mixing time

	Step 1			Step 2		
No.	Mixing speed of the motor [rpm]	Lifting speed of the motor [rpm]	Time [min]	Mixing speed of the motor [rpm]	Lifting speed of the motor [rpm]	Time [min]
1	2000	1500	3	250	800	15
2	2000	1500	6	250	800	15
3	2000	1500	9	250	800	15

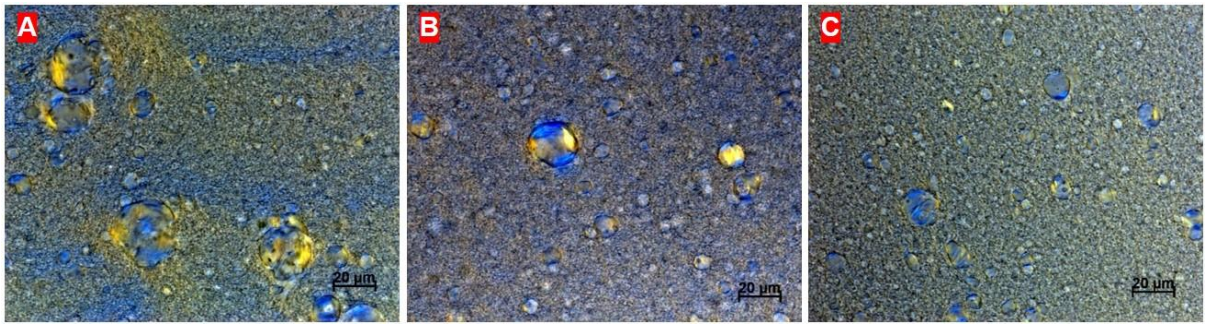

Fig. S2 Polarization micrographs of 5% L-BC prepared by Unguator® for screening proper mixing time, A: 3 min, B: 6 min and C: 9 min.

Fig. S2A shows the microscopic image of 5% L-BC after high-speed mixing with Unguator® for 3 min. Anisotropic structures were clearly seen in the mixture. Oil droplets of different sizes (up to 20 µm in diameter) were observed and they dispersed randomly in the microscopic field, indicating inhomogeneity of the formulation. In Fig. S2B, cream was prepared by high-speed mixing for 6 min with Unguator®. Lamellar phase formation was characterized by distorted Maltese crosses when observed under polarized light. However, when the mixing time was increased to 9 min, formulation texture was remarkably improved by showing even smaller sized oil droplets with reduced birefringence at the border. Thus, high-speed mixing time had a direct influence on the formulation properties. More specifically, longer mixing time tended to form more homogenous cream textures. Therefore, in our experiment, a proper mixing time of 9 min was chosen as it gave well-distributed cream formulation.

2.3 Temperature measurement

All components in the formulations were firstly melted at high temperature and subsequently mixed with Unguator® while cooling down. However, if the low-speed mixing time is too short, cream mixture may not cool down sufficiently. Some components (most likely lipids) may crystalize rather than participate in forming a proper cream structure. Hence, temperature of the formulation was detected by a digital thermometer (GMH 3700 Series, GHM Messtechnik GmbH, Regenstauf, Germany) after 15, 30 and 45

min of low-speed mixing. Samples were taken at the same time and observed microscopically. Operating parameters of Unguator® were described in Table S4.

Table S4 Operating parameters of Unguator® for temperature measurement

	Step 1			Step 2		
No.	Mixing speed of the motor [rpm]	Lifting speed of the motor [rpm]	Time [min]	Mixing speed of the motor [rpm]	Lifting speed of the motor [rpm]	Time [min]
1	2000	1500	9	250	800	15
2	2000	1500	9	250	800	30
3	2000	1500	9	250	800	45

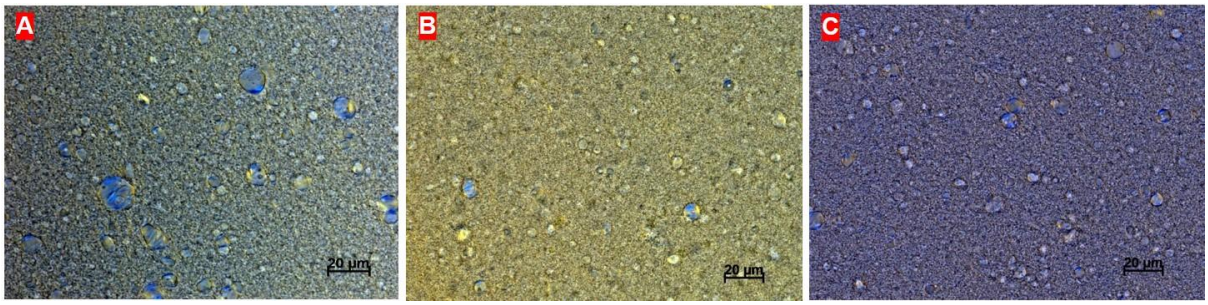

Fig. S3 Polarization micrographs of 5% L-BC prepared by Unguator®, A: after 15 min of low-speed mixing, B: after 30 min of low-speed mixing and C: after 45 min of low-speed mixing.

After low-speed mixing for 15, 30 and 45 min, the temperatures of formulation were 36.1 ± 0.5 °C, 30.2 ± 0.2 °C and 29.6 ± 0.5 °C, respectively. This shows a trend of lowered temperature along with longer mixing time. However, after 30 min this trend was not obvious, since the temperature did not statistically decrease any more. Fig. S3 are the polarization micrographs of 5% L-BC prepared by Unguator® after 15, 30 and 45 min low-speed mixing. After 15 min continuous and homogenous cream was formed despite of some oil droplets existed. However, after 30 min the number of oil droplets dramatically reduced and the size decreased to even smaller, indicating a more homogenous texture. In comparison, after 45-min mixing no obvious change was found in formulation texture compared to 30-min mixing. Thus, a proper low-speed mixing time should be set to 30 min to get homogenous cream texture.

3. Stability studies of basic cream and non-ionic cream

Fig. S4 depicts the PLM images of BC (base cream) in storage stability study. This was done as a comparison with 5% L-BC. Similar trend as 5% L-BC was seen in both accelerated stability (AS) and long-term stability (LTS). In AS, after 1 month, no indication of phase separation was found (Fig. S4D). In LTS, BC was stable after being stored for 3 months (Fig. S4E), as no clear changes were noticed compared with the initial result (Fig. S4A). Fig. S5 shows PLM images of NiC (base cream) in the stability test. In both LTS and AS, the formulation showed a homogenous texture, implying a high stability of NiC.

Fig. S6 shows the rheological behaviour of BC and NiC. From Fig. S6A, it can be seen that, BC showed no obvious changes in amplitude sweep compared with the initial values. In viscosity curves, there were also no significant variations after storage under LTS and AS conditions (Fig. S6B), indicating stable rheological behaviour of BC. Likewise, Fig. S6C and Fig. S6D show relatively stable rheological behaviour of NiC, which proves that NiC remained physically stable in both AS and LTS study.

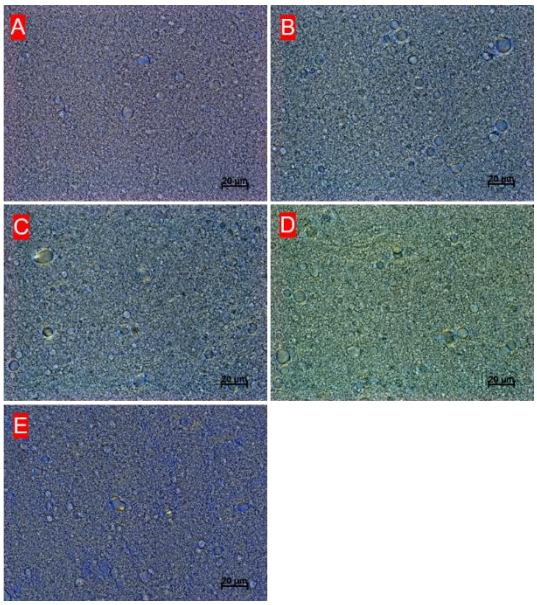

Fig. S4 Polarization micrographs of BC in stability study, A: initial image (after 24 h of the preparation), B: after 7 days in AS, C: after 14 days in AS, D: after 1 month in AS and E: after 3 months in LTS.

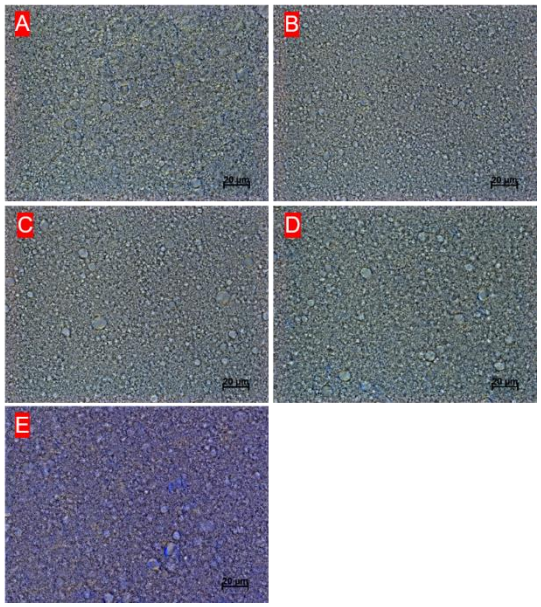

Fig. S5 Polarization micrographs of NiC in stability study, A: initial image (after 24 h of the preparation), B: after 7 days in AS, C: after 14 days in AS, D: after 1 month in AS and E: after 3 months in LTS.

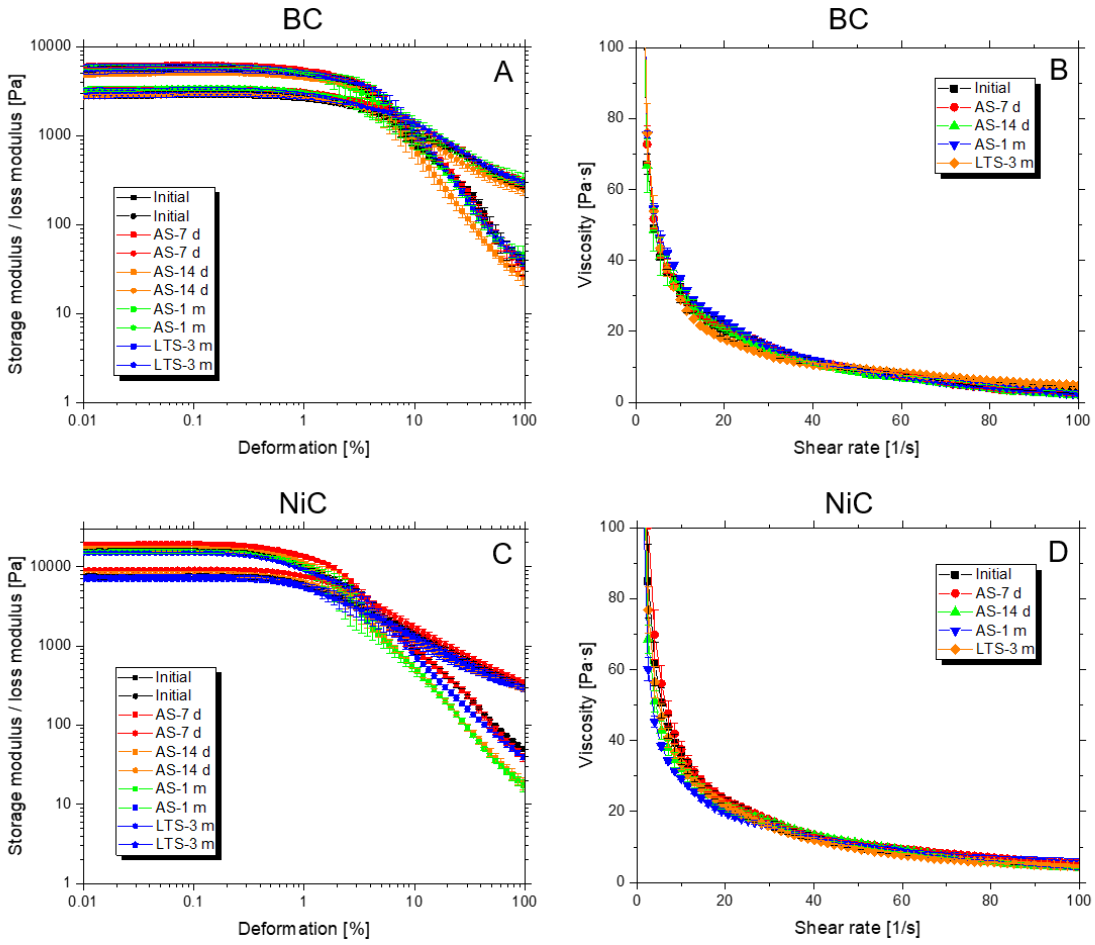

Fig. S6 Rheological behaviour of NiC and BC in the stability study. A and C results are from oscillatory test; B and D are calculated viscosity results from flow curves, n = 3.

4. Rheological behaviour of L-BC and L-NiC

The rheological behaviour of 5% L-BC in stability study is shown in Fig. S7. It can be seen that, 5% L-BC showed no obvious changes in amplitude sweep compared with the initial value (Fig. S7A). In viscosity curves (Fig. S7B), there was also no significant variation after storage under LTS and AS conditions, indicating stable rheological behaviour of 5% L-BC. Therefore, the developed 5% L-BC is proved to be as stable as the base cream of BC, and thus can be regarded stable enough for further evaluation studies.

However, 5% L-NiC showed time-dependent instability. In AS, both storage and loss modulus increased along with time (Fig. S7C). The increases in both moduli could be explained by the coalescent oil droplets and inhomogeneous texture of the formulation. In LTS, after 2 months, both storage and loss modulus increased dramatically compared to the initial results (Fig. S7C). Moreover, the viscosity of 5% L-NiC showed a trend of higher values (Fig. S7D). In combination with microscopic results, this rheological change could result from the crystals appeared in the formulations after being stored for 2 months.

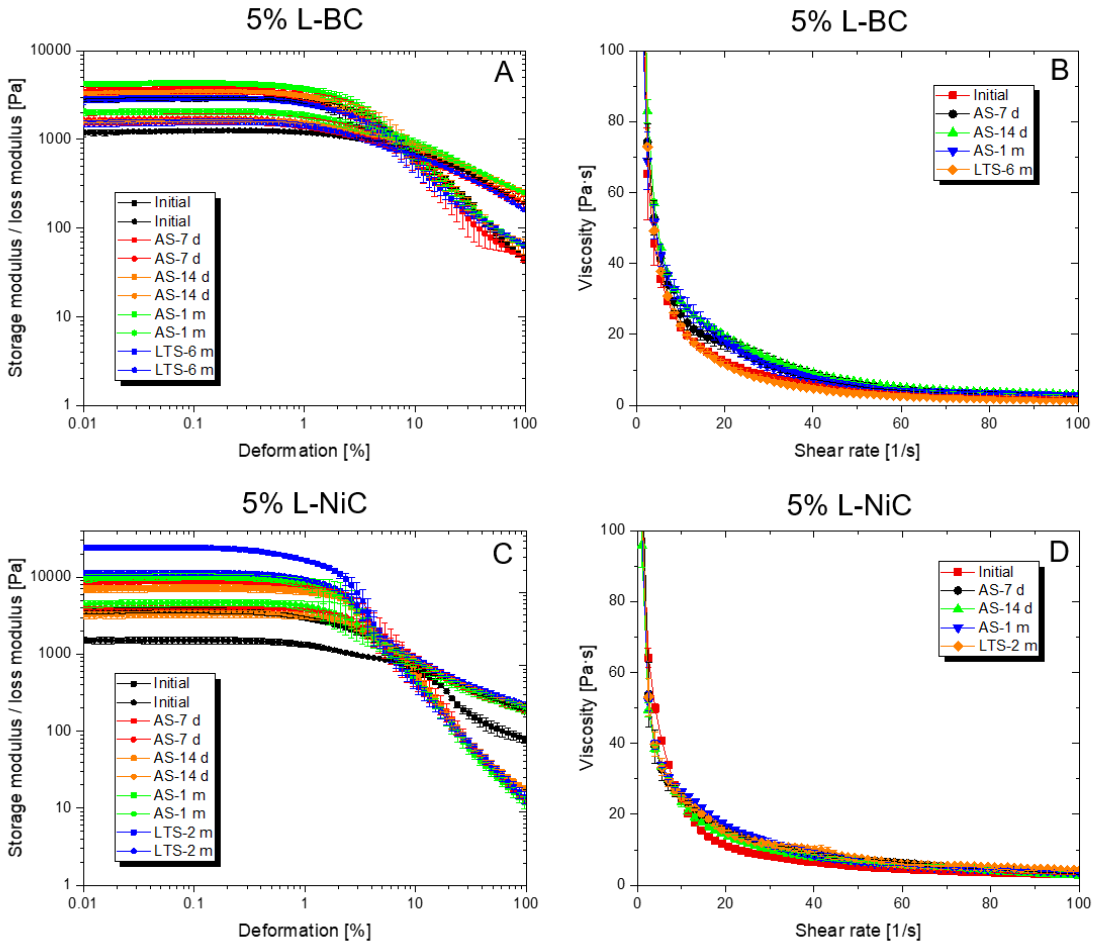

Fig. S7 Rheological behaviour of L-NiC and L-BC in the stability study. A and C results are from oscillatory test; B and D are calculated viscosity results from flow curves, n = 3.